

Electroweak Corrections to *W*-pair Production at LHC and ILC

Zur Erlangung des akademischen Grades eines
DOKTORS DER NATURWISSENSCHAFTEN
der Fakultät für Physik
der Universität Karlsruhe (TH)

genehmigte

DISSERTATION

von

Dipl.-Phys. Falk Metzler
aus Karlsruhe

Tag der mündlichen Prüfung: 03.07.2009

Referent: Prof. Dr. J.H. Kühn

Korreferent: Prof. Dr. M. Steinhauser

**Electroweak Corrections
to W -Pair Production
at LHC and ILC**

Contents

1	Introduction	3
2	Electroweak Corrections at High Energies	7
2.1	Mass Singularities	8
2.2	Sudakov Logarithms in the Electroweak Theory	10
2.3	The Goldstone Boson Equivalence Theorem	11
2.4	W -Pair Production in Leading Order	12
3	Evolution Equations	17
3.1	The Evolution Equation Approach	17
3.2	Gauge Boson Pair Production in $U(1)$ and $SU(2)$ Models . . .	26
3.3	Evolution Equations in the Electroweak Standard Model . . .	36
4	W-Pair Production in e^+e^- Annihilation (ILC)	41
4.1	One-Loop Corrections	42
4.1.1	Approach I: Transformation of Known Results	42
4.1.2	Approach II: Calculation	47
4.2	Two-Loop Corrections	51
4.2.1	Top Quark Yukawa Coupling Effects	51
4.2.2	Anomalous Dimensions	55
4.2.3	Numerical Results	60
5	W-Pair Production in $q\bar{q}$ Annihilation (LHC)	67
5.1	Anomalous Dimensions	67
5.2	Partonic Results	73
5.3	Hadronic Results	78
6	Conclusions	85
A	Appendix	87
A.1	Reduction of Gamma Matrices	87
A.2	Group Theory	88

A.3	Explicit Values of Charges	89
A.4	Summation of Light Fermion	89
A.5	Feynman Rules of $U(1)_Y$	90
A.6	Counter Terms	91
A.7	Checks of One-Loop Logarithms	96
	Bibliography	99

Chapter 1

Introduction

The Standard Model of particle physics successfully describes all fundamental forces, aside from gravitation, by quantum field theories where forces are mediated by so-called gauge bosons. In particular, this is the electromagnetic, the weak and the strong interaction. The Electroweak Standard Model explains electromagnetism, where the carrier of the electromagnetic force is the massless photon, and the weak force, mediated by the massive W - and Z -bosons. The strong force, which is responsible for the binding of atomic nucleus, is defined within the theory of Quantum Chromo Dynamics (QCD). Experimental and theoretical studies of the Standard Model have explored an energy scale up to the magnitude of the masses of the W - and Z -bosons with great accuracy. Theoretical predictions derived in the framework of the Standard Model are probed in collisions of particles in particle accelerators and, up to now, the Standard Model has successfully passed all experimental tests. Yet, there are some issues which cannot be resolved within the Standard Model of particle physics. The scientific community is, therefore, excited about possible new physics probed by the next generation of particle accelerators.

There are basically two designs of particle colliders. On the one hand circular accelerators, and on the other hand linear accelerators, both having their advantages and disadvantages. The circular collider can accelerate the particles running in the ring for as long as required. Unfortunately, the faster the particles become, the more synchrotron radiation they emit and the higher the energy loss. This leads to a natural bound of an economically justified center of mass energy for circular colliders. On the other hand, linear accelerators do not emit any synchrotron radiation and thus the energy loss is much less compared to that of circular colliders. However, the particles can only be accelerated once along their trajectory, making it technically a rather difficult task to build a linear accelerator of sensible length yielding a

high center of mass energy.

Another freedom of choice are the particles running in the collider, namely electrons or protons, and their respective antiparticles. Again, both have their advantages and disadvantages. In the beginning of the collider era, electrons were the first choice since they have only a small number of final state particles. The clear signature in the detectors makes it simpler to reconstruct the event and its kinematics. The disadvantages of electrons running in circular colliders lie in their small mass, so that the energy loss due to synchrotron radiation increases quickly. The last high energy electron circular collider most likely ever built was the Large Electron Positron Collider (LEP) at CERN, the predecessor of Large Hadron Collider (LHC). This is the reason why protons were the choice at LHC. With a mass of about 2000 times the electron mass, the center of mass energy of a proton collider is much higher than that of an electron collider, assuming a similar amount of energy loss by synchrotron radiation. However, it is the bending magnets which actually cause limitations of the center of mass energy. Due to the larger mass of the protons, the magnetic fields which keep the particles on track have to be much greater. The advantage of gaining higher center of mass energies with protons is impaired by the protons substructure, however, which makes it an extremely difficult task to reconstruct the event and momentum transfer. While the proton-proton collision at LHC takes place at a center of mass energy of 14 TeV, the actual scattering processes involves quarks and gluons, the constituents of the protons, which carry only a fraction of the protons energy. Within the theory of the Standard Model, predictions for such scattering processes are calculated for the protons constituents, also referred as partons, yielding partonic cross sections. To derive cross sections for proton colliders the partonic cross sections have to be convoluted with parton distribution function which gives the probability of finding particular constituents inside the proton carrying a certain amount of momentum fraction.

Indeed, The next colliders planed are electron linear colliders. The one most promising to be build is the International Linear Collider (ILC), which is planed to start at a center of mass energy of about 500 GeV, including the possibility of an upgrade to 1000 GeV. The status of this collider has not succeeded the planing phase yet and it remains uncertain whether it will ever be built. Much of the question as to whether to build a linear collider depends on the outcome of LHC. Another linear collider planed is the Compact Linear Collider (CLIC), which will run at center of mass energies of 3 TeV to 5 TeV. The CLIC project, however, is not expected to be build in the near future because its technical design cannot be realised with current technology. The power of electron colliders lies rather in accurate measurements of the

parameters of the Standard Model due to its clear signatures, while proton colliders are better suited for exploring new energy regimes inaccessible to electron colliders. Due to its high center of mass energy, the LHC is well suited for the discovery of new particles whose production is not possible in the energy range currently accessible. One of the most important tasks of LHC, maybe the most important one, is the search for the Higgs boson. The Higgs boson is the only particle predicted by the Standard Model of particle physics which is yet to be discovered. It is inevitably needed to generate mass terms in the Electroweak Standard Model without violating its underlying gauge symmetry.

One of the key issues is the high luminosity of LHC and ILC which enhance the experimental precision, thus allowing to probe the particles properties accurately. Therefore the precision of theoretical predictions must be at least as good as the experimental precision in order to provide an accurate determination of parameters and to disentangle various scenarios of physics beyond the Standard Model and their manifestations.

At energies around the electroweak mass scale, the main contribution to radiative corrections is of QCD nature. At the TeV-scale, the situation looks different. Here, electroweak radiative corrections which are dominated by large electroweak logarithms, commonly referred to as Sudakov logarithms, can well reach a similar magnitude as QCD corrections. These logarithms were first observed by Sudakov in the context of calculations within the theory of Quantum Electrodynamics (QED). Quantum field theories with exchange of massless gauge bosons may lead to singularities when performing loop integrations on the one hand and considering radiation of massless gauge bosons with arbitrarily soft momenta on the other hand. To regularize these singularities one commonly introduces an artificial gauge boson mass. In this way, both the virtual corrections, i.e. only virtual particle exchange is considered, and real corrections, where a massless gauge boson with soft momenta is radiated, become well defined but depend on an unphysical photon mass. Only in inclusive corrections, when virtual and real corrections are combined, the dependence of the artificial gauge boson mass drops out.

In the electroweak theory, however, loop integrals involving only virtual W - and Z -bosons are infrared safe because the masses of the weak gauge bosons provide a natural regularization. Hence exclusive weak corrections are well defined. Massive gauge bosons with arbitrarily soft momenta can be detected as individual particles, in contrast to massless gauge bosons, which go undetected if their energy becomes too soft for the resolution of the detector. Hence inclusive processes involving real gauge boson radiation differ from exclusive processes. Of course, photons are part of the electroweak theory and real QED corrections have to be included in order to get well defined

inclusive electroweak cross sections.

The electroweak Sudakov logarithms take the form $\log(s/M^2)$ where \sqrt{s} is the center of mass energy of the colliding particles and M denotes the mass of the weak gauge bosons. In the framework of perturbation theory the underlying equations are expanded in a power series of the small fine structure constant α . In particular, per loop integration double logarithms and single logarithms arise. At n -th order perturbation theory, this leads to logarithms of the form $\alpha^n \log^{2l}(s/M^2)$ with $l = 1, \dots, n$, which grow rapidly with the energy. They are commonly denoted as leading logarithms (LL) for $\alpha^n \log^{2n}(s/M^2)$, next-to-leading logarithms (NLL) for $\alpha^n \log^{2n-1}(s/M^2)$, etc. Usually, the subleading logarithms are of comparable size to the leading ones due to large coefficients. Furthermore, the coefficients may have alternating signs which eventually lead to large cancellations between leading and next-to-leading logarithms. Therefore, subleading logarithms have to be taken into account to derive precise results. In this thesis, the electroweak NNLL corrections to the production of onshell W pairs are presented both for proton-proton collisions (LHC) and electron-positron collisions (ILC).

This work is organized as follows. In chapter two, we give a brief introduction of the high energy behaviour of the Electroweak Standard Model and address the Sudakov logarithms associated with mass singularities. In chapter three, the approach of the infrared evolution equation is introduced for a single mass scale theory and is applied to a massive Abelian and a non-Abelian gauge group. Subsequently, it is shown how to work with this approach for the somewhat more complicated Electroweak Standard Model. This approach is applied to W -pair production at electron colliders in chapter 4. Finally, W -pair production at LHC is handled in chapter 5. The conclusion of this work is presented in chapter 6.

Chapter 2

Electroweak Corrections at High Energies

The fundamental object of the standard model of particle physics is the Lagrange density \mathcal{L} . It governs all known interactions among particles except gravity. It can be found in any textbook on Quantum Field Theory and will not be discussed here in detail. A common approach to calculate interaction amplitudes is the concept of Feynman diagrams, where interactions are assumed to be perturbations to the free field theory. With this approach, the Lagrangian is expanded in small coupling constants leading to a sum of Feynman diagrams in any expansion order perturbation theory. In that sense each of the three gauge groups of the standard model, $U(1)_Y$, $SU(2)_w$ and $SU(3)_c$ which describe the electromagnetic, the weak and the strong force respectively, has its own coupling constant which can be expanded in. We restrict this work to calculations within the Electroweak Standard Model made up of $SU(2)_w \times U(1)_Y$. This gauge symmetry is, however, spontaneously broken, as described in the context of the Higgs mechanism. Due to this symmetry breaking, the gauge bosons and the coupling constants of these two particular gauge groups mix and only the symmetry $U(1)_{em}$ survives, related to Quantum Electrodynamics. The relation between the gauge boson B_μ and coupling constant g' of $U(1)_Y$ and the three gauge bosons W_i , $i = 1, \dots, 3$ and coupling g of $SU(2)_w$ are given by

$$\begin{aligned} A_\mu &= \cos \theta_W B_\mu - \sin \theta_W W_\mu^3 \\ Z_\mu &= \sin \theta_W B_\mu + \cos \theta_W W_\mu^3 \\ W_\mu^\pm &= \frac{1}{\sqrt{2}}(W_\mu^1 \mp iW_\mu^2) \end{aligned} \tag{2.1}$$

and

$$e = \sin \theta_W g = \cos \theta_W g', \tag{2.2}$$

where θ_W is the weak mixing angles. The remaining two weak gauge bosons W_2 and W_3 form the electrically charged gauge bosons W^+ and W^- . Since only the symmetry $U(1)_{\text{em}}$ remains after symmetry breaking, the corresponding gauge boson A_μ , the photon, stays massless while the gauge bosons W^\pm and Z gain masses. At high energies, when all kinematic invariants are far larger than the masses of the weak gauge bosons so that these masses can be neglected, the symmetric and broken phase of $SU(2)_w \times U(1)_Y$ become equivalent.

As expansion parameter we use, if not stated otherwise, the fine structure constant $\alpha = \frac{e^2}{4\pi}$. For the sines and cosines of the mixing angle the abbreviations $s_W = \sin \theta_W$ and $c_W = \cos \theta_W$ are introduced. Throughout this work we use natural units $c = \hbar = 1$.

In this chapter, the high energy structure of the Electroweak Standard Model will be briefly introduced. The origin and properties of Sudakov logarithms are discussed in sections 2.1 and 2.2. In section 2.3 we address the Goldstone boson equivalence theorem at leading and next-to-leading order. Finally we present the leading order cross section of W -pair production at high energies in section 2.4.

2.1 Mass Singularities

When performing higher order calculations, one encounters singularities arising from loop integrations. On one hand there are UV-divergences related to loop momenta tending to infinity. These divergences are commonly handled by dimensional regularization. On the other hand, Feynman amplitudes may become divergent when massless particles are running in the loop. These singularities are commonly referred to as mass singularities and occur for virtual as well as for real radiative corrections. These mass singularities can be classified in two types, soft singularities and collinear singularities.

Soft singularities arise in diagrams where a massless virtual particle is exchanged between external on-shell particles and the momentum flow through the massless particle uniformly tends to zero. Consider a vertex diagram with exchange of a massless gauge boson between on-shell fermions,

$$\begin{aligned} & \int d^4\ell \frac{1}{\ell^2[(\ell + p_i)^2 - m_i^2][(\ell + p_j)^2 - m_j^2]} \\ &= \int d^4\ell \frac{1}{\ell^2(2 p_i \ell)(2 p_j \ell)} \sim \int_\omega \frac{d\ell}{\ell} \sim \log(\omega). \end{aligned} \quad (2.3)$$

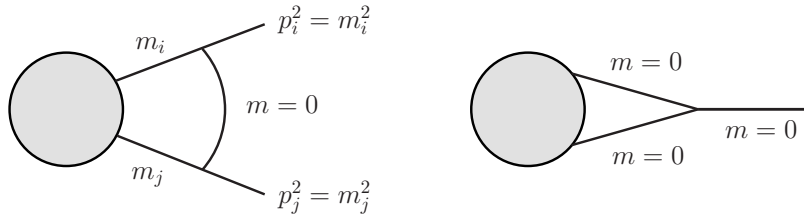


Figure 2.1: Diagrams leading to soft (left hand side) and collinear (right hand side) singularities

Here, ω was introduced as lower integration cutoff. The logarithm blows up for $\omega \rightarrow 0$. However, introducing an integration cutoff violates Lorentz and gauge invariance. For Abelian theories, a convenient way to handle this singularities is to introduce an artificial mass λ for the exchanged gauge boson. This leads to logarithms of the ratio of the kinematic invariants q^2 and the artificial mass $\log(q^2/\lambda^2)$. The soft divergences are connected with vanishing momenta and are thus long distance effects (i.e. soft divergences are local in momentum space).

Collinear singularities appear when a massless external particle splits into two massless particles attached to a loop. Consider a massless onshell particle with momentum p , emitting a virtual massless particle. The denominator of the corresponding amplitude has the form

$$\int d^4\ell \frac{1}{\ell^2(\ell^2 - 2p \cdot \ell) \dots} \quad (2.4)$$

This integral diverges when ℓ becomes collinear to p . This divergence can be handled by introducing a mass either for the emitting particle or for the emitted particle. In other words, one may introduce either a fermion mass m or a gauge boson mass λ leading to $\log(q^2/m^2)$ or $\log(q^2/\lambda^2)$, respectively. Obviously, this class of diagrams exhibits soft divergences as well when the loop momentum of a propagator attached to an external leg tends to zero. These soft-collinear singularities lead to double logarithms. The collinear (and soft-collinear) logarithms depend only on the properties of the external on-shell particles but not on a specific process [1, 2, 3, 4, 5, 6]. This fact is especially clear if a physical (Coulomb or axial) gauge is used for the calculation. In this gauge the collinear divergences are present only in the self energy insertions to the external particles [2, 5, 6].

Real emission of soft or collinear massless particles gives rise to similar divergences when integrating over the phase space of the emitted particles. The

virtual and real divergences are intrinsically connected and in many cases one obtains a finite result for inclusive corrections. This is stated by the Kinoshita-Lee-Nauenberg theorem [7, 8]. Technically, the real radiation of massless particles can be detected only up to a certain resolution threshold, since any detector has a finite energy resolution E_{res} . For an inclusive correction of an Abelian theory involving massless gauge bosons which is regulated by a artificial gauge boson mass, the dependence of the artificial mass drops out and the detector resolution comes into play instead. The logarithms related to mass singularities are usually referred to as Sudakov logarithms. In the following we use the expression “infrared singularities” for both soft and collinear singularities.

2.2 Sudakov Logarithms in the Electroweak Theory

In contrast to the energy scale around the W -mass and below, radiative corrections on an energy scale far higher than the W -mass are dominated by large Sudakov logarithms. In theories with massless gauge bosons like QED, the Sudakov logarithms depend on an unphysical gauge boson mass and well defined observables are only obtained in inclusive processes. For massive gauge bosons this is not the case. In contrast to QED, the masses of the W - and Z -bosons provide a natural cutoff and the emitted massive gauge bosons can be detected as distinguishable particles. Hence, exclusive cross sections involving Sudakov logarithms are well defined and lead to large corrections at high energies. In [9] it is shown that real and virtual logarithmic corrections do not cancel in electroweak corrections. This fact is known as Bloch-Nordsieck violation.

At n -loop level, Sudakov logarithms are of the form $\alpha^n \log^{2n-l}(s/M^2)$ with $l = 0, \dots, 2n - 1$. They are commonly denoted as leading logarithms (LL) for $\alpha^n \log^{2n}(s/M^2)$, next-to-leading logarithms (NLL) for $\alpha^n \log^{2n-1}(s/M^2)$, etc. The particular logarithmic corrections can amount to several ten percent at one-loop and still several percent at the two-loop level in the TeV region. However, the subleading logarithms may be comparable in size to the leading logarithms due to large numerical coefficients. Moreover, the coefficients of higher order subleading logarithms may have alternating sign, such that large cancellations between leading and subleading logarithms may take place. Thus, subleading logarithms have to be taken into account to guaranty reasonable accuracy of theoretical predictions.

The one-loop leading and next-to-leading logarithms can be found in [10], derived in a process independent way. Indeed, it is shown up to this approximation, that the corrections depend only on Casimir operators of the external particles. The first approach in including Sudakov logarithms beyond next-to-leading logarithms was presented in [11] where the leading logarithms were resummed in exponential form by means of evolution equations. In [12, 13, 14] this approach was applied to the four fermion process up to NLL, NNLL and NNNLL approximation successively. Recently, the NNLL correction to W -pair production in e^+e^- collisions was presented [15].

2.3 The Goldstone Boson Equivalence Theorem

The equivalence theorem on tree level

Gauge symmetry demands all gauge fields to be massless. The only known way to introduce masses without violating gauge symmetry is the Higgs mechanism, which is based on spontaneous symmetry breaking. In this framework massless gauge bosons absorb a massless scalar would-be-Goldstone boson giving the gauge fields a mass term associated with a third degree of freedom, the longitudinal polarization. At high energies, where the momentum transfer $q^2 \gg M^2$, M being the mass of the gauge boson, the longitudinal degrees of freedom exhibit their original nature. The amplitude for emission or absorption of longitudinally polarized gauge boson becomes equal to the amplitude for emission or absorption of the corresponding Goldstone boson [16]. Let us write the momentum vector of the outgoing gauge boson in the form

$$k_{\pm}^{\mu} = E(1, \beta \vec{e}_{\pm}),$$

where $\beta = \sqrt{1 - M^2/E^2}$ and \vec{e}_{\pm} are the unit-vectors of the three-momentum directions of the gauge bosons. In the high energy approximation the longitudinal polarization vector reads

$$\epsilon_L^{\mu}(k_{\pm}) = \frac{1}{M} k_{\pm}^{\mu} + v_{\pm}^{\mu},$$

where $v_{\pm}^{\mu} = -\frac{M}{E(1-\beta)}(1, \vec{e}_{\pm})$ is of $\mathcal{O}(M/E)$. Thus, in the high energy limit the longitudinal polarization vector is equivalent to k^{μ}/M , which corresponds to an external scalar boson. Therefore, in a leading order scattering the external

longitudinally polarized vector bosons may be replaced by the corresponding would-be-Goldstone bosons. The mixing contributions of production of one Goldstone boson and one longitudinally polarized gauge boson are suppressed by $\mathcal{O}(M/E)$ [17].

The equivalence theorem at one-loop

At the one-loop level one has to take care of the field strength renormalization of the would-be-Goldstone bosons. Since the Goldstone bosons are no real physical particles the field strength renormalization is not as straight forward as for physical particles. The the field strength renormalization of the would be Goldstone bosons needs to be modified, as shown in [18, 19]. The field strength renormalization of the charged Goldstone boson ϕ , related to the W -boson, is given by

$$Z_\phi^{1/2} = \left[1 - \frac{\Sigma_L^W(M_W^2)}{M_W^2} - \frac{\Sigma^{W\phi}(M_W^2)}{M_W} + \frac{1}{2} \frac{\delta M_W^2}{M_W^2} + \frac{1}{2} \delta Z_W \right] + \mathcal{O}(\alpha^2), \quad (2.5)$$

where relevant self energies and mass counterterms can be found in Appendix A.6.

2.4 W -Pair Production in Leading Order

In this section we discuss the onshell W -pair production. The full process, of course, is $f\bar{f} \rightarrow W^+W^- \rightarrow 4$ fermions. This reaction is, however, only gauge invariant when all intermediate states are taken into account. We restrict ourselves to the production of onshell states, where the W -decay has to be attached for the complete reaction.

In the high energy limit the cross section of W pair production is significantly different for transverse and longitudinally polarized W bosons. Therefore the particular cross sections are treated separately. For the production of longitudinally polarized W bosons we use the Goldstone boson equivalence theorem and calculate the production of the corresponding charged would-be-Goldstone bosons instead.

For $f(p_1)\bar{f}(p_2) \rightarrow W^+(k_1)W^-(k_2)$ the Mandelstam variables, the kinematic invariants of the process, take the form

$$s = (p_1^2 + p_2^2), \quad t = (p_1 - k_1)^2, \quad u = (p_1 - k_2)^2. \quad (2.6)$$

Alternatively we often use the center of mass energy squared s and the dimensionless variables x_- and x_+ which are defined as

$$x_- = -\frac{t}{s} = \frac{1}{2}(1 - \cos \theta), \quad x_+ = -\frac{u}{s} = \frac{1}{2}(1 + \cos \theta), \quad (2.7)$$

where θ is the scattering angle. The CKM matrix is set to unity, so quark mixing effects are not taken into account.

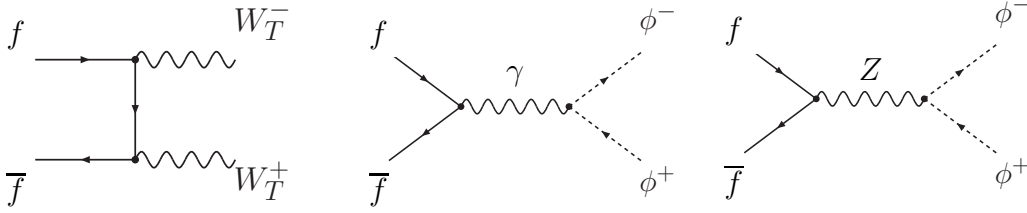


Figure 2.4: Diagrams contributing to the leading order cross section. The t -channel diagram corresponds to the production of transversely polarized W -boson, the s -channel to the production of Goldstone boson related to the corresponding longitudinally polarized W -bosons.

First we present the Born amplitudes for both transverse and longitudinally polarized W -bosons and left-handed initial state fermions. Here, and in the following, we refer to left-handed spinors such that the fermion is left-handed and the antifermion is right-handed. The diagrams contributing to the Born cross section are depicted in fig. 2.4. Note that for the production of a pair of transversely polarized W -pairs only the t -channel diagram contributes at leading order. In principle s -channel diagrams involving triple gauge boson couplings W^+W^-Z and $W^+W^-\gamma$ do contribute as well, but vanish in the high energy limit. This is because only vanishing scalar products of combinations of four momenta of the W -bosons and its polarization vectors appear when contracting the amplitude. For the production of longitudinally polarized gauge bosons the t -channel does not contribute because scalar bosons describing the longitudinal degree of freedom of the gauge bosons do not couple to massless fermions.

The Feynman rules are adopted from [20]. For the production of a pair of transversely polarized W bosons the Born amplitude depends only on the $SU(2)$ coupling of the initial fermions to the W boson which is essentially the same for electrons and quarks. The longitudinal parts of the Born amplitude and cross section are presented for initial state fermions carrying electric charge Q_f and weak isospin T_f^3 . Whereas for the cross section related to the transverse part only left-handed initial states contribute, both left-handed

and right-handed initial states are involved in the production of longitudinally polarized W -bosons. In the center of mass frame, the momenta are parameterised according to

$$p_{1/2} = \frac{s}{2}(1, 0, 0, \pm 1), \quad k_{1/2} = \frac{s}{2}(1, \mp \sin \theta, 0, \mp \cos \theta). \quad (2.8)$$

The polarization vectors of the transversely polarized W -bosons read

$$\begin{aligned} \epsilon_{\kappa}^{*\mu}(k_1) &= \frac{1}{\sqrt{2}}(0, \cos \theta, \kappa i, -\sin \theta), \\ \epsilon_{\kappa}^{*\mu}(k_2) &= \frac{1}{\sqrt{2}}(0, -\cos \theta, \kappa i, \sin \theta). \end{aligned} \quad (2.9)$$

where $\kappa = \pm$ represents the polarization and corresponds to helicity ± 1 respectively. Note that the vector bosons have to have opposite helicity due to helicity conservation in the high energy regime. For the longitudinally polarized W bosons, we make use of the Goldstone boson equivalence theorem. To give the amplitudes in a compact form we make use of the opposite polarizations of the transversely polarized W -bosons, such that $\epsilon_{\kappa}^{\mu}(k_1) = -\epsilon_{-\kappa}^{\mu}(k_2) = \epsilon_{\kappa}^{\mu}$ where $\kappa = \pm$ corresponds to polarization $(+, -)$ and $(-, +)$ respectively. The amplitudes are presented for fixed chirality of the initial state fermions labeled by $-$ and $+$ for left-handed and right-handed initial states respectively,

$$\mathcal{A}_{-T}^B = \frac{e^2}{s_W^2} \frac{1}{t} \bar{\psi}(p_2) \not{\epsilon}_{\kappa}^* p_1 \cdot \epsilon_{\kappa}^* \omega_- \psi(p_1), \quad \mathcal{A}_{+T}^B = 0, \quad (2.10)$$

$$\mathcal{A}_{\mp L}^B = e^2 \frac{1}{s} \frac{(2T_f^3 - Q_f)s_W^2 - T_f^3}{c_W^2 s_W^2} \bar{\psi}(p_2) \not{k}_1 \omega_{\mp} \psi(p_1), \quad (2.11)$$

where $\omega_- = \frac{1-\gamma^5}{2}$ and $\omega_+ = \frac{1+\gamma^5}{2}$ are the projectors on left-handed and right-handed initial states respectively. The polarization parameter κ has to be summed up when calculating the cross section of the transversely polarized W -bosons.

The Born cross sections for polarized initial state fermions and final state W -bosons read

$$\frac{d\sigma_{-T}^B}{d\Omega} = \frac{\alpha^2(M_W^2)}{s_W^4} \frac{1}{4s} \frac{x_+(x_+^2 + x_-^2)}{x_-}, \quad (2.12)$$

$$\frac{d\sigma_{-L}^B}{d\Omega} = \alpha^2(s) \frac{((Q_f - 2T_f^3)s_W^2 + T_f^3)^2}{c_W^4 s_W^4} \frac{x_+ x_-}{4s}, \quad (2.13)$$

$$\frac{d\sigma_{+L}^B}{d\Omega} = \alpha^2(s) \frac{Q_{\psi}^2}{c_W^4} \frac{x_+ x_-}{4s}. \quad (2.14)$$

We restrict, however, our calculation to left-handed initial states because, for right-handed initial state fermions, the Born cross section is saturated by the hypercharge gauge boson.

In order to be thorough, we emphasize that additional amplitudes contribute to the W -pair production which are, however, suppressed at high energies. In particular for e^+e^- initial states these are [21]

$$\frac{d\sigma_{+T}^B}{d\Omega} = \frac{\alpha^2 M_W^4}{c_W^4 s^3} x_+ x_-, \quad (2.15)$$

$$\frac{d\sigma_{-M}^B}{d\Omega} = \frac{\alpha^2 M_W^2}{s_W^4 c_W^4 s^2} (x_+^2 + x_-^2 + 4c_W^2 x_+ (x_+ - x_-) + 8c_W^4 x_+^2), \quad (2.16)$$

$$\frac{d\sigma_{+M}^B}{d\Omega} = \frac{\alpha^2 M_W^2}{c_W^4 s^2} (x_+^2 + x_-^2), \quad (2.17)$$

The label M denotes the production of one transverse and one longitudinally polarized W -boson. These processes will not be discussed in the following.

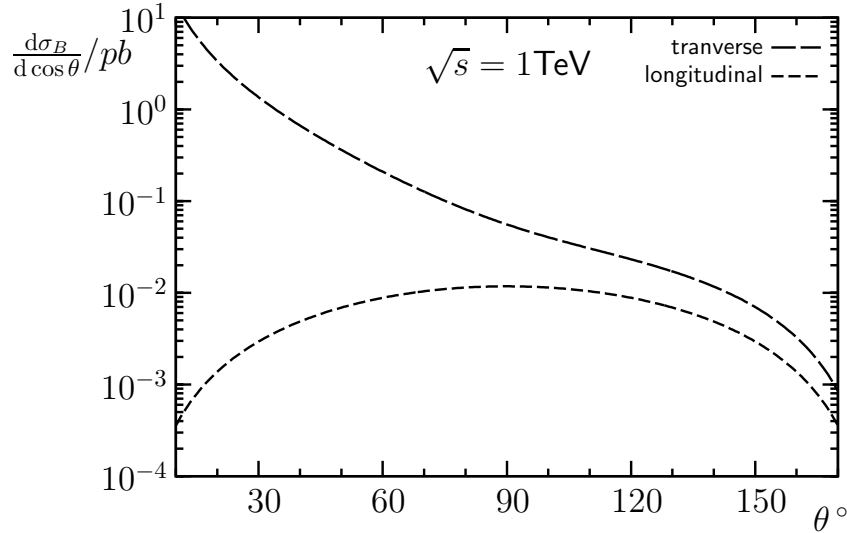


Figure 2.2: The differential distribution of the leading order cross section for pair-production of transverse and longitudinally polarized W -bosons in e^+e^- annihilation.

The leading order differential and total cross section for W -pair production in e^+e^- annihilation are depicted in figures 2.2 and 2.3. Note that a spin average factor of $1/4$ for the polarized cross sections is included to account for

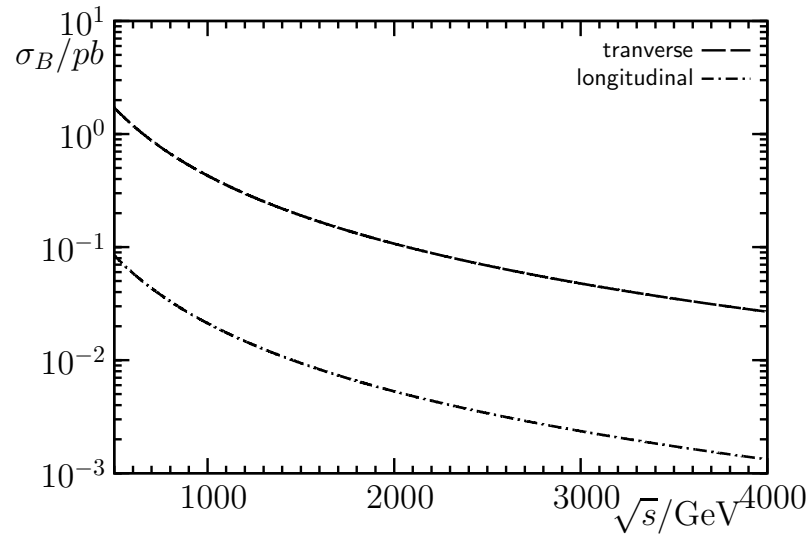


Figure 2.3: The total cross section at leading order with an angular cutoff of 30° .

incomplete polarization. As input parameters we use $\overline{\text{MS}}$ values, $\alpha = 1/128/1$ and $s_W^2 = 0.231$. For the total cross sections we integrate over the angular region $\frac{\pi}{6} \leq \theta \leq \frac{5\pi}{6}$.

Chapter 3

Evolution Equations

In this chapter we present the framework of the infrared evolution equation approach. In section 3.1 we discuss this approach within the model of a single gauge group $SU(N)$. We give a detailed discussion of $2 \rightarrow 2$ processes with final state particles transforming either according to the fundamental representation or the adjoint representation. The initial state particles are assumed to transform according to the fundamental representation.

Subsequently, we apply this approach to $U(1)$ and $SU(2)$ corrections to the production of a pair of scalar bosons and vector bosons in section 3.2. Finally, in section 3.3, we extend the evolution equation approach introduced in 3.1 to the case of the spontaneously broken Electroweak Standard Model.

With the evolution equation approach, it is possible to relate coefficients of logarithms in n -th order perturbation theory to those of orders lower than n . Thus, the evolution equation approach provides a powerful tool to derive the dominant terms in higher orders without performing a complete calculation in the desired order perturbation theory.

3.1 The Evolution Equation Approach

In this section we extend the Infrared Evolution Equation approach, devised in the context of resummation of subleading logarithms in the four fermion process [12, 13], to a more general case of the production of two arbitrary particles. To keep the discussion general, we consider a $SU(N)$ theory. In that sense, by isospin we refer to the charge of this group. In the context of electroweak corrections this corresponds to (weak) isospin and for QCD to colour.

As mentioned before, in the high energy approximation radiative correc-

tions are dominated by Sudakov logarithms originating from exchange of soft and collinear gauge bosons. The collinear logarithms are known to factorize and depend only on the properties of the external particles but not on a specific process. Thus, a factor \mathcal{Z} is introduced containing all factorized logarithms. These are, in particular, soft-collinear double-logarithms and collinear single-logarithms. Let us denote by $\tilde{\mathcal{A}}$ the reduced amplitude containing the remaining soft logarithms, such that any $SU(N)$ amplitude may be expressed as

$$\mathcal{A} = \mathcal{Z}\tilde{\mathcal{A}}. \quad (3.1)$$

In general, the reduced amplitude $\tilde{\mathcal{A}}$ can be represented as a vector in the isospin/chiral basis. In this work we restrict ourselves to fixed chirality of initial state fermions. In that sense, we restrict ourselves to one specific component of the chiral basis. The choice of the isospin basis depends only on the representation of the external particles and will be discussed in more detail in the following. The asymptotic Q -dependence of the \mathcal{Z} -factor and the reduced amplitude in this limit is governed by the evolution equations as introduced in [4, 5] and [12, 6] respectively. The evolution equations are presented in terms of a Euclidian four vector $Q^2 = -q^2$, where q denotes the momentum transfer in Minkowskian space. The factor \mathcal{Z} and the reduced amplitude $\tilde{\mathcal{A}}$ satisfy the following linear evolution equations

$$\frac{\partial}{\partial \log Q^2} \mathcal{Z} = \left[\int_{M^2}^{Q^2} \frac{dx}{x} \gamma(\alpha(x)) + \zeta(\alpha(Q^2)) + \xi(\alpha(M^2)) \right] \mathcal{Z}, \quad (3.2)$$

$$\frac{\partial}{\partial \log Q^2} \tilde{\mathcal{A}} = \chi(\alpha(Q^2)) \tilde{\mathcal{A}}, \quad (3.3)$$

with the solution

$$\mathcal{Z} = \exp \left\{ \int_{M^2}^{Q^2} \frac{dx}{x} \left(\int_{M^2}^x \frac{dx'}{x'} \gamma(\alpha(x')) + \zeta(\alpha(x)) + \xi(\alpha(M^2)) \right) \right\}, \quad (3.4)$$

$$\tilde{\mathcal{A}} = \text{P} \left[\exp \left(\int_{M^2}^{Q^2} \frac{dx}{x} \chi(\alpha(x)) \right) \right] \tilde{\mathcal{A}}_0(\alpha(M^2)), \quad (3.5)$$

where $\alpha = \frac{g^2}{4\pi}$, g being the $SU(N)$ coupling, is renormalized within the $\overline{\text{MS}}$ scheme. In eq. 3.4 the initial condition was fixed to $\mathcal{Z}_i|_{Q^2=M^2} = 1$. The matrices $\chi(\alpha(Q^2))$ for different values of Q do not commute and the solution of eq. 3.3 is given by the path-ordered exponent [6], where P denotes the path ordering. This becomes relevant in $O(\alpha^3)$ since one needs at least second power of χ and first power of β_0 to have the non-commutative effect. The coefficients of the latter equations

$$f(\alpha) = \{\gamma(\alpha), \zeta(\alpha), \xi(\alpha), \chi(\alpha), \tilde{\mathcal{A}}_0(\alpha)\}$$

are expanded according to

$$f(\alpha) = \sum_{n=0}^{\infty} \left(\frac{\alpha}{4\pi} \right)^n f^{(n)}, \quad (3.6)$$

with

$$\gamma^{(0)} = \zeta^{(0)} = \xi^{(0)} = \boldsymbol{\chi}^{(0)} = 0, \quad \tilde{\mathcal{A}}_0^{(0)} = \mathcal{A}_B,$$

and $\alpha = \alpha(M^2)$ while $\alpha(x) = \alpha(M^2) - \alpha^2(M^2)\beta_0 \log(\frac{x}{M^2}) + \mathcal{O}(\alpha^3)$. Thereby renormalization group logarithms come into play, which are also resummed by the evolution equation approach. How to obtain β_0 for a specific gauge group is discussed in appendix A.4. The Born amplitude is denoted by \mathcal{A}_B . Note that this amplitude is given as a vector in isospin space.

Let us give a briefly introduce the coefficients of the evolution equation and discuss them in more detail subsequently.

In the \mathcal{Z} factor, γ is the coefficient of the soft-collinear double logarithm, ζ and ξ are the coefficients of the collinear single logarithm. For the reduced amplitude the matrix of soft anomalous dimensions $\boldsymbol{\chi}$, defined in isospin space, gives the coefficients of soft logarithms.

The coefficients of the evolution equation can be related to specific regions regarding the loop momentum, the hard momentum region where the loop momentum is of order Q and the soft momentum region where the loop momentum is of order M . We merely want to clarify the relationship between the coefficients and the region of loop momentum without going into explicit details about the expansion by region method. For a detailed discussion we refer to [12, 14] and references therein. In particular, γ , ζ and χ are related to the hard momentum region. and ξ and the constant $\tilde{\mathcal{A}}_0^{(n)}$, $n \geq 1$, are related to the soft momentum region. Hence only ξ and $\tilde{\mathcal{A}}_0$ are sensitive to the mass structure of the theory.

The initial conditions of the differential equations 3.4 and 3.5 read $\mathcal{Z}_i|_{Q^2=M^2} = 1$ and $\tilde{\mathcal{A}}|_{Q^2=M^2} = \mathcal{A}_0$ respectively. Yet, we still have some freedom to fix the initial condition ξ . This coefficient depends on the mass structure of the theory. In the context of a single mass scale $SU(N)$ where the infrared cutoff is the gauge boson mass one has $\xi = 0$. These coefficients will be discussed in more detail below.

While the coefficients of the factor \mathcal{Z} , related to collinear and soft-collinear logarithms, only depend on the group properties of the external particles, this is not true for the matrix of soft anomalous dimensions. In particular, the factor \mathcal{Z} can, in principle, be applied to a process involving an arbitrary number of external particles but the matrix $\boldsymbol{\chi}$ in the reduced amplitude $\tilde{\mathcal{A}}$ is

essentially dependent on the number of external particles. In this framework, we restrict ourselves to $2 \rightarrow 2$ processes concerning the reduced amplitude.

We present the expansion of the \mathcal{Z} -factor and the reduced amplitude $\tilde{\mathcal{A}}$ in α up to the desired order. The particular contributions are given by

$$\begin{aligned}\mathcal{Z}^{(0)} &= 1, \\ \mathcal{Z}^{(1)} &= \frac{1}{2}\gamma^{(1)}\log^2\left(\frac{Q^2}{M^2}\right) + (\zeta^{(1)} + \xi^{(1)})\log\left(\frac{Q^2}{M^2}\right).\end{aligned}\quad (3.7)$$

$\mathcal{Z}^{(2)}$ we decompose into powers of logarithms up to NNLL

$$\mathcal{Z}^{(2)} = \mathcal{Z}_{LL}^{(2)} + \mathcal{Z}_{NLL}^{(2)} + \mathcal{Z}_{NNLL}^{(2)}$$

with

$$\begin{aligned}\mathcal{Z}_{LL}^{(2)} &= \frac{1}{8}(\gamma^{(1)})^2\log^4\left(\frac{Q^2}{M^2}\right), \\ \mathcal{Z}_{NLL}^{(2)} &= \frac{1}{2}(\zeta^{(1)} + \xi^{(1)} - \frac{1}{3}\beta_0)\gamma^{(1)}\log^3\left(\frac{Q^2}{M^2}\right), \\ \mathcal{Z}_{NNLL}^{(2)} &= \frac{1}{2}(\gamma^{(2)} + (\zeta^{(1)} + \xi^{(1)})^2 - \beta_0\zeta^{(1)})\log^2\left(\frac{Q^2}{M^2}\right).\end{aligned}\quad (3.8)$$

The reduced amplitude is expanded according to

$$\begin{aligned}\tilde{\mathcal{A}} &= \tilde{\mathcal{A}}_0^{(0)} + \frac{\alpha}{4\pi}[\boldsymbol{\chi}^{(1)}\tilde{\mathcal{A}}_0^{(0)}\log\left(\frac{Q^2}{M^2}\right) + \tilde{\mathcal{A}}_0^{(1)}] \\ &+ \left(\frac{\alpha}{4\pi}\right)^2\left[\frac{1}{2}\left((\boldsymbol{\chi}^{(1)})^2 - \beta_0\boldsymbol{\chi}^{(1)}\right)\tilde{\mathcal{A}}_0^{(0)}\log^2\left(\frac{Q^2}{M^2}\right)\right. \\ &\left.+ \left(\boldsymbol{\chi}^{(1)}\tilde{\mathcal{A}}_0^{(1)} + \boldsymbol{\chi}^{(2)}\tilde{\mathcal{A}}_0^{(0)}\right)\log\left(\frac{Q^2}{M^2}\right) + \tilde{\mathcal{A}}_0^{(2)}\right] + \mathcal{O}(\alpha^3).\end{aligned}\quad (3.9)$$

In the following, the one-loop coefficients of the evolution equation will be discussed in detail.

The coefficients of the one-loop soft-collinear leading and collinear next-to-leading logarithms $\gamma^{(1)}$ and $\zeta^{(1)}$ are given by

$$\gamma^{(1)} = \sum_k C_k^\gamma, \quad \zeta^{(1)} = \sum_k C_k^\zeta \quad \text{with} \quad (3.10)$$

$$\begin{aligned}C_k^\gamma &= \begin{cases} -C_F & \text{for EWSM fermions and scalar bosons} \\ -C_A & \text{for gauge bosons} \end{cases} \\ C_k^\zeta &= \begin{cases} \frac{3}{2}C_F & \text{for EWSM fermions} \\ 2C_F & \text{for EWSM scalar bosons} \\ 0 & \text{for gauge bosons} \end{cases}\end{aligned}$$

for a $SU(N)$ theory, where k runs over all external legs. $C_F = (N^2 - 1)/(2N)$ is the quadratic Casimir operator of the fundamental representation, $C_A = N$ is the quadratic Casimir operator of the adjoint representation. For an Abelian theory $U(1)_Y$, where the particles carry charge Y_k , one has to replace $C_F \rightarrow (Y_k/2)^2$ and $C_A \rightarrow 0$. We emphasize that although fermions and scalar bosons transform according to the fundamental representation in the Electroweak Standard Model (EWSM) this does not hold in general in theories beyond the EWSM. For QED, the infrared cutoff M corresponds to an artificial photon mass and the structure of the logarithms and its coefficients depend on whether the external particles are massive and which mass hierarchy they obey. For a detailed discussion of this, see e.g. [10].

The matrix of soft anomalous dimensions χ defined in isospin space is the only part of the evolution equation depending on the isospin structure of the process. Before we continue with the discussion of the matrix χ , let us review the underlying isospin structure. Let us emphasize once again that the part concerning the matrix χ works only for $2 \rightarrow 2$ processes.

As stated before, a isospin basis is introduced due to the non-factorization of soft logarithms regarding the isospin structure of the Born amplitude. In particular, there are two sets of bases, one for the production of a pair of particles which transform under the fundamental representation, and another for particles which transform according to the adjoint representation. The initial state fermions are assumed to transform under the fundamental representation.

First, we consider the case of the fundamental representation. This concerns the production of a pair of fermions or a pair of scalar bosons. The Born isospin structure is given by $\mathbf{T}^a \otimes \mathbf{T}^a$, where \mathbf{T}^a are the generators of $SU(N)$ in the fundamental representation. A brief introduction to group theory is provided in appendix A.2.

In general, the isospin structure becomes more complicated in higher order calculations. However, the product of generators can, in this case, be reduced to two contributions ($\mathbf{T}^a \otimes \mathbf{T}^a$) and ($\mathbf{1} \otimes \mathbf{1}$). Thus the structure of radiative corrections is given in respect to a isospin basis ($\mathbf{T}^a \otimes \mathbf{T}^a, \mathbf{1} \otimes \mathbf{1}$). Let us examine the reduction to the isospin basis of a one-loop box diagram for the production of a pair of particles transforming under the fundamental representation as an example. The Born isospin structure $\mathbf{T}^a \times \mathbf{T}^a$ reads in components $T_{ik}^a T_{nl}^a$. The isospin structure of the direct box diagram can be reduced according to

$$T_{ij}^a T_{jk}^b T_{nm}^b T_{ml}^a = \left(C_F - \frac{T_F}{N} \right) T_{ik}^a T_{nl}^a + \frac{C_F T_F}{N} \delta_{ik} \delta_{nl}, \quad (3.11)$$

where the relations

$$T_{ij}^a T_{kl}^a = T_F \left(\delta_{il} \delta_{jk} - \frac{1}{N} \delta_{ij} \delta_{kl} \right), \quad (3.12)$$

$$T_{ij}^a T_{jk}^a = C_F \delta_{ik} \quad (3.13)$$

were used and $T_F = 1/2$ is the index of the fundamental representation of the $SU(N)$ group. In matrix form this reads $(C_F - \frac{T_F}{N})(\mathbf{T}^a \times \mathbf{T}^a) + \frac{C_F T_F}{N}(\mathbf{1} \times \mathbf{1})$. For the crossed box one obtains $(C_F - \frac{C_A}{2} - \frac{T_F}{N})(\mathbf{T}^a \times \mathbf{T}^a) + \frac{C_F T_F}{N}(\mathbf{1} \times \mathbf{1})$. The matrix of soft anomalous dimensions for the production of a pair of particles transforming under the fundamental representation reads [12]

$$\chi_F^{(1)} = \begin{pmatrix} -2C_A (\log(x_+) + i\pi) + 4\left(C_F - \frac{T_F}{N}\right) \log\left(\frac{x_+}{x_-}\right) & 4 \log\left(\frac{x_+}{x_-}\right) \\ 4\frac{C_F T_F}{N} \log\left(\frac{x_+}{x_-}\right) & 0 \end{pmatrix}. \quad (3.14)$$

The matrix χ is labeled by the index F to illustrate that this matrix belongs to the process in which particles transforming under the fundamental representation are produced. Note that this index refers only to the final state particles, the initial state particles are always assumed to transform according to the fundamental representation.

Next, we examine the isospin structure regarding the adjoint representation, describing the isospin algebra for the production of a pair of gauge bosons. The basic idea is the same as for fundamental representation. As an isospin basis we choose $(\mathbf{T}^a \mathbf{T}^b, \mathbf{T}^a \mathbf{T}^b, \delta^{ab} \mathbf{1})$. The corresponding matrix of soft anomalous dimensions can be extracted from the results of Refs. [22, 23] and reads

$$\chi_A^{(1)} = \begin{pmatrix} -N(\log(x_-) + i\pi) & 0 & \log\left(\frac{x_+}{x_-}\right) \\ 0 & -N(\log(x_+) + i\pi) & \log\left(\frac{x_-}{x_+}\right) \\ (\log(x_+) + i\pi) & (\log(x_-) + i\pi) & 0 \end{pmatrix}. \quad (3.15)$$

This matrix related to the the production of particles transforming under the adjoint representation is labeled by A . An alternative choice of an isospin basis would be $(if^{abc} \mathbf{T}^c, d^{abc} \mathbf{T}^c, \delta^{ab} \mathbf{1})$, where f^{abc} is the totally antisymmetric constant of $SU(N)$ and d^{abc} symmetric structure constants of $SU(N)$. Note that angular dependent logarithms appear only in the matrix of soft anomalous dimensions.

The form of the amplitude vector $\tilde{\mathcal{A}}_0$ regarding the isospin basis depends on the process being dealt with and incorporates the non-logarithmic part of the amplitude and its leading order expansion gives the Born amplitude

vector $\tilde{\mathcal{A}}_0^{(0)} = \mathcal{A}_{\text{Born}}$. Let us consider an exemplary case for both of the bases introduced above.

As examples we choose the production of a pair of scalar bosons and a pair of vector bosons representing the cases fundamental and adjoint representations, respectively. The corresponding Feynman diagrams are depicted in fig. 3.1. For the production of a pair of scalar bosons by an s-channel process, which is in one-to-one correspondence to the production of a pair of fermions, the Born process reads $(\mathbf{T}^a \otimes \mathbf{T}^a) \mathcal{A}_{\mathcal{L}}$. Here, for the Lorentz structure, which is a common factor regarding the isospin algebra, we write $\mathcal{A}_{\mathcal{L}}$ and the isospin vector in leading order is given by $(1, 0)$. Note that in contrast to $\tilde{\mathcal{A}}_0$ (and $\mathcal{A}_{\text{Born}}$) $\mathcal{A}_{\mathcal{L}}$ is not a vector in isospin space. The production of a pair of vector bosons in a $SU(N)$ theory involves two different Born processes, a t-channel and u-channel process (the s-channel is suppressed at high energies). Thus, these amplitudes obey also a different angular dependence beside the isospin structure. Again, we write the Born amplitude, up to a common factor $\mathcal{A}'_{\mathcal{L}}$ as $(\mathbf{T}^i \mathbf{T}^j / x_- + \mathbf{T}^j \mathbf{T}^i / x_+) \mathcal{A}'_{\mathcal{L}}$ which corresponds to $(1/x_-, 1/x_+, 0) \mathcal{A}'_{\mathcal{L}}$.

The coefficient ξ depends only on the lower bound of the integration in eq. 3.2 and, therefore, depends on the mass structure of the underlying theory. Hence this initial condition is fixed according to this mass structure. In the context of calculations within the Electroweak Standard Model particles with non-negligible masses different from the W -mass, which would be a natural choice as cutoff scale, this can also lead to soft-collinear double logarithms. To restore the leading logarithmic structure, provided by the evolution equation, the mass dependence of particles with masses different to the mass used as cutoff, the logarithmic structure can be rearranged in such a way that only Sudakov logarithms with one mass scale in the argument appear. Let us clarify this with a simple example of a double logarithm arising from the exchange of a Z -boson with a mass different to M , which corresponds to the mass of the W -boson. Here, the corresponding logarithm is rewritten according to $\log^2(s/M_Z^2) = \log^2(s/M^2) + 2 \log(M^2/M_Z^2) \log(s/M^2) + \log^2(M_Z^2/M^2)$, where the Z -mass dependent logarithm of the second term would fix the initial condition ξ . In this way, non-negligible masses different to the cutoff mass can be implemented in the evolution equation approach, without spoiling the infrared structure.

While the Sudakov logarithms factorize with respect to the Lorentz structure of the Born amplitude, this does not necessarily hold for the non-logarithmic constant part. It is because of this non-factorization that we take the solution of the evolution equation where \mathcal{A} is a vector in isospin space and process

it to the cross section. Expanding the cross section in the $\overline{\text{MS}}$ renormalized coupling α yields

$$\left(\frac{d\sigma}{d\Omega}\right) = \left[1 + \left(\frac{\alpha}{4\pi}\right)\delta^{(1)} + \left(\frac{\alpha}{4\pi}\right)^2\delta^{(2)} + \mathcal{O}(\alpha^3)\right] \left(\frac{d\sigma}{d\Omega}\right)_B \quad (3.16)$$

and the following corrections with respect to the Born cross section are obtained

$$\delta^{(1)} = \gamma^{(1)} \log^2\left(\frac{s}{M^2}\right) + 2(\zeta^{(1)} + \xi^{(1)} + \tilde{\chi}^{(1)}) \log\left(\frac{s}{M^2}\right) + \sigma_0^{(1)}. \quad (3.17)$$

Furthermore, we expand the two-loop contribution in leading logarithms up to

$$\delta^{(2)} = \delta_{LL}^{(2)} + \delta_{NLL}^{(2)} + \delta_{NNLL}^{(2)} + \mathcal{O}(N^3 LL), \quad (3.18)$$

where the particular contributions read

$$\begin{aligned} \delta_{LL}^{(2)} &= \frac{1}{2}(\gamma^{(1)})^2 \log^4\left(\frac{s}{M^2}\right), \\ \delta_{NLL}^{(2)} &= \left(2(\zeta^{(1)} + \xi^{(1)} + \tilde{\chi}^{(1)}) - \frac{1}{3}\beta_0\right) \gamma^{(1)} \log^3\left(\frac{s}{M^2}\right), \\ \delta_{NNLL}^{(2)} &= \left[\gamma^{(2)} + 2(\zeta^{(1)} + \xi^{(1)})^2 + 4(\zeta^{(1)} + \xi^{(1)})\tilde{\chi}^{(1)} + (\tilde{\chi}^{(1)})^2 + (\tilde{\chi}^2)^{(1)}\right. \\ &\quad \left. - \beta_0(\zeta^{(1)} + \tilde{\chi}^{(1)}) + \gamma^{(1)}\sigma_0^{(1)}\right] \log^2\left(\frac{s}{M^2}\right). \end{aligned} \quad (3.19)$$

Here, we introduced

$$\tilde{\chi}^{(1)} = \frac{\tilde{\mathcal{A}}_0^\dagger \chi^{(1)} \tilde{\mathcal{A}}_0}{\tilde{\mathcal{A}}_0^\dagger \tilde{\mathcal{A}}_0}, \quad (3.20)$$

which is related to the matrix elements of χ regarding final states transforming according to the fundamental and adjoint representation respectively, such that

$$\begin{aligned} \tilde{\chi}_A^{(1)} &= \chi_{11}^{(1)} + \chi_{31}^{(1)} + \frac{x_-}{x_+} (\chi_{12}^{(1)} + \chi_{32}^{(1)}), \\ (\tilde{\chi}_A^2)^{(1)} &= (\chi_{11}^{(1)})^2 + \chi_{31}^{(1)}\chi_{11}^{(1)} + \chi_{12}^{(1)}\chi_{21}^{(1)} + \chi_{13}^{(1)}\chi_{31}^{(1)} + \chi_{21}^{(1)}\chi_{32}^{(1)} + \chi_{31}^{(1)}\chi_{33}^{(1)} \\ &\quad + \frac{x_-}{x_+} (\chi_{11}^{(1)}\chi_{12}^{(1)} + \chi_{12}^{(1)}\chi_{22}^{(1)} + \chi_{12}^{(1)}\chi_{31}^{(1)} + \chi_{13}^{(1)}\chi_{32}^{(1)} + \chi_{22}^{(1)}\chi_{32}^{(1)} \\ &\quad + \chi_{32}^{(1)}\chi_{33}^{(1)}), \end{aligned} \quad (3.21)$$

$$\begin{aligned} \tilde{\chi}_F^{(1)} &= \chi_{11}^{(1)} + 4\chi_{12}^{(1)}, \\ (\tilde{\chi}_F^2)^{(1)} &= (\chi_{11}^{(1)})^2 + \chi_{12}^{(1)}\chi_{21}^{(1)} + 4(\chi_{11}^{(1)}\chi_{12}^{(1)} + \chi_{22}^{(1)}\chi_{12}^{(1)}). \end{aligned} \quad (3.22)$$

For clarity we omitted the indices F and A in the matrix elements. The matrix elements on the right hand side refer to eq. 3.14 for $\tilde{\chi}_F$ and to eq. 3.15 for $\tilde{\chi}_A$.

We should emphasize that we have switched from Euclidian momentum Q^2 to the center of mass energy squared s . Note that the one-loop constant $\sigma_0^{(1)}$ is altered according to $\sigma_0^{(1)} = \mathcal{A}_0^{(1)} \mathcal{A}_B^* + \mathcal{A}_0^{(1)*} \mathcal{A}_B - \pi^2 \gamma^{(1)} - 2i\pi \Im[\chi^{(1)}]$ due to the evaluation of the imaginary part of the Sudakov logarithms $\log(-s/M^2)$. Higher order corrections can be easily obtained by an adequate expansion of eqs. 3.4 and 3.5.

Within this framework, one can evaluate the leading logarithmic corrections in all orders of perturbation with little input. The LL approximation includes all the terms of the form $\alpha^n \log^{2n}(Q^2/M^2)$ and is determined by the one-loop value of $\gamma(\alpha)$. The NLL approximation includes all the terms of the form $\alpha^n \log^{2n-m}(Q^2/M^2)$ with $m = 0, 1$. This requires the one-loop values of $\gamma(\alpha)$, $\zeta(\alpha)$, $\xi(\alpha)$ and the one-loop running of α in $\gamma(\alpha)$. The NNLL approximation includes all the terms of the form $\alpha^n \log^{2n-m}(Q^2/M^2)$ with $m = 0, 1, 2$. In this case, $\gamma(\alpha)$ is required up to $\mathcal{O}(\alpha^2)$, $\zeta(\alpha)$, $\xi(\alpha)$, $\chi(\alpha)$ and $\mathcal{A}_0(\alpha)$ up to $\mathcal{O}(\alpha)$ together with the one-loop running of α in $\gamma(\alpha)$, $\zeta(\alpha)$ and $\chi(\alpha)$. The only two-loop value needed is $\gamma^{(2)}$, which was calculated for the fermion form factor ,i.e. the vertex of a fermion current coupling to a vector field, in [24]

$$\gamma_{f\bar{f}}^{(2)} = -2C_F \left[\left(\frac{67}{9} - \frac{\pi^2}{3} \right) C_A - \frac{4}{9}(5n_f + 2n_s)T_F \right], \quad (3.23)$$

where the n_f is the number of (light) fermions and n_s is the number of scalar multiplets.

To calculate the two-loop value of γ for a pair of external gauge bosons, one has to exchange the Casimir operator of the fundamental representation by the one of the adjoint representation, whereas the one for external Goldstone bosons is the same as for external fermions,

$$\begin{aligned} \gamma_{V^\dagger V}^{(2)} &= (C_A/C_F) \gamma_{f\bar{f}}^{(2)}, \\ \gamma_{\phi^\dagger \phi}^{(2)} &= \gamma_{f\bar{f}}^{(2)}. \end{aligned} \quad (3.24)$$

The leading order expansion of the β -function required for the NNLL expansion reads

$$\beta_0 = \frac{11}{3}C_A - \frac{4}{3}T_F n_f - \frac{1}{3}T_F n_s. \quad (3.25)$$

While the one-loop expansion of the coefficients of leading logarithms $\gamma^{(1)}$ and $\zeta^{(1)}$, as well as the matrix of soft anomalous dimension $\chi^{(1)}$, are known

for arbitrary ($2 \rightarrow 2$) processes, this is not true for $\xi^{(1)}$ and $\sigma_0^{(1)}$. To determine these coefficients an explicit one-loop calculation is necessary. Now, having all the necessary components to construct the two-loop NNLL corrections on the basis of a one-loop calculation, let us turn to some toy model examples. The evolution equation approach was applied to the four fermion process quite intensively. For readers interested in that reaction we refer to the corresponding literature [12, 13, 14] and do not discuss this reaction in the framework of this thesis. It is, however, quite similar to the production of scalar bosons, which is discussed in the following section, due to its similar isospin structure.

3.2 Gauge Boson Pair Production in $U(1)$ and $SU(2)$ Models

In this section we investigate radiative corrections in a spontaneously broken $U(1)$ theory and an $SU(2)$ theory for the massive gauge boson pair production in e^+e^- collisions. We work in the high energy limit where all the kinematic invariants are much greater than the gauge boson mass. All fermions are assumed to be massless. Due to helicity conservation a pair of either transverse or longitudinally polarized gauge bosons can be produced in the high energy limit. The transverse gauge bosons transform according to the adjoint representation while the longitudinal gauge bosons, as a consequence of the Goldstone boson equivalence theorem, behave like scalar particles in the fundamental representation. The structure of the Sudakov logarithms in these cases is significantly different and we consider them separately.

We work within the 't Hooft-Feynman gauge and use dimensional regularization to handle UV structure, adopting the $\overline{\text{MS}}$ renormalization scheme. The $\overline{\text{MS}}$ renormalization scale μ is set to M for the transverse part and to \sqrt{s} for the longitudinal part. It is assumed that the mass of the Higgs boson is the same as the mass of the gauge boson(s). First, we demonstrate how to obtain the two-loop next-to-next-to-leading logarithmic corrections in an Abelian toy model and subsequently in the non-Abelian $SU(2)$ theory. The results are presented in a power series with respect to the corresponding coupling, namely

$$\delta_{U(1)} = \sum_n \left(\frac{\alpha_Y}{4\pi} \right)^n \delta_{U(1)}^{(n)}, \quad (3.26)$$

$$\delta_{SU(2)} = \sum_n \left(\frac{\alpha_w}{4\pi} \right)^n \delta_{SU(2)}^{(n)}, \quad (3.27)$$

where $\alpha_Y = \frac{g'^2}{4\pi}$ and $\alpha_w = \frac{g^2}{4\pi}$.

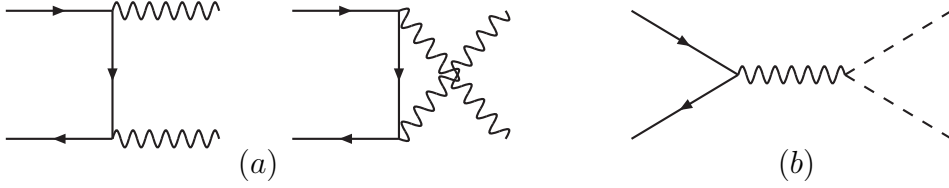


Figure 3.1: These diagrams represent (a) transverse and (b) longitudinal gauge boson pair production in fermion-antifermion annihilation at high energy in the Born approximation.

Let us now consider the hypercharge $U(1)$ correction to the pair production of scalar bosons charged under $U(1)$. The corresponding Feynman rules and quantum charges can be found in appendices A.5 and A.3. We only consider left-handed initial states like for the case of electroweak corrections. This basically corresponds the production of electroweak Goldstone bosons related to the W -bosons. Here, the expansion parameter α is related the hypercharge coupling. The Born cross section for polarized left-handed initial states reads

$$\frac{d\sigma_{-,L}^B}{d\Omega} = \alpha_Y^2(s) \frac{x_+ x_-}{16s}. \quad (3.28)$$

For the one-loop correction we obtain

$$\begin{aligned} \delta_{U(1),L}^{(1)} = & -\log^2\left(\frac{s}{M^2}\right) + \left(2\log\left(\frac{x_+}{x_-}\right) + \frac{7}{2}\right)\log\left(\frac{s}{M^2}\right) \\ & - \frac{1}{2x_+}\log^2(x_-) + \frac{1}{2x_-}\log^2(x_+) - \frac{697}{36} - \frac{17\pi}{3\sqrt{3}} + \frac{5\pi^2}{9}. \end{aligned} \quad (3.29)$$

The anomalous dimension coefficients can be read from this result to be

$$\gamma_{U(1),L}^{(1)} = -1, \quad \zeta_{U(1),L}^{(1)} = \frac{7}{4}, \quad \xi_{U(1),L}^{(1)} = 0 \quad \text{and} \quad \chi_{U(1),L}^{(1)} = \log\left(\frac{x_+}{x_-}\right),$$

while $\sigma_{0U(1),L}^{(1)}$ is given by eq. (3.29) setting $\log(s/M^2) \rightarrow 0$. Note that the soft anomalous dimension χ is scalar for Abelian theories. In addition one needs β_0 and $\gamma^{(2)}$. The hypercharge beta function is $\beta_0 = -\frac{41}{6}$. The two-loop coefficient $\gamma_{U(1),L}^{(2)} = \frac{416}{9}$ is obtained from eq. (3.23). One has to take care implementing the number of fermions in β_0 and $\gamma^{(2)}$, as discussed in appendix A.4.

Plugging these values into the two-loop NNLL expansion, one obtains

$$\delta_{U(1),L}^{(2)} = \frac{1}{2}\log^4\left(\frac{s}{M^2}\right) + \left(2\log\left(\frac{x_+}{x_-}\right) - \frac{52}{9}\right)\log^3\left(\frac{s}{M^2}\right)$$

$$\begin{aligned}
& + \left[\frac{1}{2x_+} \log^2(x_-) - \frac{1}{2x_-} \log^2(x_+) + 2 \log^2\left(\frac{x_+}{x_-}\right) + \frac{83}{6} \log\left(\frac{x_+}{x_-}\right) \right. \\
& \left. + \frac{389}{9} + \frac{17\pi}{3\sqrt{3}} - \frac{5\pi^2}{9} \right] \log^2\left(\frac{s}{M^2}\right) + \mathcal{O}(N^3LL). \quad (3.30)
\end{aligned}$$

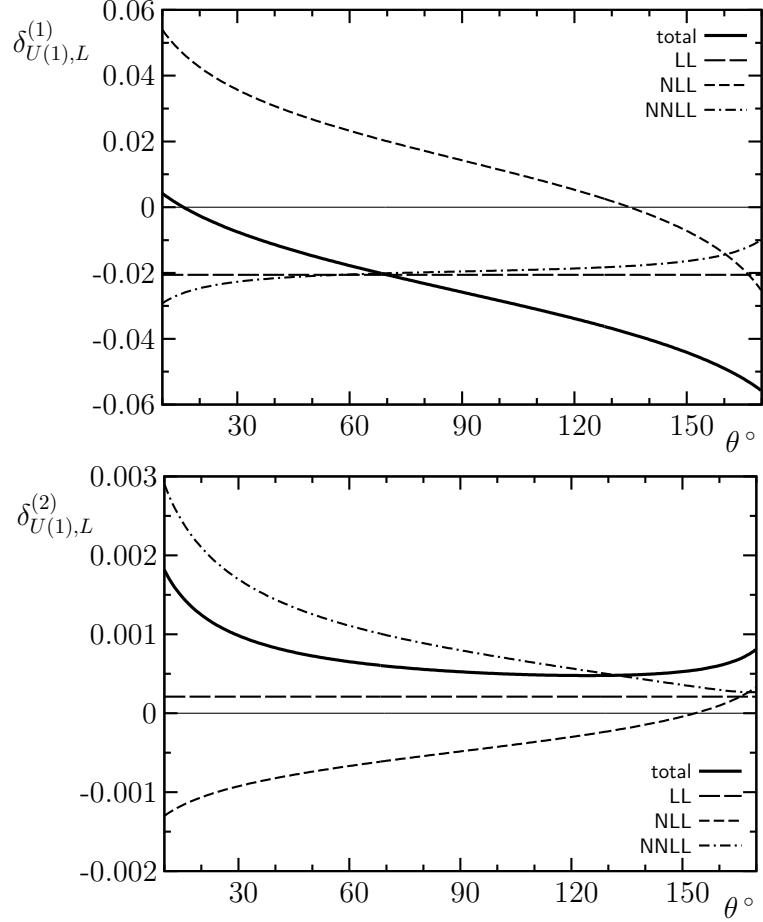


Figure 3.2: The one-loop and two-loop $U(1)_Y$ corrections to the differential cross section relative to the Born approximation for the production of scalar bosons at $\sqrt{s} = 1$ TeV.

To apply the evolution equation approach to the production of transversely polarized gauge bosons, we do not restrict ourselves to a pure Abelian Theory. Since we want to mimic the W -pair production, we adopt the electroweak Born cross section eq. 2.12 and calculate the hypercharge $U(1)$ correction to this process. The procedure works similar to the treatment of longitudinal

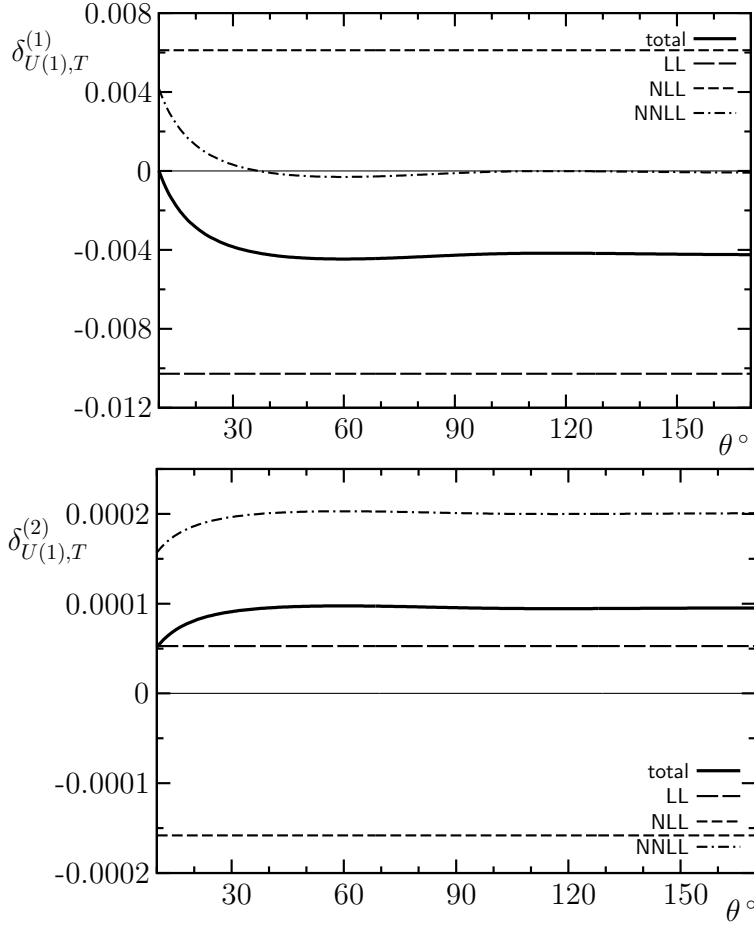


Figure 3.3: The one-loop and two-loop $U(1)_Y$ corrections to the differential cross section relative to the Born approximation for the production of transversely polarized W bosons at $\sqrt{s} = 1$ TeV.

polarization, and we obtain

$$\gamma_{U(1),T}^{(1)} = -\frac{1}{2}, \quad \zeta_{U(1),T}^{(1)} = \frac{3}{4}, \quad \xi_{U(1),T}^{(1)} = 0, \quad \chi_{U(1),T}^{(1)} = 0 \quad \text{and} \quad \gamma_T^{(2)} = \frac{52}{9}.$$

The corrections to the differential cross sections read

$$\begin{aligned} \delta_{U(1),T}^{(1)} &= -\frac{1}{2} \log^2 \left(\frac{s}{M^2} \right) + \frac{3}{2} \log \left(\frac{s}{M^2} \right) + \left(\frac{3x_- - 1}{2(x_-^2 + x_+^2)} + \frac{1}{x_+} \right) \log^2(x_-) \\ &\quad - \frac{x_- - 3}{2(x_-^2 + x_+^2)} \log(x_-) + \frac{x_+}{2(x_-^2 + x_+^2)} + \frac{\pi^2}{6} - \frac{7}{4}. \end{aligned} \quad (3.31)$$

$$\delta_{U(1),T}^{(2)} = \frac{1}{8} \log^4 \left(\frac{s}{M^2} \right) - \frac{17}{9} \log^3 \left(\frac{s}{M^2} \right) + \left[\left(\frac{1 - 3x_-}{4(x_-^2 + x_+^2)} + \frac{1}{2x_+} \right) \log^2(x_-) \right]$$

$$\begin{aligned}
& + \frac{x_- - 3}{4(x_-^2 + x_+^2)} \log(x_-) - \frac{x_+}{4(x_-^2 + x_+^2)} - \frac{\pi^2}{12} + \frac{929}{72} \Big] \log^2\left(\frac{s}{M^2}\right) \\
& + \mathcal{O}(N^3 LL). \tag{3.32}
\end{aligned}$$

Again, the constant $\sigma_{0U(1),T}^{(1)}$ can be read from the one-loop correction eq. 3.31.

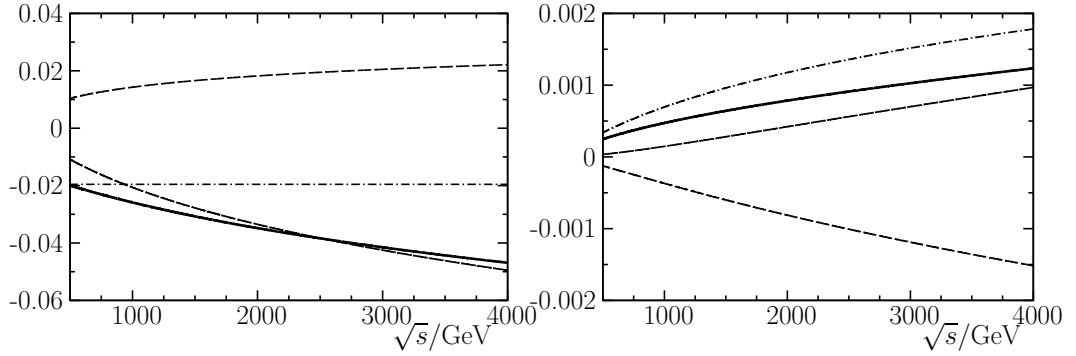


Figure 3.4: The one-loop (left diagram) and two-loop (right diagram) $U(1)_Y$ corrections to the total cross section relative to the Born approximation for the production of scalar bosons. The long-dashed, short-dashed and dot-dashed lines denote the LL, NLL and NNLL corrections, as defined in the legend of figs. 3.2, 3.3

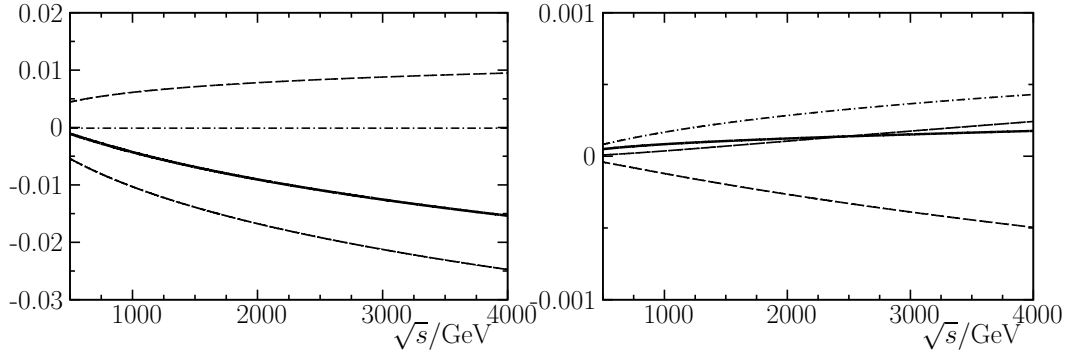


Figure 3.5: The same as fig. 3.4 but for the transverse case.

The mass of the gauge boson is set to the W -mass $M = 80.41\text{GeV}$. In this simple example of the production of scalar bosons one can observe the cancellation of subleading logarithms. This feature will emerge also in electroweak corrections.

The $U(1)$ corrections to the production of a pair of transversely polarized W -bosons barely show an angular dependence. This is because the angular

variables enter through box diagrams and, due to the non-coupling of the $U(1)$ gauge boson to the external W -bosons, the only box diagram which contributes is the one where the gauge boson is exchanged between the two initial state fermions.

Now let us examine radiative corrections in the spontaneously broken $SU(2)$ model, which comes close to the real world since the radiative corrections within the Electroweak Standard Model are dominated by the $SU(2)$ gauge group. Basically, the only difference with regards to the $U(1)$ correction is the matrix structure of the reduced amplitude.

For this model, we do not perform a calculation, rather we extract the $SU(2)$ coefficients from the full electroweak calculation by taking the $SU(2)$ limit of the corresponding correction. The same procedure is applied to the $U(1)$ limit reproducing the $U(1)$ corrections presented above. For the transverse part we obtain

$$\begin{aligned}
\delta_{SU(2),T}^{(1)} = & -\frac{11}{2}\log^2\left(\frac{s}{M^2}\right) \\
& + \left[\left(-8 + \frac{4x_-}{x_+}\right)\log(x_-) + 4\log(x_+) + \frac{9}{2} \right] \log\left(\frac{s}{M^2}\right) \\
& + \left(\frac{5 + 3x_-}{2(x_-^2 + x_+^2)} - \frac{5}{x_+} \right) \log^2(x_-) + \frac{3x_-}{x_-^2 + x_+^2} \log(x_+^2) \\
& + \frac{4}{x_+} \log(x_-) \log(x_+) + \left(\frac{9 - 19x_-}{2(x_-^2 + x_+^2)} \right) \log(x_-) - \frac{5x_+}{2(x_-^2 + x_+^2)} \\
& - \frac{7\pi^2}{18} - \frac{13\pi}{3\sqrt{3}} - \frac{25}{36}, \tag{3.33}
\end{aligned}$$

$$\begin{aligned}
\delta_{SU(2),T}^{(2)} = & \frac{121}{8}\log^4\left(\frac{s}{M^2}\right) \\
& + \left[\left(44 - \frac{22x_-}{x_+}\right)\log(x_-) - 22\log(x_+) - \frac{341}{18} \right] \log^3\left(\frac{s}{M^2}\right) \\
& + \left[\left(32 + \frac{4x_-^2}{x_+^2} - \frac{55 + 33x_-}{4(x_-^2 + x_+^2)} + \frac{55 - 40x_-}{2x_+} \right) \log^2(x_-) \right. \\
& - \left. \left(28 + \frac{22 - 4x_-}{x_+}\right)\log(x_-)\log(x_+) + \frac{35}{3}\log(x_+) \right. \\
& + \left. \left(-\frac{70}{3} + \frac{35x_-}{3x_+} - \frac{99 - 209x_-}{4(x_-^2 + x_+^2)}\right)\log(x_-) \right. \\
& + \left. \left(8 - \frac{33x_-}{2(x_-^2 + x_+^2)}\right)\log^2(x_+) + \frac{55x_+}{4(x_-^2 + x_+^2)} + \frac{209\pi^2}{36} \right]
\end{aligned}$$

$$+\frac{143\pi}{6\sqrt{3}} - \frac{863}{24}] \log^2\left(\frac{s}{M^2}\right) s + \mathcal{O}(N^3 LL), \quad (3.34)$$

where the coefficients of soft anomalous dimensions derived from the one-loop calculation are

$$\gamma_{SU(2),T}^{(1)} = -\frac{11}{2}, \quad \zeta_{SU(2),T}^{(1)} = \frac{9}{4}, \quad \xi_{SU(2),T}^{(1)} = 0 \quad (3.35)$$

and $\sigma_{0,SU(2),T}^{(1)}$ corresponds to the part of eq. 3.33 involving no Sudakov logarithms $\log(s/M^2)$. The method for obtaining $\tilde{\chi}$ is discussed in the previous section. For the transverse case they take the form

$$\begin{aligned} \tilde{\chi}_{SU(2),T}^{(1)} &= -4 \log(x_-) + 2 \frac{x_-}{x_+} \log(x_-) + 2 \log(x_+), \\ (\tilde{\chi}^2)_{SU(2),T}^{(1)} &= 16 \log^2(x_-) - 8 \log(x_+) \log(x_-) - 8 \frac{x_-}{x_+} \log(x_+) \log(x_-) \\ &\quad + 8 \frac{x_-}{x_+} \log\left(\frac{x_+}{x_-}\right) \log(x_-) + 4 \log(x_+) \log\left(\frac{x_+}{x_-}\right). \end{aligned} \quad (3.36)$$

The coefficients needed for the two-loop corrections read

$$\gamma_{SU(2),T}^{(2)} = -\frac{385}{9} + \frac{11}{3}\pi^2, \quad \beta_0 = \frac{19}{6}, \quad (3.37)$$

and are obtained from eqs. 3.23 and 3.25 with $C_A = 2$ and $C_F = 3/4$.

For the longitudinal part we find

$$\begin{aligned} \delta_{SU(2),L}^{(1)} &= -3 \log^2\left(\frac{s}{M^2}\right) + \left[-10 \log(x_-) + 2 \log(x_+) + \frac{21}{2}\right] \log\left(\frac{s}{M^2}\right) \\ &\quad - \frac{5}{2x_+} \log^2(x_-) + \frac{1}{2x_-} \log^2(x_+) - \frac{7\pi^2}{3} + \frac{32\pi}{3\sqrt{3}} - \frac{505}{36}, \end{aligned} \quad (3.38)$$

$$\begin{aligned} \delta_{SU(2),L}^{(2)} &= \frac{9}{2} \log^4\left(\frac{s}{M^2}\right) + \left[30 \log(x_-) - 6 \log(x_+) - \frac{85}{3}\right] \log^3\left(\frac{s}{M^2}\right) \\ &\quad + \left[\left(38 + \frac{15}{2x_+}\right) \log^2(x_-) + \left(2 - \frac{3}{2x_-}\right) \log^2(x_+)\right] \\ &\quad - 8 \log(x_-) \log(x_+) - \frac{535}{6} \log(x_-) + \frac{107}{6} \log(x_+) + 9\pi^2 \\ &\quad - \left[\frac{32\pi}{\sqrt{3}} + \frac{229}{4}\right] \log^2\left(\frac{s}{M^2}\right) + \mathcal{O}(N^3 LL), \end{aligned} \quad (3.39)$$

where the corresponding coefficients are given by

$$\gamma_{SU(2),L}^{(1)} = -3, \quad \zeta_{SU(2),L}^{(1)} = \frac{21}{4}, \quad \xi_{SU(2),L}^{(1)} = 0, \quad \gamma_{SU(2),L}^{(2)} = -\frac{70}{3} + 2\pi^2 \quad (3.40)$$

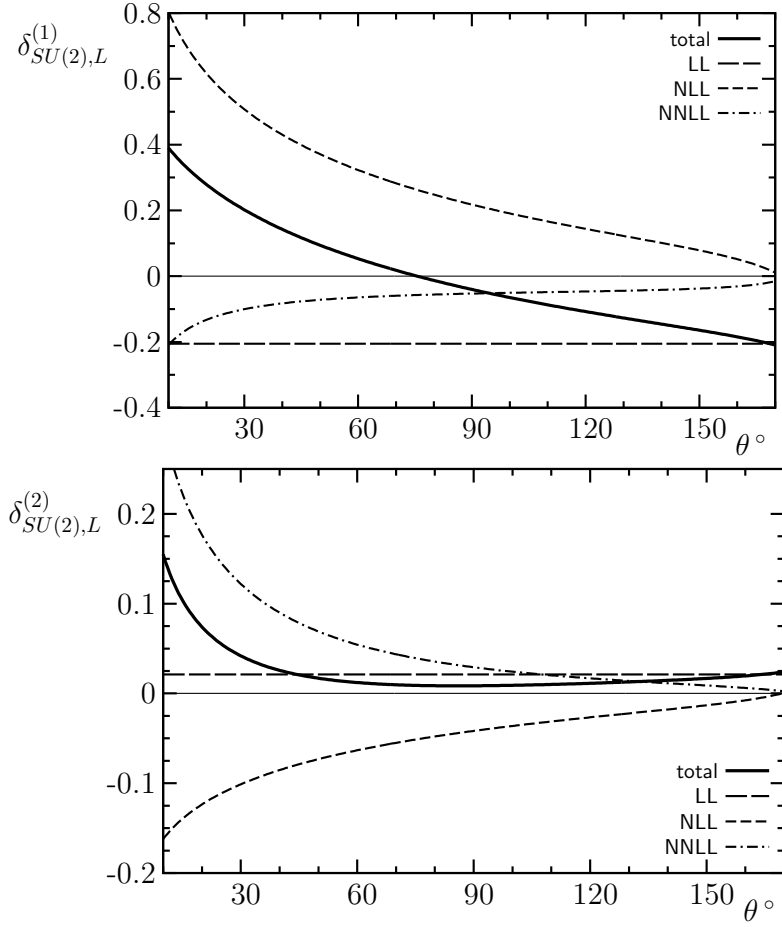


Figure 3.6: The one-loop and two-loop $SU(2)$ corrections to the differential cross section relative to the Born approximation for the production of scalar bosons at $\sqrt{s} = 1$ TeV.

and $\sigma_{0,SU(2),L}^{(1)}$ can be read from eq. 3.33. The coefficients of the matrix of soft anomalous dimensions read

$$\begin{aligned}
 \tilde{\chi}_{SU(2),L}^{(1)} &= 5 \log\left(\frac{x_+}{x_-}\right) - 4(\log(x_+) + i\pi), \\
 (\tilde{\chi}^2)_{SU(2),L}^{(1)} &= 13 \log^2\left(\frac{x_+}{x_-}\right) - 28 \log\left(\frac{x_+}{x_-}\right) \log(x_+) + 16 \log^2(x_+) - 16\pi^2 \\
 &\quad - i\pi \left(28 \log\left(\frac{x_+}{x_-}\right) - 32 \log(x_+) \right). \tag{3.41}
 \end{aligned}$$

The $SU(2)$ corrections to the W -pair production exceed the $U(1)$ correction

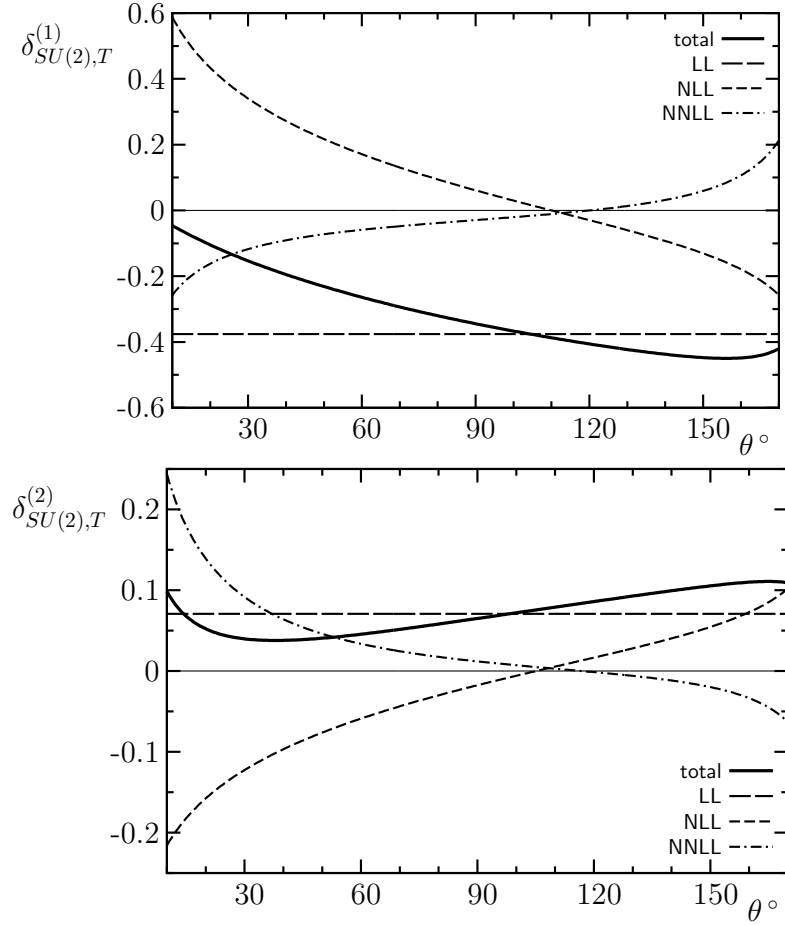


Figure 3.7: The one-loop and two-loop $SU(2)$ corrections to the differential cross section relative to the Born approximation for the production of transversely polarized W bosons at $\sqrt{s} = 1$ TeV.

by several factors. It is, therefore, expected that the $SU(2)$ corrections dominate the electroweak corrections. While both the $U(1)$ and $SU(2)$ corrections show similar behaviour, up to some factor, for the production of a pair of scalar bosons, this is not the case for the production of a pair of transversely polarized W -bosons. This is because the $U(1)$ gauge boson does not couple to the external W -bosons.

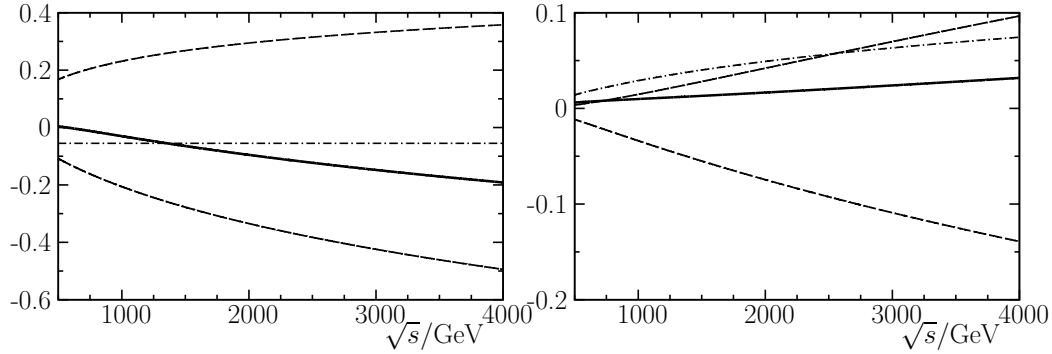


Figure 3.8: The one-loop (left diagram) and two-loop (right diagram) $SU(2)$ corrections to the total cross section relative to the Born approximation for the production of scalar bosons. The long-dashed, short-dashed and dot-dashed lines denote the LL, NLL and NNLL corrections, as defined in the legend of figs. 3.6, 3.7

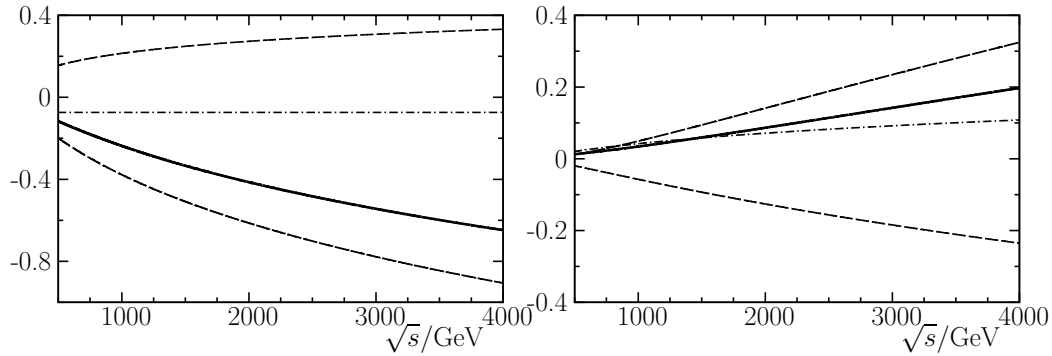


Figure 3.9: The same as fig. 3.4 but for the transverse case.

Now, having illustrated how to work with the evolution equation approach in an $U(1)$ and a $SU(2)$ theory, let us compete with electroweak corrections. However, to transfer this approach to the Electroweak Standard Model is not straightforward. In the next section it is shown how to handle this approach within the standard model.

3.3 Evolution Equations in the Electroweak Standard Model

We are interested in the electroweak Sudakov logarithmic enhanced corrections. Yet, the evolution equation approach introduced in section 3.1 cannot be directly applied to electroweak corrections because the Z boson and the photon are a mixture of W_μ^3 , pure $SU(2)_L$, and B_μ , the Abelian hypercharge components. In this section we demonstrate how to circumvent this issue and how to work with the infrared evolution equation in the spontaneously broken Electroweak Standard Model.

The concept of evolution equations in the context of the electroweak corrections was first introduced in [11] for the resummation of double logarithms. Successively, it was extended to subleading logarithms for the fermion pair production in ref. [12, 13, 14]. The approach of the latter references basically extends to the gauge boson pair production as briefly described below. The only potential subtlety in the analysis of gauge boson production is that the effects of spontaneous symmetry breaking can change the asymptotic states as it happens with photon and Z -boson in the standard model. This would require additional consideration. We restrict the analysis to the production of W -bosons which have the same gauge quantum numbers in broken and symmetric phases and do not encounter this problem.

The electroweak Standard Model with the spontaneously broken $SU_L(2) \times U(1)$ gauge group involves the massive W and Z bosons and the massless photon. The corrections to fully exclusive cross sections are infrared divergent due to virtual photon exchange and should be combined with soft real photon emission to obtain infrared finite physical observables.

We want to identify the logarithms related to exchange of only the massive gauge bosons and, therefore, have to separate pure QED logarithms. However, the mixing effect which leads to the mass gap of the neutral gauge bosons involves difficulties, which are circumvented by considering two different regimes regarding the lower bound of the integration of the solution of the evolution equation. For $\sqrt{s} \gg \mu \gg M_W$, the effects of spontaneous symmetry breaking and, in particular, gauge boson masses can be neglected. Hence one may work with the hard evolution equation in terms of effectively massless gauge fields B_μ and W_μ^a of the symmetric phase $SU(2) \times U(1)_Y$.

To get the desired result one also has to consider the region in which the lower bound of the integration is $\mu \ll M_W$. In this regime, only the electromagnetic part contributes and μ can be identified as the artificial photon mass λ . These

two regimes have to be matched at $\mu = M$. Therefore, to derive the pure electroweak corrections related to Sudakov logarithms originating from W - and Z -boson exchange, the electromagnetic corrections have to be subtracted from the corrections in the symmetric phase with $\lambda = M_W$.

Let us clarify this approach by considering the example of only leading logarithmic corrections. In the first regime $|Q| \gg \mu \gg M_W$, the solution of the evolution equation takes the form

$$\mathcal{A}_{\mu \gg M_W}^{LL}(Q, \mu) = \exp \left[-\frac{1}{2} \sum_i \left(\frac{\alpha_w}{4\pi} C_i^{SU(2)} + \frac{\alpha_Y}{4\pi} \left(\frac{Y_i}{2} \right)^2 \right) \log^2 \left(\frac{Q^2}{\mu^2} \right) \right] \mathcal{A}_{\text{Born}}, \quad (3.42)$$

where the sum i runs over all external particles, and $C_i^{SU(2)} = (C_F, C_A)$ for particles transforming under the fundamental or the adjoint representation respectively. The initial condition is fixed according to $\mathcal{A}^{LL}|_{\mu^2=s} = \mathcal{A}_{\text{Born}}$. In the second regime the evolution equation reads

$$\frac{\partial}{\partial \log(\mu^2)} \mathcal{A}_{\mu \ll M_W}^{LL}(Q, \mu) = \frac{\alpha}{4\pi} \sum_i Q_i^2 \log^2 \left(\frac{Q^2}{\mu^2} \right) \mathcal{A}_{\mu \ll M_W}^{LL}(Q, \mu). \quad (3.43)$$

Here, the appropriate initial condition is fixed by matching the two regimes at $\mu = M_W$, such that the solution of the latter differential equation is

$$\begin{aligned} \mathcal{A}_{\mu \ll M_W}^{LL}(Q, \mu) = & \exp \left[-\frac{1}{2} \sum_i \left(\frac{\alpha_w}{4\pi} C_i^{SU(2)} + \frac{\alpha_Y}{4\pi} \left(\frac{Y_i}{2} \right)^2 - \frac{\alpha}{4\pi} Q_i^2 \right) \log^2 \left(\frac{Q^2}{M_W^2} \right) \right] \\ & \times \exp \left[\frac{1}{2} \frac{\alpha}{4\pi} \sum_i Q_i^2 \log^2 \left(\frac{Q^2}{\mu^2} \right) \right] \mathcal{A}_{\text{Born}} \end{aligned} \quad (3.44)$$

The first exponential function corresponds to the resummation of Sudakov double logarithms related to W and Z exchange, while the second exponential function represents the pure QED double logarithmic correction. Note that the latter equations in this example are actually only correct as presented if the masses of external particles are smaller than μ , otherwise the mass of an heavy external particles would act as a natural cutoff in the integration.

To disentangle the electroweak and QED logarithms we use the approach of ref. [11, 13, 14]. While the dependence of the amplitudes on the large momentum transfer is governed by the hard evolution equations (see eqs. (3.2, 3.3)), their dependence on the photon mass is governed by the infrared evolution equations [11]. In the limit $\lambda^2 \ll M_W^2$, $m_t^2 \ll Q^2$ the infrared evolution equations in the full theory are the same as in QED. To formulate this approach with respect to the amplitude $\mathcal{A}(Q, M_W, \lambda)$, related to the full Electroweak

Standard Model, we introduce the factor $\mathcal{U}_{\text{QED}}(Q, \lambda, M_W)$, which refers to all virtual electromagnetic correction, such that the amplitude can be split according to

$$\mathcal{A}(Q, M_W, \lambda) = \mathcal{A}_{\text{EW}}(Q, M_W) \mathcal{U}_{\text{QED}}(Q, \lambda, M_W) + \mathcal{O}(\lambda/M_W), \quad (3.45)$$

where the electroweak amplitude $\mathcal{A}_{\text{EW}}(Q, M_W)$ we are interested in contains the electroweak logarithms $\log(Q^2/M_W^2)$ related to W^\pm and Z exchange and reads

$$\mathcal{A}_{\text{EW}}(Q, M_W) = \mathcal{A}(Q, M_W) \mathcal{U}_{\text{QED}}^{-1}(Q, \lambda, M_W) + \mathcal{O}(\lambda/M_W). \quad (3.46)$$

The QED factor $\mathcal{U}_{\text{QED}}(Q, \lambda, M_W)$ obeys the infrared evolution equation governing the λ -dependence of the virtual QED corrections. It contains the virtual electromagnetic logarithms $\log(Q^2/\lambda^2)$ and eventually also $\log(Q^2/M_W^2)$ of electromagnetic origin which cancel against the real corrections. The dependence of the weak scale M_W in \mathcal{U}_{QED} appears only if the process considered involves heavy external gauge bosons. It is convenient to normalize $\mathcal{U}_{\text{QED}}(Q, \lambda, M_W)$ according to $\mathcal{U}_{\text{QED}}(M_W, M_W, M_W) = 1$ such that it is of pure exponential nature. In that case a QED subtraction is not necessary for $\tilde{\mathcal{A}}_0$.

It is worth noting at this point that, up to next-to-leading logarithmic corrections, the electroweak amplitude $\mathcal{A}_{\text{EW}}(Q, M_W)$ can be related to either the amplitude of the Electroweak Standard Model or to the amplitude in the symmetric phase \mathcal{A}_{sym} , such that

$$\mathcal{A}_{\text{EW}}(Q, M_W) = \mathcal{A}_{\text{sym}}(Q, M_W) \mathcal{U}_{\text{QED}}^{-1}(Q, M_W, M_W). \quad (3.47)$$

Here, $\mathcal{A}_{\text{sym}}(Q, M_W)$ represents the amplitude derived within the symmetric phase with all particles having the same mass M_W . For NNLL corrections the one-loop constant comes into play, which in general contributes to both the symmetric phase and the QED part. Therefore eq. 3.46 is the adequate approach compatible with the initial condition $\mathcal{U}_{\text{QED}}(M_W, M_W, M_W) = 1$, since the initial condition of eq. 3.47 reads $\mathcal{A}_{\text{EW}}(M_W, M_W) = \tilde{\mathcal{A}}_{0,\text{sym}}$. For massless external states, however, the constant $\tilde{\mathcal{A}}_0$ does not involve any QED contribution and eqs. 3.46 and 3.47 become equivalent, as it is the case for the four fermion process [12, 13, 14].

The infrared evolution equation related to \mathcal{U}_{QED} can be dealt with independently. This part, however, is infrared divergent and the corresponding real corrections accompanied by real soft photon radiation integrated to some resolution energy E_{res} have to be included to obtain an infrared safe cross

section independent on an auxiliary photon mass. For the detector resolution $E_{res} \ll M$, the soft photon emission is of pure QED nature. Therefore, the kernel of infrared evolution is essentially Abelian. The proper inclusive corrections should be derived within Monte Carlo routines providing an adequate cancelation of the infrared divergence. We, however, restrict ourselves in this framework to exclusive corrections. Note that the \mathcal{U}_{QED} factor contains only logarithmic contributions and the constant is completely incorporated in \mathcal{A}_{EW} .

So far we have assumed that $M_Z = M_W$ and fermion masses $m_f = 0$. For the full electroweak corrections, we incorporate the mass hierarchy

$$\sqrt{s} \gg M_W \neq M_Z \neq M_H \neq m_t \neq 0. \quad (3.48)$$

To implement, for example, $M_Z \neq M_W$ one simply replaces the Sudakov logarithms originating from Z exchange $\log(Q^2/M_Z^2)$ by $\log(M_Z^2/M_W^2)$ and $\log(Q^2/M_W^2)$, which governs the dynamic of the evolution equation. At one-loop level, the double logarithm $\log^2(Q^2/M_Z^2)$ leads to a contribution of the form $\log(M_Z^2/M_W^2) \log(Q^2/M_W^2)$ which fixes the initial condition $\xi^{(1)}$ and $\log(M_Z^2/M_W^2)$, originating from the single logarithm $\log(Q^2/M_Z^2)$ is fixed by adjusting $\tilde{\mathcal{A}}_0^{(1)}$. The implementation of the top quark mass is more subtle and will be discussed in section 4.2.

Chapter 4

W -Pair Production in e^+e^- Annihilation (ILC)

In this chapter we discuss the virtual electroweak one-loop and leading two-loop corrections to W -pair production in e^+e^- annihilation in the high energy approximation. The reaction $e^+e^- \rightarrow W^+W^-$ provides an important precision test of the Electroweak Standard Model due to the W -boson being the only particle which interacts solely with $SU(2)$ couplings. In particular, processes where W -bosons participate are the only reaction within the standard model involving triple gauge boson couplings. Therefore, accurate predictions and measurements regarding W -pair production are highly desirable. Radiative corrections to W -pair production in e^+e^- collisions have been covered quite intensively. Exclusive and inclusive electroweak one-loop corrections can be found for example in [25, 26, 27, 21]. For the complete process one has to take into account the decay of the W -bosons which yields a four fermions final state. However, such a process where only W -bosons as intermediate states are considered is not gauge invariant and all possible intermediate states have to be included. The complete process with a four fermions final state is presented in [28].

We, however, restrict ourselves to one-loop corrections to on-shell W -pair production and to process this result by means of evolution equations in order to estimate the leading contributions at two-loop level. To consider the production of on-shell W -bosons and subsequently including the decay of the W -bosons is the dominant contribution to the process with four fermion final states and gives a good approximation of that reaction.

In section 4.1 we show how to obtain the one-loop corrections in a form suitable to process within the evolution equation approach by proper modifications of known results. Subsequently, we discuss these one-loop corrections

derived in an independent calculation and why there is a slight difference with respect to the first approach. In section 4.2 we give the coefficients of the solution of the evolution equation obtained by one-loop calculations and present the electroweak two-loop corrections up to next-to-next-to-leading logarithms at two-loop level.

4.1 One-Loop Corrections

In this section we shall discuss the electroweak virtual one-loop corrections to the on-shell W -pair production in electron-positron colliders in the high energy approximation where all kinematic invariants s , t and u are much larger than any mass.

These corrections are derived in two independent ways. On one hand, we use the results of a one-loop calculation performed by Beenakker et al. [21]. We adopt their result and transform it into a form suitable for our approach. On the other hand, we perform the one-loop calculation in the high energy approximation both within the $\overline{\text{MS}}$ and the on-shell renormalization scheme. First we present how to transform the result of [21] and afterwards we discuss our calculation. For convenience we present the one-loop results together with the two-loop corrections in section 4.2 .

4.1.1 Approach I: Transformation of Known Results

In our first approach we adopt the one-loop correction to the W -pair production from [21] to derive the coefficients needed for the evolution equation approach. However, this calculation is performed in the on-shell scheme and using an electron mass to regularize collinear singularities while we employ the $\overline{\text{MS}}$ renormalization scheme and use an artificial photon mass to regularize both soft and collinear singularities. Furthermore, they present inclusive corrections, whereas we are interested in exclusive ones. Thus some modifications have to be taken into account which lead to additional contributions to their one-loop correction factor.

The starting point is the inclusive correction with respect to the Born cross section in the on-shell scheme δ_B , presented in [21]. This correction factor is related to the one we use within the evolution equation approach, denoted by $\delta^{(1)}$, by adding proper modification factors

$$\delta^{(1)} = \delta_B + \delta_m + \delta_{\text{RS}} - \delta_{\text{real}} . \quad (4.1)$$

In particular, δ_m accommodates the exchange of the electron mass by the photon mass as a regulator for the collinear singularities. The term δ_{RS} , responsible for changing the renormalization scheme from on-shell to $\overline{\text{MS}}$, basically contains the finite parts of the on-shell counterterms. Finally, the QED real radiation contribution δ_{real} is to be subtracted. Eventually, an additional contribution δ_μ related to a change of the renormalization scale has to be included. While δ_m and δ_{real} are essentially the same for the production of both transverse and longitudinally polarized W -pairs, the term δ_{RS} depends on the structure of the leading order cross section. The precise form of these coefficients is presented at the end of this section. In the following we shall discuss the particular modifications in more detail.

Changing the mass hierarchy δ_m

The authors of [21] used an electron mass to regularize collinear divergences. Therefore, we have to switch the mass hierarchy from $m_e \gg \lambda$ to $\lambda \gg m_e$. This only affects logarithms which are related to external electron legs and do not depend on the topology of the process. Therefore the modification is the same for both the transverse and longitudinal case. To adjust the amplitude we simply consider QED one-loop correction to the fermion form factor (i.e. the vertex of a fermion current coupling to an external vector field) for both mass hierarchies and subtract the corresponding difference.

We calculate the one-loop corrections to the fermion form factor \mathcal{F} with a photon mass λ as sole regulator on one hand and a photon and a fermion mass m on the other. For the one-loop corrections $\mathcal{F}^{(1)}$ given in $\frac{\alpha}{4\pi}$ we have

i) $|Q| \gg \lambda \gg m$:

$$\mathcal{F}_i^{(1)} = -\log^2\left(\frac{Q^2}{\lambda^2}\right) + 3\log\left(\frac{Q^2}{\lambda^2}\right) - \frac{7}{2} - \frac{2\pi^2}{3}, \quad (4.2)$$

ii) $|Q| \gg m \gg \lambda$:

$$\mathcal{F}_{ii}^{(1)} = \log^2\left(\frac{Q^2}{m^2}\right) - 2\log\left(\frac{Q^2}{m^2}\right)\log\left(\frac{Q^2}{\lambda^2}\right) + \log\left(\frac{Q^2}{m^2}\right) + 2\log\left(\frac{Q^2}{\lambda^2}\right) - 4 + \frac{\pi^2}{3}, \quad (4.3)$$

such that

$$\delta_m = \frac{\alpha}{2\pi}(\mathcal{F}_i^{(1)} - \mathcal{F}_{ii}^{(1)}). \quad (4.4)$$

Actually, one may simply replace the fermion masses in the argument of logarithms by the photon mass everywhere (i.e. in δ_B , δ_{real} and δ_m) such that only the non-logarithmic constant in has to be included δ_m , yielding

$$\delta_m|_{m \rightarrow \lambda} = \frac{\alpha}{4\pi}(1 - 2\pi^2). \quad (4.5)$$

Converting the renormalization scheme δ_{RS}

To convert the correction factor of [21] into the five flavour $\overline{\text{MS}}$ scheme we use relations between these two schemes provided in [29, 30, 31]. This scheme transformation affects two parameters, the fine structure constant and the weak mixing angle. For the parameters renormalized in the $\overline{\text{MS}}$ scheme at the scale $\mu = M_Z$ and defined in a five flavour theory we introduce

$$\alpha_{OS} = \alpha_{\overline{\text{MS}}}(1 + \delta_\alpha(M_Z^2)), \quad \alpha_{\overline{\text{MS}}} = \alpha_{\overline{\text{MS}}}^{(5)}(M_Z^2), \quad (4.6)$$

$$\frac{1}{s_{W,OS}^4} = \frac{1}{s_{W,\overline{\text{MS}}}^4}(1 + \delta_s(M_Z^2)), \quad s_{W,\overline{\text{MS}}} = s_{W,\overline{\text{MS}}}^{(5)}(M_Z^2), \quad (4.7)$$

$$\frac{1}{c_{W,OS}^4} = \frac{1}{c_{W,\overline{\text{MS}}}^4} \left(1 - \frac{s_W^2}{c_W^2} \delta_s(M_Z^2) \right), \quad c_{W,\overline{\text{MS}}} = c_{W,\overline{\text{MS}}}^{(5)}(M_Z^2).$$

The scheme transformations of these parameters are directly related to the corresponding counterterms in the on-shell scheme without the UV pole. We only need these transformation formulae at the one-loop level because the two-loop corrections are only approximated up to next-to-next-to-leading logarithms. For the fine structure constant the transformation coefficient reads [29]

$$\delta_\alpha(\mu^2) = -\Pi_{\gamma\gamma}^{(f)}(0) - \frac{\alpha}{4\pi} \left(7 \log \left(\frac{M^2}{\mu^2} \right) - \frac{2}{3} \right), \quad (4.8)$$

where $\Pi^{(f)}$ is the f -flavour fermion contribution to the photon self energy and the latter contribution comes from the bosonic sector. With the fermionic contribution in a five flavour theory given by

$$\Pi_{\gamma\gamma}^{(5)}(0) = -\frac{4}{3} \frac{\alpha}{4\pi} \sum_{f \neq t} N_c Q_f^2 \log \left(\frac{m_f^2}{\mu^2} \right) \quad (4.9)$$

it is

$$\delta_\alpha(M_Z^2) = \frac{\alpha}{4\pi} \left(\Delta\alpha + \frac{17}{9} \log \left(\frac{M_Z^2}{M_W^2} \right) + \frac{2}{3} \right). \quad (4.10)$$

For convenience we adopted

$$\begin{aligned} \Delta\alpha = & \frac{4}{3} \frac{\alpha}{4\pi} \left[\log \left(\frac{m_e^2}{M_W^2} \right) + \log \left(\frac{m_\mu^2}{M_W^2} \right) + \log \left(\frac{m_\tau^2}{M_W^2} \right) + \frac{4}{3} \left(\log \left(\frac{m_u^2}{M_W^2} \right) \right. \right. \\ & \left. \left. + \log \left(\frac{m_c^2}{M_W^2} \right) \right) + \frac{1}{3} \left(\log \left(\frac{m_d^2}{M_W^2} \right) + \log \left(\frac{m_s^2}{M_W^2} \right) + \log \left(\frac{m_b^2}{M_W^2} \right) \right) \right] \end{aligned} \quad (4.11)$$

as introduced in [21]. The renormalization scheme transformation of the fine structure constant is of course the same for the transverse and longitudinal case.

Now let us turn to the transformation coefficient of the weak mixing angle. The transformation from the onshell scheme to the six flavour $\overline{\text{MS}}$ scheme is given by

$$\delta_s^{(6)}(M_Z^2) = 2 \frac{c_W^2}{s_W^2} \text{Re} \left[\frac{\Sigma_{WW}(M_W^2)}{M_W^2} - \frac{\Sigma_{ZZ}(M_Z^2)}{M_Z^2} \right] \quad (4.12)$$

where $\Sigma_{WW}(M_W^2)$ and $\Sigma_{ZZ}(M_Z^2)$ are the W - and Z -boson self energies respectively. The fermionic contributions to these self energies are obtained from [30] and the bosonic contributions are derived from [31]. The analytical values of these contributions are rather lengthy and are not presented here explicitly. However, the mixing angle is still defined in a six flavour theory and one can not entirely decouple the top quark contribution because this breaks $SU(2)$ symmetry. The scheme adopted here only decouples the $\log(m_t^2/M_Z^2)$ contributions from the $\gamma - Z$ mixing. The relation between the five flavour and the six flavour mixing angle is provided in [30] and reads

$$s_W^{2(5)} = s_W^{2(6)} \left(1 + \frac{\alpha}{\pi} d \right), \quad (4.13)$$

where

$$d = \frac{1}{3} \left(\frac{1}{s_W^2} - \frac{8}{3} \right) \left[\left(1 + \frac{\alpha_s}{\pi} \right) \log \left(\frac{m_t}{M_Z} \right) - \frac{15}{8} \frac{\alpha_s}{\pi} \right]. \quad (4.14)$$

Thus, one obtains for the transformation of the sinus of the mixing angle into a five flavour $\overline{\text{MS}}$ scheme

$$\delta_s = \delta_s^{(6)} - 2 \frac{\alpha}{\pi} d. \quad (4.15)$$

In our approximation we do not include the QCD terms proportional to α_s in eq. 4.14. The modification terms of $\sin \theta_W$ and $\cos \theta_W$ depend on the structure of the Born cross section and are different for transverse and longitudinal polarization. The proper coefficients related to both cases are given at the end of this section.

Changing the renormalization scale δ_μ

With the transformation discussed above we obtain corrections renormalized in the $\overline{\text{MS}}$ -scheme where the scale is chosen to be $\mu = M_Z$ as it is convenient for electroweak corrections. However, this scale we only adopt for the transverse part. For the longitudinal part we choose $\mu = \sqrt{s}$ since here only s -channel amplitudes contribute at leading order. Thus, for the longitudinal

case we have an additional running coupling contribution

$$\delta_\mu = 2\frac{\alpha}{4\pi} (\beta_0^Y P_Y + \beta_0^W P_W) \log\left(\frac{s}{M_Z^2}\right) \quad (4.16)$$

with

$$\begin{aligned} \beta_0^W &= -\frac{4}{3}N_g + \frac{43}{6}, \\ \beta_0^Y &= -\frac{20}{9}N_g - \frac{1}{6}, \end{aligned} \quad (4.17)$$

and

$$\begin{aligned} P_Y &= \frac{\frac{Y_f Y_\phi}{2} \frac{1}{c_W^2}}{\frac{Y_f Y_\phi}{2} \frac{1}{c_W^2} + T_f^3 T_\phi^3 \frac{1}{s_W^2}}, \\ P_W &= \frac{T_f^3 T_\phi^3 \frac{1}{s_W^2}}{\frac{Y_f Y_\phi}{2} \frac{1}{c_W^2} + T_f^3 T_\phi^3 \frac{1}{s_W^2}}. \end{aligned} \quad (4.18)$$

With explicit hypercharge and isospin quantum numbers one obtains with respect to the cross section

$$\delta_\mu = \frac{\alpha}{4\pi} \left(\frac{22}{3} + \frac{19}{3} \frac{1}{s_W^2} - \frac{41}{3} \frac{1}{c_W^2} \right) \log\left(\frac{s}{M_Z^2}\right). \quad (4.19)$$

Subtraction of real QED contribution δ_{real}

Now let us turn to the subtraction of real radiation. The authors of [21] give the inclusive QED logarithmic correction separate from the electroweak corrections and reads

$$\Delta_{\text{QED}} = \frac{\alpha}{4\pi} \left[6 \log\left(\frac{s}{m^2}\right) + 4 \log\left(\frac{\Delta E^2}{E^2}\right) \left(\log\left(\frac{s}{m^2}\right) + \log\left(\frac{s}{M^2}\right) + 2 \log\left(\frac{t}{u}\right) - 2 \right) \right]. \quad (4.20)$$

The pure real corrections are presented in [26] and read in the high energy approximation

$$\begin{aligned} \delta_{\text{real}} &= \frac{\alpha}{4\pi} \left[-2 \log^2\left(\frac{s}{m^2}\right) + 4 \log\left(\frac{\Delta E^2}{\lambda^2}\right) \log\left(\frac{s}{m^2}\right) - 2 \log^2\left(\frac{s}{M_W^2}\right) \right. \\ &\quad + 4 \log\left(\frac{s}{m^2}\right) + 4 \log\left(\frac{s}{M_W^2}\right) + 4 \log\left(\frac{s}{M_W^2}\right) \log\left(\frac{\Delta E^2}{\lambda^2}\right) \\ &\quad - 8 \log\left(\frac{\Delta E^2}{\lambda^2}\right) - 8 \log\left(\frac{u}{t}\right) \log\left(\frac{\Delta E^2}{\lambda^2}\right) - 4 \log^2\left(-\frac{u}{t}\right) \\ &\quad \left. - 16 \text{Li}_2\left(-\frac{u}{t}\right) - 4\pi^2 \right]. \end{aligned} \quad (4.21)$$

Thus, the virtual QED corrections are given by $\delta_V^{(m)} = \Delta_{\text{QED}} - \delta_{\text{real}}$, where m indicates that collinear singularities are regularized by an electron mass. When the replacement of the mass hierarchy $\lambda \gg m$ is included one obtains the virtual QED corrections

$$\begin{aligned} \delta_{\text{QED}}^{\text{virt}} = & \frac{\alpha}{4\pi} \left[2 \log^2 \left(\frac{s}{M_W^2} \right) - 4 \log \left(\frac{s}{\lambda^2} \right) \log \left(\frac{s}{M_W^2} \right) - 2 \log^2 \left(\frac{s}{\lambda^2} \right) \right. \\ & - 4 \log \left(\frac{s}{M_W^2} \right) + 8 \log \left(\frac{u}{t} \right) \log \left(\frac{s}{\lambda^2} \right) + 10 \log \left(\frac{s}{\lambda^2} \right) + 4 \log \left(-\frac{u}{t} \right) \\ & \left. + 16 \text{Li}_2 \left(-\frac{u}{t} \right) + 2\pi^2 + 1 \right]. \end{aligned} \quad (4.22)$$

These QED corrections are essentially the same for both the transverse and longitudinal W -pair production.

Complete modification

When summing up all the contributions discussed above one obtains

$$\begin{aligned} \left(1 + \frac{\alpha}{4\pi} \delta_T^{\prime(1)} \right) \sigma_B^T(M_Z^2) &= \left(1 + \delta_B^T + \delta_m - \delta_{\text{real}} + 2\delta_\alpha + \delta_s \right) \sigma_B^T, \\ \left(1 + \frac{\alpha}{4\pi} \delta_L^{\prime(1)} \right) \sigma_B^L(s) &= \left(1 + \delta_B^L + \delta_m - \delta_{\text{real}} + 2\delta_\alpha + \delta_s + \delta_c + \delta_\mu \right) \sigma_B^L, \end{aligned} \quad (4.23)$$

where $\delta^{\prime(1)}$ is the one-loop virtual corrections within five flavour $\overline{\text{MS}}$ renormalization and a photon mass as infrared regulator. This correction factor is marked with a prime to emphasize that it is slightly different to the one obtained from a direct calculation within the $\overline{\text{MS}}$ scheme. This issue and the comparison with respect to our own calculation are discussed at the end of this section. For convenience we give the numerical values for the parameters related to scheme transformation

$$\begin{aligned} \delta_\alpha &= -24.774 \frac{\alpha}{4\pi}, \\ \delta_s &= 127.870 \frac{\alpha}{4\pi}, \\ \delta_c &= 38.411 \frac{\alpha}{4\pi}. \end{aligned} \quad (4.24)$$

The input parameters are given in eq. 4.57.

4.1.2 Approach II: Calculation

We give a brief discussion of our calculation of virtual one-loop corrections within the Electroweak Standard Model to the leading order processes presented in section 2.4. The Feynman diagrams are generated by *QGRAF3.1*

[32] and are calculated in *Mathematica* using the package *FeynCalc* [33]. The Feynman rules are taken from [20] and the 't Hooft Feynman gauge is adopted. We make use of the high energy approximation, neglecting mass terms in relation to kinematic invariants whenever possible. In particular all fermion masses are neglected except for the top quark. To regularize infrared divergences, the photon is given an artificial mass λ . Tensor integrals are reduced to scalar integrals according to the Passarino-Veltman reduction method [34]. The scalar integrals are computed in the high approximation according to [35] and are checked against *LoopTools* [36]. The calculation is performed in two different renormalization schemes, the $\overline{\text{MS}}$ scheme and the on-shell scheme. The precise form of the on-shell counterterms can be found in appendix A.6. In contrast to approach I, we do not decouple the top quark in the sinus of the mixing angle. This can be easily included by taking into account the corresponding contribution presented in the previous section. To bring the radiative corrections in a form factorized with respect to the Born cross section we use relations presented in appendix A.1. Therewith, the Dirac structure of higher order amplitudes can be reduced to a simple Dirac structure, often proportional to the Born amplitude. While for the process of the production of longitudinally polarized W -pairs we obtain a factorization with respect to the Born amplitude, this does not hold for the production of a pair of transversely polarized W -bosons. Thus, besides the Born amplitude 2.10, we introduce an additional leading order contribution \mathcal{A}_T^k to decompose the one-loop correction factorized with respect to leading order contributions according to

$$\mathcal{A}_T^{(1)} = \delta_A^B \mathcal{A}_T^B + \delta_A^k \mathcal{A}_T^k \quad (4.25)$$

with

$$\mathcal{A}_T^k = \frac{e^2}{s_W^2} \frac{1}{t} \bar{\psi}(p_2) \not{k}_1 (p_1 \cdot \epsilon_\kappa^*)^2 \omega_- \psi(p_1). \quad (4.26)$$

This only affects the non-logarithmic constant part though. Note that this decomposition concerns the Dirac structure and must not be confused with the isospin structure introduced in section 3.1. For the evolution equation approach we work with radiative corrections with respect to the Born cross section instead of the Born amplitude to accommodate factorization. The correction with respect to the Born cross section is then given by

$$\frac{d\sigma_T^{(1)}}{d\Omega} = \delta_T^{(1)} \frac{d\sigma_T^B}{d\Omega} \quad \text{with} \quad \delta_T^{(1)} = 2 \left[\delta_A^B + \delta_A^B \frac{d\sigma_T^k/d\Omega}{d\sigma_T^B/d\Omega} \right], \quad (4.27)$$

where $d\sigma_T^k/d\Omega = \frac{\alpha^2}{8s_W^4} x_+^2 (x_+ - x_-)$ is the cross section related to \mathcal{A}_T^k .

The final results are presented in the $\overline{\text{MS}}$ scheme while the on-shell scheme is only used to check against known one-loop results (4.1.1). In order to be concise, we do not present the one-loop corrections but the coefficients of soft anomalous dimension and initial conditions derived by comparing the one-loop expansion of the evolution equation with the calculated one-loop correction. These results are presented in section 4.2 along with the corresponding two-loop results.

Subtraction of QED Logarithms

The virtual one-loop corrections we calculated are derived within the Electroweak Standard Model. We are, however, interested in radiative corrections related to W - and Z -boson exchange. As stated in section 3.3 one has to separate the virtual QED contribution and one obtains two evolution equations. The hard evolution equation for the electroweak logarithms $\log(s/M_W^2)$ and the infrared evolution equation for the QED logarithms $\log(s/\lambda^2)$. For the infrared evolution equation, the QED factor \mathcal{U} is introduced.

Obviously, all logarithms containing the artificial photon mass are to be embedded in \mathcal{U} . Yet besides logarithms of the form $\log(s/\lambda^2)$, logarithms involving the W -mass contribute to \mathcal{U} as well. The latter logarithms arise from diagrams with virtual photons coupling to external onshell W -bosons leading to integrals where the W -mass acts as an infrared cutoff. Yet, logarithms of the form $\log(s/M_W^2)$ drop out when real QED corrections are included. To disentangle the contributions of $\log(s/M_W^2)$ related to the electroweak and the QED part respectively, we investigate the real corrections provided in [26] to identify the virtual QED logarithms $\log(s/M_W^2)$. At the one-loop level obtain

$$\begin{aligned} \mathcal{U}_{\text{QED}}^{(1)}(Q, \lambda, M_W) = \frac{\alpha}{4\pi} \left[-\log^2\left(\frac{Q^2}{\lambda^2}\right) - 2\log\left(\frac{Q^2}{\lambda^2}\right)\log\left(\frac{s}{M_W^2}\right) + \log^2\left(\frac{Q^2}{M_W^2}\right) \right. \\ \left. - 2\log\left(\frac{Q^2}{M_W^2}\right) + 4\log\left(\frac{x_+}{x_-}\right)\log\left(\frac{Q^2}{\lambda^2}\right) + 5\log\left(\frac{Q^2}{\lambda^2}\right) \right]. \end{aligned} \quad (4.28)$$

Note that we only take into account logarithmic contributions due to the initial condition $\mathcal{U}_{\text{QED}}(M_W, M_W, M_W) = 1$. Up to the constant, the one-loop expansion of the factor \mathcal{U}_{QED} reproduces the virtual QED corrections derived in eq. 4.22.

In order to solve the infrared evolution equation in NNLL approximation, also the coefficients $\beta_0^{\text{QED}} = -\frac{80}{9}$ and $\gamma_{\text{QED}}^{(2)} = \frac{800}{27}$ are needed. How to derive

these coefficients is shown in appendix A.3 and one obtains

$$\begin{aligned} \mathcal{U}_{\text{QED}} = U_0(\alpha) \exp \left\{ -\frac{\alpha(\lambda^2)}{4\pi} \left[\left(2 - \left(\frac{290}{27} + \frac{40}{9} \log \left(\frac{x_+}{x_-} \right) \right) \frac{\alpha}{\pi} \right) \log^2 \left(\frac{Q^2}{\lambda^2} \right) \right. \right. \\ \left. \left. - \left(3 + 4 \log \left(\frac{x_+}{x_-} \right) \right) \log \left(\frac{Q^2}{\lambda^2} \right) + \frac{40}{27} \frac{\alpha}{\pi} \log^3 \left(\frac{Q^2}{\lambda^2} \right) \right. \right. \\ \left. \left. - \left(\log \left(\frac{M_W^2}{\lambda^2} \right) - 1 \right)^2 \right] + \mathcal{O}(\alpha^3) \right\}. \end{aligned} \quad (4.29)$$

Let us clarify this subtraction procedure by considering the example of one-loop leading logarithmic corrections in the transverse case. In the full EWSM calculation we find with respect to the Born cross section

$$\delta_{T,\text{full}}^{(1)LL} = -\frac{\alpha}{4\pi} \left[\left(\frac{11}{2} \frac{1}{s_W^2} + \frac{1}{2} \frac{1}{c_W^2} - 6 \right) \log^2 \left(\frac{s}{M_W^2} \right) + 2 \log^2 \left(\frac{s}{\lambda^2} \right) \right]. \quad (4.30)$$

From eq. 4.28 we know that $+2\frac{\alpha}{4\pi} \log^2(s/M_W^2)$ and all $2 \log^2(s/\lambda^2)$ contribute to the infrared evolution equation. Thus we are left with

$$\delta_{T,\text{EW}}^{(1)LL} = -\frac{\alpha}{4\pi} \left(\frac{11}{2} \frac{1}{s_W^2} + \frac{1}{2} \frac{1}{c_W^2} - 4 \right) \log^2(s/M_W^2). \quad (4.31)$$

The coefficient of this logarithm corresponds to $\gamma^{(1)}$ and enters the hard evolution equation which gives the electroweak logarithms related to virtual W - and Z -exchange.

Since the QED corrections are sensitive to only the electromagnetic charge the factor \mathcal{U}_{QED} is essentially the same for both the transverse and longitudinal W -pair production. In order to cancel the singular dependence on the photon mass, the QED Sudakov exponent (4.29) should be combined with the real photon emission, which is also of pure QED nature if the energy of the emitted photons is much smaller than M_W .

The results of these calculations are presented in section 4.2 in terms of coefficients entering the solution of the evolution equation.

Comparison of the two approaches

We have presented two independent approaches to derive the one-loop corrections for W -pair production in e^+e^- collisions within the $\overline{\text{MS}}$ scheme. Yet, the results of both approaches are slightly different from each other. In our first approach we obtained the electroweak two-loop NNLL correction using $\delta^{(1)}$ derived from [21]. Here we had to include appropriate modifications as mentioned above. The corresponding results are published in [15].

When we performed the one-loop calculation on our own we reproduced the result of [21] in the on-shell scheme but found slight difference within the $\overline{\text{MS}}$ scheme. This is because the authors of [21] made use of the on-shell relation $M_Z = M_W/c_W$, which is legitimate as long the calculation is performed in the on-shell scheme of course, to simplify the expressions. However, the use of this relation is no longer valid when one turns to the $\overline{\text{MS}}$ scheme. The transformation of the one-loop correction in the on-shell scheme, where $M_Z = M_W/c_W$ was used, into the $\overline{\text{MS}}$ scheme causes an error which is formally of next-to-next-to-leading order. The results presented in the next section are derived from the exact $\overline{\text{MS}}$ calculation and therefore slightly different to the results presented in [15].

4.2 Two-Loop Corrections

In principle, one can derive the leading logarithms at any order perturbation theory by means of the evolution equation approach. Practically, however, the two-loop leading logarithms are sufficient to match the experimental accuracy. Before we present the results, let us discuss effects related to the massive top quark which do not contribute until the two-loop level.

4.2.1 Top Quark Yukawa Coupling Effects

The large Yukawa coupling of the third generation quarks to the scalar (Higgs and Goldstone) bosons results in specific logarithmic corrections proportional to m_t^2/M_W^2 . In the longitudinal case with Goldstone boson final states, these corrections do not obey the evolution equation introduced in section 3.3 in the NNLL approximation. Regarding the Yukawa coupling effects it is suitable to split the \mathcal{Z} factor into two form factor-like factors

$$\mathcal{Z} = \mathcal{Z}_\psi \mathcal{Z}_\Phi \tag{4.32}$$

where \mathcal{Z}_ψ and \mathcal{Z}_Φ are related to the form factors where a vector boson couples to a fermion current and a scalar current respectively. In our approximation, the Yukawa type corrections affect only \mathcal{Z}_Φ .

The high energy evolution of the form factors in a theory with Yukawa interaction is completely analogous to the one of ϕ^3 scalar theory in six dimensions, see the second paper of Ref. [37]. The structure of factorization and evolution equations is much simpler than in a gauge theory because Yukawa interaction itself does not contribute to the anomalous dimension $\gamma_i(\alpha)$. It results only in single logarithmic corrections completely determined by the

ultraviolet field renormalization of the external on-shell particles, which includes $\log(\mu^2/M_W^2)$ while the vertex correction includes $\log(Q^2/\mu^2)$ terms. In the finite vector form factor they are combined to $\log(Q^2/M_W^2)$. Thus, there is a one-to-one correspondence between the ultraviolet field renormalization and the anomalous dimension of \mathcal{Z} -functions.

These corrections can be taken into account through the modification of the evolution equations for the corresponding \mathcal{Z} -functions. The analysis is straightforward but complicated because the Yukawa interaction mixes evolution of the quark and scalar boson form factors and in general does not commute with the $SU(2)$ and hypercharge couplings.

However, due to the factorization of the double Sudakov logarithms, the Yukawa enhanced contribution to NLL approximation is given simply by the product of the one-loop Yukawa corrections and the double logarithmic exponent, as observed in Ref. [38]. The structure of the NNLL contribution is more complicated and we restrict the analysis to $SU(2)$ corrections.

Since the scalar bosons interact in a different way to itself and other scalar bosons, left-handed and right-handed, up-type and down-type quark components, we have to consider the corresponding \mathcal{Z} functions separately. It is convenient to introduce the following five-component vector in the space of \mathcal{Z}_Φ -functions $\mathcal{Z} = (\mathcal{Z}_\phi, \mathcal{Z}_\chi, \mathcal{Z}_{b-}, \mathcal{Z}_{t-}, \mathcal{Z}_{t+})$, where the subscript $+$ ($-$) stand for the right-handed (left-handed) quark fields and \mathcal{Z}_χ corresponds to the transition of the Higgs boson into the neutral Goldstone boson in the external singlet vector field. The evolution equation for this vector takes the form

$$\frac{\partial}{\partial \log Q^2} \mathcal{Z} = \left[\int_{M_W^2}^{Q^2} \frac{dx}{x} \gamma(\alpha_w(x)) + \zeta(\alpha_w(Q^2), \alpha_{Yuk}(Q^2)) + \xi(\alpha_w(M_W^2)) \right] \mathcal{Z}, \quad (4.33)$$

with the solution

$$\mathcal{Z} = P \left[\exp \left\{ \int_{M_W^2}^{Q^2} \frac{dx}{x} \left(\int_{M_W^2}^x \frac{dx'}{x'} \gamma(\alpha_w(x')) + \zeta(\alpha_w(x), \alpha_{Yuk}(x)) + \xi(\alpha_w(M_W^2)) \right) \right\} \right] \mathcal{Z}_0, \quad (4.34)$$

where $\gamma^{(1)} = (-3/2) \cdot \mathbf{1}$ and $\xi = 0$ is given for $SU(2)$. The anomalous dimension matrix ζ includes all the dependence on the Yukawa coupling α_{Yuk} . We eliminate the latter by means of the relation $\alpha_{Yuk} = \frac{m_t^2}{2M_W^2} \alpha_w$, and consider the one-parameter series for the anomalous dimension in α_w . The

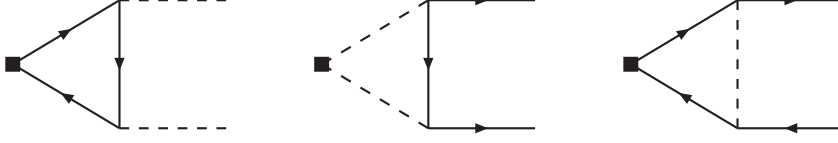


Figure 4.1: The one-loop diagrams contributing to the anomalous dimension matrix ζ . The arrow lines correspond to the third generation quarks. The dashed lines correspond to the Higgs, neutral or charged Goldstone bosons. The black square represent an external singlet vector field

one-loop coefficient reads

$$\zeta^{(1)} = \frac{1}{4} \begin{pmatrix} 12 & 0 & 0 & 0 & 0 \\ 0 & 12 & 0 & 0 & 0 \\ 0 & 0 & 9 & 0 & 0 \\ 0 & 0 & 0 & 9 & 0 \\ 0 & 0 & 0 & 0 & 0 \end{pmatrix} + \frac{m_t^2}{4M_W^2} \begin{pmatrix} 0 & 0 & 6 & 0 & -6 \\ 0 & 0 & 0 & 6 & -6 \\ 1 & 0 & 0 & 0 & -1 \\ 0 & 1 & 0 & 0 & -1 \\ -1 & -1 & -1 & -1 & 0 \end{pmatrix}, \quad (4.35)$$

where the first term representing the pure $SU_L(2)$ contribution follows from the result of sect. 3.1 and the second term represents the Yukawa contribution. It can be extracted from the known one-loop result (see e.g. ref. [38, 39]). The relevant diagrams are given in fig. 4.1.

As stated above, instead of the \mathcal{Z} -functions associated with the form factors one can directly consider the ultraviolet field renormalization. In this case the non-diagonal form of the anomalous dimension matrix is due to the mixing of the bilinear quark and scalar boson operators, which is specific for Yukawa interaction and is absent in a gauge theory.

The first two diagrams in fig. 4.1 correspond to the mixing of the quark and the scalar boson form factors. Moreover the Yukawa coupling changes quark chirality and/or flavour and the last diagram corresponds to the pure mixing of \mathcal{Z}_{b-} , \mathcal{Z}_{t-} and \mathcal{Z}_{t+} functions. As a consequence, all the diagonal matrix elements in the second term of Eq. (4.35) vanish.

The proper initial condition for the evolution equation which corresponds to the Born amplitudes of the quark and scalar boson production in e^+e^- annihilation is given by the vector $\mathcal{Z}_0 = (1, -1, -1, 1, 0)$. In NNLL approximation one needs also the one-loop running of the Yukawa coupling with the corresponding beta-function $\beta_0^{Yuk} = \frac{9}{4} - \frac{3m_t^2}{4M_W^2}$. By expanding the solution for the component \mathcal{Z}_ϕ we obtain the two-loop corrections enhanced by the second or fourth power of the top quark mass. Note that in the production amplitude one has to take into account also the interference between the one-loop Yukawa contribution to \mathcal{Z}_ϕ and the one-loop logarithmic term in

the reduced amplitude and the electron \mathcal{Z}_ψ function.

To derive the correct m_t dependence at two-loop NNLL level we remove all terms proportional to m_t^2 and m_t^4 from $\zeta^{(1)}$ in the two-loop NNLL expansion and treat these terms in an extra Yukawa contribution $\delta_{Yuk}^{(2)NNLL}$. Like for the matrix structure of the reduced amplitude we introduce coefficients which are given in respect to the Born cross section, such that

$$\langle \zeta_\phi^{(1)} \rangle = \mathcal{Z}_P \zeta^{(1)} \mathcal{Z}_0, \quad (4.36)$$

$$\langle \zeta_\phi^{(1)2} \rangle = \mathcal{Z}_P \zeta^{(1)} \zeta^{(1)} \mathcal{Z}_0, \quad (4.37)$$

where $\mathcal{Z}_P = (1, 0, 0, 0, 0)$. For reasons of traceability, we give the particular terms contributing to the two-loop NNLL Yukawa enhanced contributions explicitly. We split the two-loop NNLL Yukawa correction into (2loop \times Born) and (1loop \times 1loop)

$$\delta_{Yuk}^{(2)NNLL} = \delta_{Yuk,1\text{loop} \times 1\text{loop}}^{(2)NNLL} + \delta_{Yuk,2\text{loop} \times \text{born}}^{(2)NNLL}, \quad (4.38)$$

and obtain

$$\begin{aligned} \delta_{Yuk,2\text{loop} \times \text{born}}^{(2)NNLL} &= [\langle \zeta_\phi^{(1)2} \rangle + (2\zeta_\psi^{(1)} + 2\tilde{\chi}^{(1)} - \beta_0^{Yuk}) \langle \zeta_\phi^{(1)} \rangle]_{Yuk} \log^2 \left(\frac{s}{M_W^2} \right), \\ \delta_{Yuk,1\text{loop} \times 1\text{loop}}^{(2)NNLL} &= [\langle \zeta_\phi^{(1)} \rangle^2 + 2(\zeta_\psi^{(1)} + \tilde{\chi}^{(1)}) \langle \zeta_\phi^{(1)} \rangle]_{Yuk} \log^2 \left(\frac{s}{M_W^2} \right). \end{aligned} \quad (4.39)$$

With the coefficients $\zeta_\psi^{(1)} = 9/4$, $\tilde{\chi}^{(1)} = \log(x_+) - 5 \log(x_-)$ and the Yukawa β -function the particular contributions read

$$\langle \zeta_\phi^{(1)2} \rangle_{Yuk} = \frac{3}{8} \frac{m_t^4}{M_W^4} - \frac{63}{8} \frac{m_t^2}{M_W^2}, \quad (4.40)$$

$$\zeta_\psi^{(1)} \langle \zeta_\phi^{(1)} \rangle_{Yuk} = -\frac{27}{8} \frac{m_t^2}{M_W^2}, \quad (4.41)$$

$$\tilde{\chi}^{(1)} \langle \zeta_\phi^{(1)} \rangle_{Yuk} = \left(\frac{15}{2} \log(x_-) - \frac{3}{2} \log(x_+) \right) \frac{m_t^2}{M_W^2}, \quad (4.42)$$

$$\beta_0^{Yuk} \langle \zeta_\phi^{(1)} \rangle_{Yuk} = \frac{9}{8} \frac{m_t^4}{M_W^4} - \frac{27}{8} \frac{m_t^2}{M_W^2}, \quad (4.43)$$

$$\langle \zeta_\phi^{(1)} \rangle^2_{Yuk} = \frac{9}{4} \frac{m_t^4}{M_W^4} - 9 \frac{m_t^2}{M_W^2}. \quad (4.44)$$

So far, the Yukawa enhanced NNLL correction have been examined within a $SU(2)$ theory. To extend this approach to electroweak corrections one has

to adjust the couplings properly, such that the correction with respect to the cross section reads

$$\delta_{Yuk}^{(2)NNLL} = \frac{c_W^2}{s_W^4} \left[\frac{3}{2} \frac{m_t^4}{M_W^4} + \frac{m_t^2}{M_W^2} (30 \log(x_-) - 6 \log(x_+) - 27) \right] \log^2 \left(\frac{s}{M_W^2} \right). \quad (4.45)$$

This expression approximates the full result up to the terms suppressed by $\sin^2 \theta_W \sim 0.2$.

4.2.2 Anomalous Dimensions

We present the analytic form of the results in terms of soft anomalous dimensions. To give the formulae of the electroweak radiative corrections in a compact form we introduce the following notations

$$\begin{aligned} L_Z &= \log \left(\frac{M_Z^2}{M_W^2} \right), \\ L_H &= \log \left(\frac{M_H^2}{M_W^2} \right), \\ L_{top} &= \log \left(\frac{m_t^2}{M_W^2} \right), \\ L_{x_Z} &= \log \left(\frac{1 - \beta_Z}{1 + \beta_Z} \right), \quad \beta_Z = -i \sqrt{4 \frac{M_W^2}{M_Z^2} - 1}, \\ L_{x_H} &= \log \left(\frac{1 - \beta_H}{1 + \beta_H} \right), \quad \beta_H = -i \sqrt{4 \frac{M_W^2}{M_H^2} - 1}, \\ L_{x_{ZH}} &= \log \left(\frac{1 - \beta_{ZH}}{1 + \beta_{ZH}} \right), \quad \beta_{ZH} = -i \sqrt{4 \frac{M_Z^2}{M_H^2} - 1}, \\ L_{x_{Zt}} &= \log \left(\frac{1 - \beta_{Zt}}{1 + \beta_{Zt}} \right), \quad \beta_{Zt} = -i \sqrt{4 \frac{m_t^2}{M_Z^2} - 1}, \\ L_{Wtop} &= \log \left(1 - \frac{M_W^2}{m_t^2} \right). \end{aligned} \quad (4.46)$$

The logarithms L_{x_P} and square roots β_P ($P = Z, H, ZH, Zt$) are purely imaginary. In the radiative corrections these terms actually only exist in combinations which are real, for example $\beta_P L_{x_P}$.

The one-loop coefficients are obtained by comparing the coefficients of the one-loop expansion of $\mathcal{Z}\tilde{\mathcal{A}}$ with the one-loop calculation performed within the

$\overline{\text{MS}}$ renormalization scheme. For convenience, we project the one-loop coefficients on the particular gauge group contributions $\alpha_w = \alpha/s_W^2$, $\alpha_Y = \alpha/c_W^2$ and α . In the following these coefficients are presented first for the transverse part and subsequently for the longitudinal part.

Transverse polarization

For one-loop coefficients the renormalization scale is chosen to $\mu = M_Z$ and we obtain

$$\begin{aligned}
\gamma_T^{(1)} &= -\frac{11}{2s_W^2} - \frac{1}{2c_W^2} + 4, \\
\zeta_T^{(1)} &= \frac{9}{4s_W^2} + \frac{3}{4c_W^2} - 3, \\
\xi_T^{(1)} &= \left(\frac{5}{2s_W^2} + \frac{1}{2c_W^2} - 4 \right) \log\left(\frac{M_Z^2}{M_W^2}\right), \\
\tilde{\chi}_T^{(1)} &= \frac{1}{s_W^2} \left[\left(\frac{2x_-}{x_+} - 4 \right) \log(x_-) + 2 \log(x_+) \right] + 4 \log\left(\frac{x_-}{x_+}\right) \quad (4.47)
\end{aligned}$$

and

$$\begin{aligned}
\sigma_{0T}^{(1)} &= \frac{1}{s_W^2} \left[-\frac{23x_+^2 - 28x_+ + 10}{2x_+(x_-^2 + x_+^2)} \log^2(x_-) + \frac{3x_-}{x_-^2 + x_+^2} \log^2(x_+) \right. \\
&\quad + \frac{4}{x_+} \log x_- \log x_+ + \frac{19x_+ - 10}{2(x_-^2 - x_+^2)} \log(x_-) - \frac{1}{2} L_Z^2 \\
&\quad + \left(-\frac{3}{2} \frac{M_Z^6}{M_W^6} + \frac{31}{4} \frac{M_Z^4}{M_W^4} - \frac{17}{2} \frac{M_Z^2}{M_W^2} + 4 \log\left(\frac{x_-}{x_+}\right) - \frac{1}{6} \right) L_Z \\
&\quad + 2L_{x_z}^2 + \left(-6 \frac{M_Z^6}{M_W^6} + 43 \frac{M_Z^4}{M_W^4} - 84 \frac{M_Z^2}{M_W^2} + 68 \right) \frac{M_Z^2}{4(M_Z^2 - 4M_W^2)} \beta_Z L_{x_z} \\
&\quad + \left(-\frac{1}{6} \frac{M_H^6}{M_W^6} + \frac{3}{4} \frac{M_H^4}{M_W^4} - \frac{3}{2} \frac{M_H^2}{M_W^2} + 1 \right) L_H \\
&\quad + \left(-2 \frac{M_H^6}{M_W^6} + 13 \frac{M_H^4}{M_W^4} - 32 \frac{M_H^2}{M_W^2} + 36 \right) \frac{M_H^2}{12(M_H^2 - 4M_W^2)} \beta_H L_{x_H} \\
&\quad + 2L_{top} + 2 \left(1 - \frac{m_t^6}{M_W^6} \right) L_{Wtop} - \frac{90x_+}{x_-^2 + x_+^2} + 3 \frac{M_Z^4}{M_W^4} - 11 \frac{M_Z^2}{M_W^2} \\
&\quad + \frac{1}{3} \frac{M_H^4}{M_W^4} - \frac{M_H^2}{M_W^2} - 2 \frac{m_t^4}{M_W^4} - \frac{m_t^2}{M_W^2} + \frac{\pi^2}{2} + \frac{575}{36} \left. \right] \\
&\quad + \frac{1}{c_W^2} \left[\frac{x_+^2 - 2x_+ + 2}{2x_+(x_-^2 + x_+^2)} \log^2(x_-) + \frac{x_+ + 2}{2(x_-^2 + x_+^2)} \log(x_-) \right. \\
&\quad \left. - \frac{1}{2} L_Z^2 - \left(\frac{M_Z^2}{M_W^2} + \frac{1}{2} \right) L_Z - \left(\frac{M_Z^2}{M_W^2} - 3 \right) \frac{M_Z^2}{M_Z^2 - 4M_W^2} \beta_Z L_{x_z} \right]
\end{aligned}$$

$$\begin{aligned}
& + \frac{x_+}{2(x_-^2 + x_+^2)} + \frac{\pi^2}{6} + \frac{1}{4} \Big] \\
& + \left[2L_Z^2 + \left(8 \log \left(\frac{x_+}{x_-} \right) + \frac{4}{3} \frac{M_Z^6}{M_W^6} - 7 \frac{M_Z^4}{M_W^4} + 9 \frac{M_Z^2}{M_W^2} + 10 \right) L_Z - 2L_{xz}^2 \right. \\
& + \left(4 \frac{M_Z^6}{M_W^6} - 29 \frac{M_Z^4}{M_W^4} + 61 \frac{M_Z^2}{M_W^2} - 60 \right) \frac{M_Z^2}{3(M_Z^2 - 4M_W^2)} \beta_Z L_{xz} \\
& \left. - \frac{8}{3} \frac{M_Z^4}{M_W^4} + 10 \frac{M_Z^2}{M_W^2} - 2\pi^2 \right] \tag{4.48}
\end{aligned}$$

The coefficient $\tilde{\chi}_T^{(1)}$ can also be obtained using the matrix of soft anomalous dimension eq. 3.15. The reduced amplitude is essentially the same as for the $SU(2)$ case. To get the electroweak coefficient of $\tilde{\chi}_T^{(1)}$ one has to include the hypercharge and electromagnetic contribution to the matrix of soft anomalous dimensions according to $\chi^{(1)} = \chi_{SU(2)}^{(1)} + \chi_{U(1)_Y}^{(1)} \mathbf{1} - \chi_{\text{QED}}^{(1)} \mathbf{1}$ (see section 3.3). Note that there is no hypercharge contribution to $\tilde{\chi}_T^{(1)}$ because the gauge boson of the $U(1)_Y$ does not couple to W -bosons. For the two-loop expansion one also needs

$$\begin{aligned}
(\tilde{\chi}^2)_T^{(1)} &= \frac{1}{s_W^4} \left[4 \left(4 - \frac{x_-}{x_+} \right) \log^2(x_-) + 4 \log^2(x_+) - 4 \left(\frac{x_-}{x_+} + 3 \right) \log(x_-) \log(x_+) \right] \\
&+ \frac{16}{s_W^2} \left[\log \left(\frac{x_-}{x_+} \right) \left(\log(x_+) + \left(\frac{x_-}{x_+} - 2 \right) \log(x_-) \right) \right] + 16 \log^2 \left(\frac{x_+}{x_-} \right), \tag{4.49}
\end{aligned}$$

which is obtained according to eq. 3.21 using the electroweak matrix $\chi^{(1)}$ discussed above. For the two-loop expansion of γ_T one obtains with eq. 3.23

$$\gamma_T^{(2)} = \frac{1}{s_W^4} \left[-\frac{385}{9} + \frac{11}{3} \pi \right] + \frac{52}{9c_W^4} - \frac{1600}{27}.$$

Note that one must not simply plug in the number of light fermions n_f and scalar doublets n_s but take into account the proper charges as shown in appendix A.4. In this appendix one also finds how to properly implement the beta functions.

For $M = M_W = M_Z = M_H$ and the limit $m_t \rightarrow 0$ the particular gauge contributions reproduce the coefficients of the toy model of $SU(2)$ and $U(1)$ presented in section 3.2.

Longitudinal polarization

In the case of longitudinal polarization, the Born process involves two s-channel amplitudes with a Z -boson and a photon as mediating gauge bosons,

or a W_3 -boson and the hypercharge boson in the symmetric phase. Therefore, the isospin structure of the Born vector is more involved. For a $SU(N)$ theory, the basis $(\mathbf{T}^a \otimes \mathbf{T}^a, \mathbf{1} \otimes \mathbf{1})$ was introduced and the Born vector is given by $(1, 0)$. To extend the matrix structure to the the electroweak standard model the leading order hypercharge contribution has to be included. While the isospin basis stays the same, the Born vector has to be modified since at Born level an additional Hypercharge boson contributes to the isospin neutral part of the isospin basis. The electroweak Born amplitude for the s-channel process therefore reads $(\frac{1}{s_W^2}, \frac{1}{c_W^2} \frac{Y_\psi Y_\phi}{4})$. In contrast to the pure $SU(2)$ model a factor of $\frac{1}{s_W^2}$ appears in the $SU(2)$ contribution due to the change of the expansion parameter from the weak coupling to the electroweak coupling. With the renormalization scale set to $\mu = \sqrt{s}$ as it is convenient for a s-channel process one obtains

$$\begin{aligned}
\gamma_L^{(1)} &= -\frac{3}{s_W^2} - \frac{1}{c_W^2} + 4, \\
\zeta_L^{(1)} &= \frac{21}{4s_W^2} + \frac{7}{4c_W^2} - 3, \\
\xi_L^{(1)} &= \left(\frac{1}{s_W^2} + \frac{1}{c_W^2} - 4 \right) \log \left(\frac{M_Z^2}{M_W^2} \right) - \frac{3}{2} \frac{m_t^2}{M_W^2}, \\
\tilde{\chi}_L^{(1)} &= \frac{1}{s_W^2} [\log(x_+) - 5 \log(x_-)] + \frac{1}{c_W^2} \log \left(\frac{x_+}{x_-} \right) + 8 \log(x_-) - 4 \log(x_+)
\end{aligned} \tag{4.50}$$

and

$$\begin{aligned}
\sigma_{0L}^{(1)} &= \frac{1}{s_W^2} \left[-\frac{5}{2x_+} \log^2(x_-) + \frac{1}{2x_-} \log^2(x_+) - \frac{1}{2} L_Z^2 \right. \\
&\quad + \left(-\frac{27}{4} \frac{M_Z^6}{M_W^6} + \frac{117}{4} \frac{M_Z^4}{M_W^4} - \frac{39}{2} \frac{M_Z^2}{M_W^2} + 2 \log \left(\frac{x_-}{x_+} \right) - \frac{13}{2} \right) L_Z \\
&\quad + \left(-27 \frac{M_Z^6}{M_W^6} + 171 \frac{M_Z^4}{M_W^4} - 250 \frac{M_Z^2}{M_W^2} + 28 \right) \frac{M_Z^2}{4(M_Z^2 - 4M_W^2)} \beta_Z L_{xz} \\
&\quad + \frac{1}{2} L_{xz}^2 + \left(-\frac{1}{4} \frac{M_H^6}{M_W^6} + \frac{5}{4} \frac{M_H^4}{M_W^4} - 3 \frac{M_H^2}{M_W^2} + 1 \right) L_H + L_{xH}^2 \\
&\quad - \left(\frac{M_H^6}{M_W^6} - 7 \frac{M_H^4}{M_W^4} + 20 \frac{M_H^2}{M_W^2} - 28 \right) \frac{M_H^2}{4(M_H^2 - 4M_W^2)} \beta_H L_{xH} \\
&\quad + 3 \frac{m_t^2}{M_W^2} L_{top} + 3 \left(\frac{m_t^2}{M_W^2} - \frac{m_t^6}{M_W^6} \right) L_{Wtop} + \frac{27}{2} \frac{M_Z^4}{M_W^4} - 34 \frac{M_Z^2}{M_W^2} \\
&\quad \left. + \frac{1}{2} \frac{M_H^4}{M_W^4} - 2 \frac{M_H^2}{M_W^2} - 3 \frac{m_t^4}{M_W^4} + 3 \frac{m_t^2}{M_W^2} - \frac{5\pi^2}{3} + \frac{575}{36} \right]
\end{aligned}$$

$$\begin{aligned}
& + \frac{1}{c_W^2} \left[-\frac{1}{2x_+} \log^2(x_-) + \frac{1}{2x_-} \log^2(x_+) \right. \\
& - \frac{1}{2} L_Z^2 - \left(\frac{1}{2} \frac{M_Z^4}{M_W^4} - \frac{7}{2} \frac{M_Z^2}{M_W^2} + 2 \log\left(\frac{x_-}{x_+}\right) - \frac{1}{2} \right) L_Z \\
& + \left(\frac{M_Z^4}{M_W^4} - 9 \frac{M_Z^2}{M_W^2} + 18 \right) \frac{M_Z^2}{2(M_Z^2 - 4M_W^2)} \beta_Z L_{xz} - \frac{1}{2} L_{xz}^2 \\
& \left. - \frac{M_Z^2}{M_W^2} + \frac{\pi^2}{3} - \frac{787}{36} \right] \\
& + \left[\frac{2}{x_+} \log^2(x_-) + 2L_Z^2 + \left(8 \log\left(\frac{x_+}{x_-}\right) + 6 \frac{M_Z^6}{M_W^6} - 22 \frac{M_Z^4}{M_W^4} + 9 \frac{M_Z^2}{M_W^2} + 10 \right) L_Z \right. \\
& + 2L_{xz}^2 - \left(-6 \frac{M_Z^6}{M_W^6} + 34 \frac{M_Z^4}{M_W^4} - 39 \frac{M_Z^2}{M_W^2} + 4 \right) \frac{M_Z^2}{4(M_Z^2 - 4M_W^2)} \beta_Z L_{xz} \\
& \left. - 12 \frac{M_Z^4}{M_W^4} + 22 \frac{M_Z^2}{M_W^2} + 6\pi^2 + \frac{32}{9} \right] \tag{4.51}
\end{aligned}$$

The two-loop contribution of γ_L reads

$$\gamma_L^{(2)} = \frac{1}{s_W^4} \left[-\frac{70}{3} + 2\pi \right] + \frac{104}{9c_W^4} - \frac{1600}{27}. \tag{4.52}$$

The procedure for deriving the matrix of soft anomalous dimensions is basically the same for the transverse part and, in addition, $\tilde{\chi}_L^{(1)}$ to one obtains

$$\begin{aligned}
(\tilde{\chi}^2)_L^{(1)} &= \frac{48s_W^8 - 128s_W^6 + 132s_W^4 - 64s_W^2 + 13}{c_W^4 s_W^4} \log^2(x_-) \\
&+ \frac{-64s_W^8 + 144s_W^6 - 108s_W^4 + 24s_W^2 + 2}{c_W^4 s_W^4} \log(x_-) \log(x_+) \\
&+ \frac{(1 - 2s_W^2)^4}{c_W^4 s_W^4} \log^2(x_+). \tag{4.53}
\end{aligned}$$

Note that the coefficients $\gamma^{(1)}$, $\zeta^{(1)}$ and $\chi^{(1)}$ can be derived either from comparison from the solution of the evolution equation with the one-loop calculation, or from the formulae eqs. 3.10, 3.22, 3.21. This provides a simple check of these coefficients.

Results in the on-shell scheme

The radiative corrections obtained within the on-shell scheme differ only in the constant $\sigma^{(1)}$ and the difference is basically related to the finite parts of the on-shell counterterms. Let us write

$$\delta_{T/L}^{(1)OS} = \delta_{T/L}^{(1)} + \delta_{T/L,ct}^{(1)}. \tag{4.54}$$

In particular it is

$$\begin{aligned}\delta_{T,ct}^{(1)} &= 2(\delta Z_e - \delta Z_{s_W})|_{\Delta=0}, \\ \delta_{L,ct}^{(1)} &= \left[\left(2\delta Z_e + \frac{2s_W^2 - 1}{2c_W s_W} \delta Z_{ZA} \right) \mathcal{P}_{AA} - \frac{1}{2}(\delta Z_{AZ} + \delta Z_{ZA})(\mathcal{P}_{ZA} + \mathcal{P}_{AZ}) \right. \\ &\quad \left. + \left(2\delta Z_e - \frac{2}{2s_W^4 - 3s_W^2 + 1} \delta Z_{s_W} + \frac{2c_W s_W}{2s_W^2 - 1} \delta Z_{AZ} \right) \mathcal{P}_{ZZ} \right]_{\Delta=0},\end{aligned}\tag{4.55}$$

where $\mathcal{P}_{AA} = 4c_W^2 s_W^2$, $\mathcal{P}_{AZ} = \mathcal{P}_{ZA} = 2c_W s_W(2s_W^2 - 1)$ and $\mathcal{P}_{ZZ} = (1 - 2s_W^2)^2$. The corresponding renormalization constants can be found in appendix A.6. Note that one has to make the same choice for the renormalization scale as for the radiative corrections, i.e. $\mu = M_Z$ for $\delta_{T,ct}^{(1)}$ and $\mu = \sqrt{s}$ for $\delta_{L,ct}^{(1)}$. With eq. 4.54 we agree with the results of [21]. Note that to obtain the correct corrections in the on-shell scheme one must not add eq. 4.55 to the numerical result eqs. 4.60 and 4.62 because here $\overline{\text{MS}}$ -values are used for the mixing angle parameters, but to the result in the analytic form using on-shell parameters.

To extend this scheme transformation to the two-loop level is straight forward since it only affects the one-loop constant which enters the two-loop NNLL, such that

$$\delta_{T/L}^{(2)OS} = \delta_{T/L}^{(2)} + \gamma_{T/L}^{(1)} \delta_{T/L,ct}^{(1)}.\tag{4.56}$$

4.2.3 Numerical Results

In this subsection we give the differential corrections factorized in respect to the Born cross section at one- and two-loop in NNLL approximation. As input parameters we use $\overline{\text{MS}}$ values for the mixing angle but onshell values for masses of the gauge bosons. This is because the higher order calculations are performed within the $\overline{\text{MS}}$ scheme, yet for the gauge boson masses we use the physical values since they act as infrared cutoff in the evolution equation approach. As parameters we use

$$\begin{aligned}M_W &= 80.41\text{GeV}, M_Z = 91.19\text{GeV}, M_H = 117\text{GeV}, m_t = 172.7\text{GeV}, \\ \alpha(M_Z^2) &= \frac{1}{128.1}, s_W^2 = 0.231.\end{aligned}\tag{4.57}$$

Since the corrections to the differential cross sections were published with respect to weak coupling constant α_w , we shall give the result in the same

form in order to ease comparison, such that

$$\frac{d\sigma_P}{d\Omega} = \left(1 + \frac{\alpha_w}{4\pi} \delta_{wP}^{(1)} + \left(\frac{\alpha_w}{4\pi} \right)^2 \delta_{wP}^{(2)} + \mathcal{O}(\alpha_w^3) \right) \frac{d\sigma_P^B}{d\Omega}, \quad (4.58)$$

for polarization $P = (T, L)$ and expand in the logarithms according to

$$\delta_w^{(l)} = \sum_{k=0}^{2l} \delta_w^{(l)N^kLL} \log^{2l-k} \left(\frac{s}{M_W^2} \right). \quad (4.59)$$

Transverse polarization

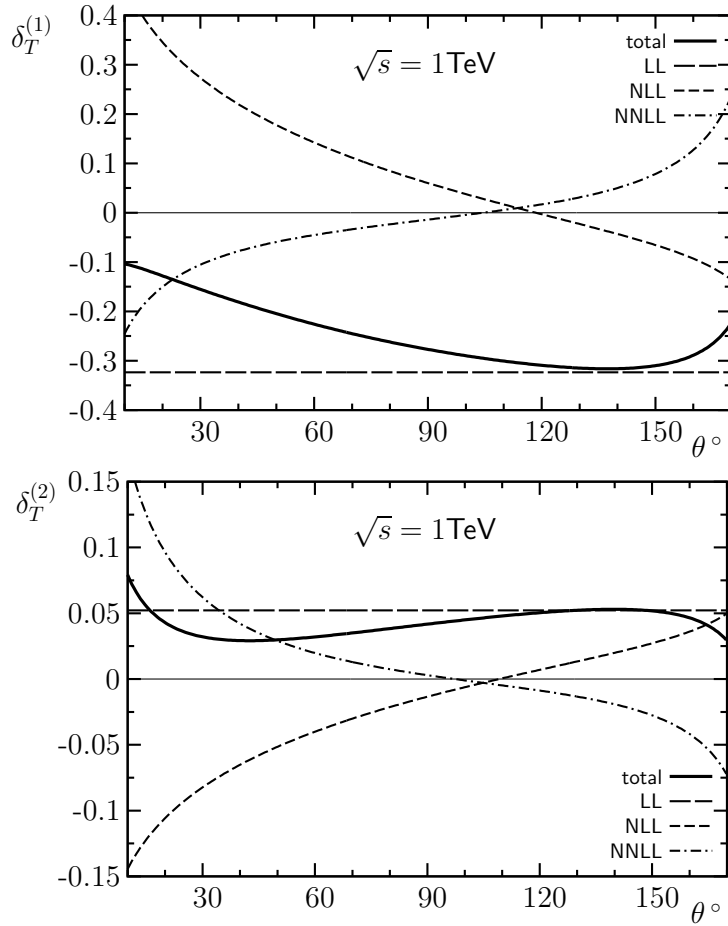


Figure 4.2: One-loop and two-loop corrections to the differential cross section relative to the Born approximation for the production of transversely polarized W bosons at $\sqrt{s} = 1 \text{ TeV}$.

$$\begin{aligned}
\delta_{\text{w}T}^{(1)LL} &= -4.726, \\
\delta_{\text{w}T}^{(1)NLL} &= \left(-6.152 + 4\frac{x_-}{x_+}\right) \log(x_-) + 2.152 \log(x_+) + 4.433, \\
\delta_{\text{w}T}^{(1)NNLL} &= \left(\frac{-4.700}{x_+} + \frac{1.951x_- + 2.350}{x_-^2 + x_+^2}\right) \log^2(x_-), \\
&\quad + \frac{4}{x_+} \log(x_-) \log(x_+) + \frac{3x_-}{x_-^2 + x_+^2} \log^2(x_+) - 0.541 \log(x_+) \\
&\quad + \left(0.541 + \frac{4.951 - 9.650x_-}{x_+}\right) \log(x_-) - 0.347. \tag{4.60}
\end{aligned}$$

$$\begin{aligned}
\delta_{\text{w}T}^{(2)LL} &= 11.169, \\
\delta_{\text{w}T}^{(2)NLL} &= \left(29.076 - \frac{18.905x_-}{x_+}\right) \log(x_-) - 10.171 \log(x_+) - 14.491, \\
\delta_{\text{w}T}^{(2)NNLL} &= \left(18.924 + \frac{22.211 - 12.608x_-}{x_+} - \frac{11.106 + 9.219x_-}{x_-^2 + x_+^2}\right. \\
&\quad \left. + \frac{4x_-^2}{x_+^2}\right) \log^2(x_-) - \left(9.239 + \frac{18.905}{x_+} + \frac{3.392x_-}{x_+}\right) \log(x_-) \log(x_+) \\
&\quad + \left(2.316 - \frac{14.179x_-}{x_-^2 + x_+^2}\right) \log^2(x_+) + 3.489 \log(x_+) \\
&\quad - \left(14.889 - \frac{11.400x_-}{x_+} + \frac{23.397 - 45.609x_-}{x_-^2 + x_+^2}\right) \log(x_-) \\
&\quad + \frac{11.106x_+}{x_-^2 + x_+^2} - 9.126, \tag{4.61}
\end{aligned}$$

Longitudinal polarization

$$\begin{aligned}
\delta_{\text{w}L}^{(1)LL} &= -2.376, \\
\delta_{\text{w}L}^{(1)NLL} &= -6.905 \log(x_-) + 0.753 \log(x_+) - 3.484, \\
\delta_{\text{w}L}^{(1)NNLL} &= -\frac{2.188}{x_+} \log^2(x_-) + \frac{0.650}{x_-} \log^2(x_+) + 0.189 (\log(x_-) - \log(x_+)) \\
&\quad + 36.823. \tag{4.62}
\end{aligned}$$

$$\begin{aligned}
\delta_{\text{w}L}^{(2)LL} &= 2.824, \\
\delta_{\text{w}L}^{(2)NLL} &= 16.409 \log(x_-) + 1.789 \log(x_+) + 11.999,
\end{aligned}$$

$$\begin{aligned}
\delta_{wL}^{(2)NNLL} = & \left(18.376 + \frac{5.200}{x_+}\right) \log^2(x_-) + \left(0.283 - \frac{1.545}{x_-}\right) \log^2(x_+) \\
& + 3.106 \log(x_-) \log(x_+) + 49.037 \log(x_-) - 17.865 \log(x_+) \\
& - 128.488.
\end{aligned} \tag{4.63}$$

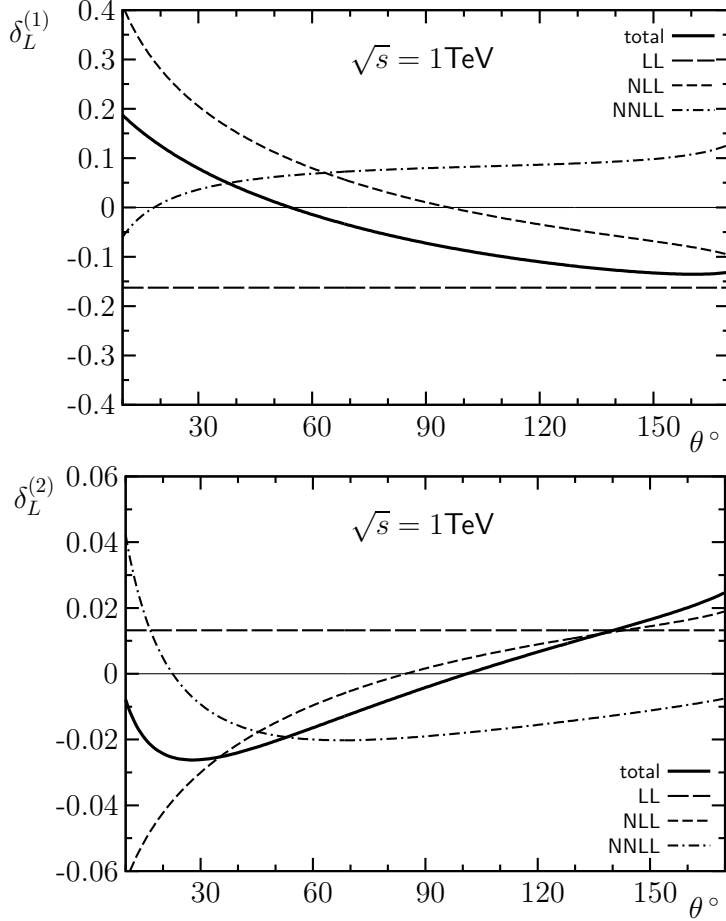


Figure 4.3: One-loop and two-loop corrections to the differential cross section relative to the Born approximation for the production of longitudinally polarized W bosons at $\sqrt{s} = 1 \text{ TeV}$.

These results differ slightly from those presented in [15]. This is basically because we adopted the on-shell calculation [21] and transformed it into the $\overline{\text{MS}}$ -scheme, where the use of $M_Z = M_W/c_W$ causes an error which is formally a higher order effect. Additionally, we did not include the top-decoupling of the weak mixing angle as described in section 4.1.1 and use a different top mass as input parameter.

In the transverse case we observe a cancellation between the huge NLL and NNLL contributions so that the sum is dominated by the LL term both at one-loop and two-loop. The two-loop radiative corrections amounts of about 5% at $\sqrt{s} \sim 1$ TeV and 20% at $\sqrt{s} \sim 3$ TeV. For the longitudinal bosons the corrections exhibit significant cancellation between the LL, NLL and NNLL terms so that the two-loop sum does not exceed 2% in absolute value for $\sqrt{s} \sim 1$ TeV. The cancellation becomes less pronounced at higher energy. The uncertainty of the theoretical prediction for the on-shell W -pair production at ILC is now determined by the unknown two-loop linear logarithmic terms. For the fermion pair production such terms are known to contribute about 1–2% of the cross section [14]. This value can be used as a rough estimate of the accuracy of our approximation.

As pointed out in [21], the high energy approximation (including one-loop corrections) reproduces the exact calculation to about one percent in the angular range $30^\circ < \theta < 150^\circ$ and at center of mass energies larger 1 TeV. Note that one can observe the dominance of the $SU(2)$ corrections when comparing the radiative corrections within the Electroweak Standard Model to the ones of the toy model $SU(2)$.

We give also the loop corrections with respect to the total Born cross section. The transverse cross section is highly sensitive on the cut-off of the angular integration, which we set to 30° , since it is peaked in the forward direction of the beam axis.

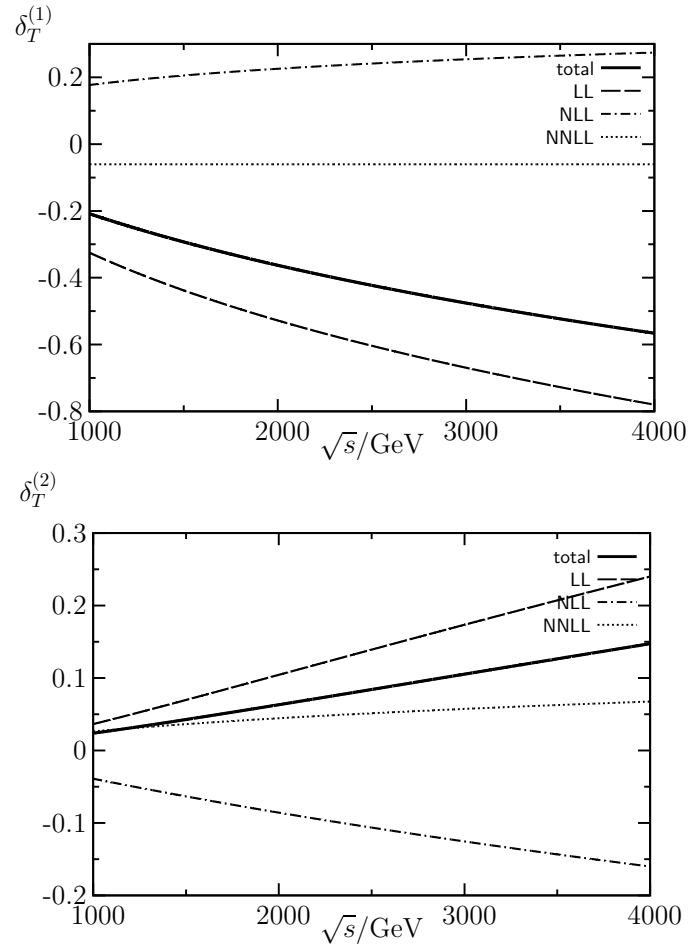


Figure 4.4: One-loop and two-loop electroweak corrections to the total cross section relative to the Born approximation for the production of transversely polarized W bosons at $\sqrt{s} = 1$ TeV with an angular cutoff of 30° .

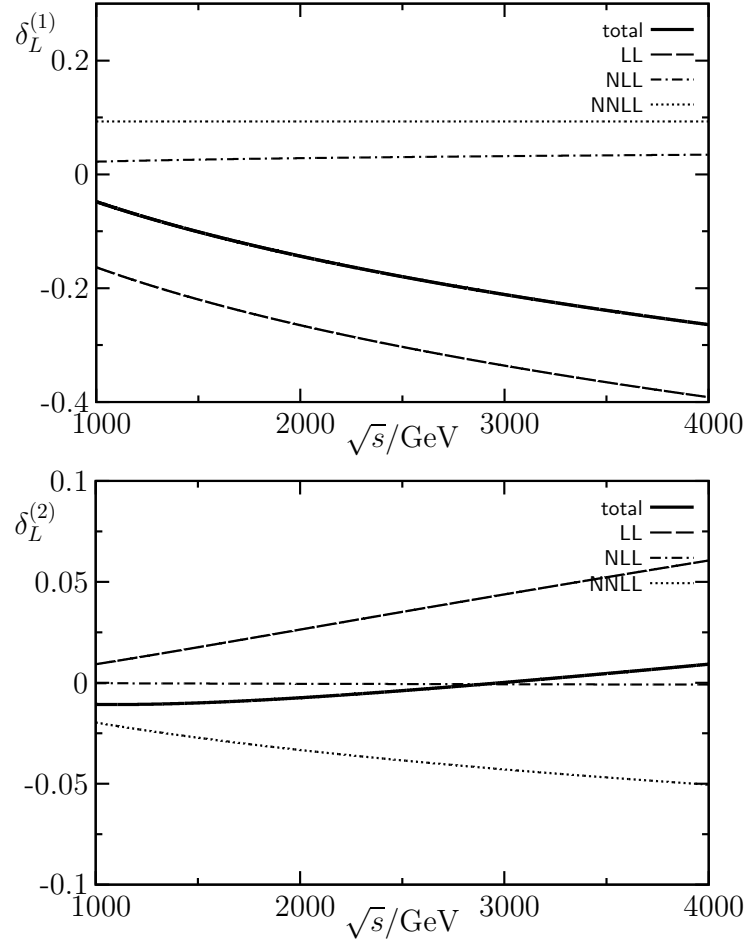


Figure 4.5: One-loop and two-loop electroweak corrections to the total cross section relative to the Born approximation for the production of longitudinally polarized W bosons at $\sqrt{s} = 1$ TeV with an angular cutoff of 30° .

Chapter 5

W -Pair Production in $q\bar{q}$ Annihilation (LHC)

In this chapter we discuss the cross section of W -pair production in hadron colliders. We restrict ourselves to the W -pair production in $q\bar{q}$ Annihilation. Indeed, the cross section of the loop induced gluon fusion process $gg \rightarrow W^+W^-$ is an order of a magnitude smaller compared to the process $q\bar{q} \rightarrow W^+W^-$ [40].

In section 5.1 the anomalous dimensions are presented, which are obtained from one-loop calculations. Numerical values for cross sections at partonic niveau are given in section 5.2. In section 5.3 we discuss the transverse momentum (p_T) and invariant mass distributions for the W -pair production at LHC. Radiative corrections to the p_T - and invariant mass distribution are presented in one-loop and up to next-to-next-to-leading logarithmic two-loop approximation.

5.1 Anomalous Dimensions

A one-loop calculation and the derivation of leading logarithms at two-loop on partonic level is performed analogously to the W -pair production in e^+e^- annihilation in the $\overline{\text{MS}}$ scheme. As in the case for e^+e^- initial states we restrict ourselves to left-handed initial states.

In the following we present the soft anomalous dimensions. The coefficients $\gamma^{(1)}$, $\zeta^{(1)}$, $\chi^{(1)}$, $\xi^{(1)}$ and the one-loop constant $\sigma_0^{(1)}$ are obtained from a one-loop corrections. The first three coefficients are checked against formulae for the one-loop expansion of γ , ζ and χ provided in section 3.1. The two-loop coefficient $\gamma^{(2)}$ is derived from eq. (3.23). We use the abbreviations of logarithmic terms introduced in eq. 4.46.

For the pair-production of transversely polarized W -bosons and up-type initial state quarks we obtain

$$\gamma_{u\bar{u},T}^{(1)} = -\frac{11}{2} \frac{1}{s_W^2} - \frac{1}{18} \frac{1}{c_W^2} + \frac{26}{9}, \quad (5.1)$$

$$\gamma_{u\bar{u},T}^{(2)} = \frac{1}{s_W^4} \left(\frac{11}{3} \pi^2 - \frac{385}{9} \right) + \frac{1}{c_W^4} \frac{52}{81} - \frac{6400}{243}, \quad (5.2)$$

$$\zeta_{u\bar{u},T}^{(1)} = \frac{9}{4} \frac{1}{s_W^2} + \frac{1}{12} \frac{1}{c_W^2} - \frac{4}{3}, \quad (5.3)$$

$$\xi_{u\bar{u},T}^{(1)} = \left(\frac{5}{2} \frac{1}{s_W^2} + \frac{1}{18} \frac{1}{c_W^2} - \frac{26}{9} \right) L_Z, \quad (5.4)$$

$$\chi_{u\bar{u},T}^{(1)} = \left[\left(\frac{2x_-}{x_+} - 4 \right) \log(x_-) + 2 \log(x_+) \right] \frac{1}{s_W^2} - \frac{8}{3} \log \left(\frac{x_+}{x_-} \right), \quad (5.5)$$

$$\begin{aligned} (\tilde{\chi}^2)_{u\bar{u},T}^{(1)} &= \frac{4}{s_W^4} \left[\left(4 - \frac{x_-}{x_+} \right) \log^2(x_-) + \log^2(x_+) - \left(\frac{x_-}{x_+} + 3 \right) \log(x_-) \log(x_+) \right] \\ &+ \frac{32}{s_W^2} \left[\left(\frac{1x_-}{3x_+} - \frac{1}{3} \right) \log^2(x_-) + \log(x_+) \left(1 - \frac{1x_-}{3x_+} \right) \log(x_-) \right. \\ &\left. - \frac{16}{3} \log^2(x_+) \right] + \frac{64}{9} \log^2 \left(\frac{x_+}{x_-} \right), \end{aligned}$$

$$\begin{aligned} \sigma_{0u\bar{u},T}^{(1)} &= \frac{1}{s_W^2} \left[2L_{xz}^2 - \frac{L_Z^2}{2} - \frac{11M_Z^2}{M_W^2} + 2L_{top} + L_{W top} \left(2 - \frac{2m_t^6}{M_W^6} \right) \right. \\ &+ L_H \left(-\frac{M_H^6}{6M_W^6} + \frac{3M_H^4}{4M_W^4} - \frac{3M_H^2}{2M_W^2} + 1 \right) \\ &+ \frac{\beta_H L_{xH}}{12M_W^6 (4M_W^2 - M_H^2)} \left(2M_H^8 - 9M_W^2 M_H^6 + 24M_W^4 M_H^4 \right. \\ &\left. - 36M_W^6 M_H^2 - 4M_W^2 (M_H^6 - 2M_H^4 M_W^2) \right) \\ &+ \frac{\beta_Z L_{xz}}{4(M_Z^2 - 4M_W^2)} M_Z^2 \left(-\frac{6M_Z^6}{M_W^6} + \frac{43M_Z^4}{M_W^4} - \frac{84M_Z^2}{M_W^2} + 68 \right) \\ &+ L_Z \left(-\frac{3M_Z^6}{2M_W^6} + \frac{31M_Z^4}{4M_W^4} - \frac{17M_Z^2}{2M_W^2} + 4 \log(x_-) - 4 \log(x_+) - \frac{13}{2} \right) \\ &+ \log^2(x_+) \left(\frac{3}{x_-} - \frac{3(x_-^2 + 2x_+ - 1)}{x_- (x_-^2 + x_+^2)} \right) + \frac{4 \log(x_-) \log(x_+)}{x_+} \\ &+ \log^2(x_-) \left(\frac{-23x_+ x_-^2 + 28x_-^2 + 10x_+}{2x_-^2 (x_-^2 + x_+^2)} - \frac{5}{x_-^2 x_+} \right) \\ &+ \frac{575x_-^2 + 485x_+^2}{36(x_-^2 + x_+^2)} - \frac{5x_- x_+}{2(x_-^2 + x_+^2)} + \frac{\log(x_-) (19x_+ - 10)}{2(x_-^2 + x_+^2)} \end{aligned}$$

$$\begin{aligned}
& + \left[\frac{M_H^4}{3M_W^4} - \frac{M_H^2}{M_W^2} + \frac{3M_Z^4}{M_W^4} - \frac{m_t^2}{M_W^2} - \frac{2m_t^4}{M_W^4} + \frac{\pi^2}{2} \right] \\
& + \frac{1}{c_W^2} \left[-\frac{L_Z^2}{18} + \left(\frac{5}{6} - \frac{M_Z^2}{M_W^2} \right) L_Z - \beta_Z L_{xz} \frac{M_Z^4 - 3M_W^2 M_Z^2}{4M_W^4 - M_W^2 M_Z^2} \right. \\
& + \frac{(390 + 4\pi^2)x_+^2 - 4(96 + \pi^2)x_+ + 2\pi^2 + 195}{108(x_-^2 + x_+^2)} \\
& + \left. \log^2(x_-) \left(\frac{x_+ x_-^2 - 2x_-^2 - 2x_+}{18x_-^2(x_-^2 + x_+^2)} + \frac{1}{9x_-^2 x_+} \right) + \frac{\log(x_-)(x_+ + 2)}{18(x_-^2 + x_+^2)} \right] \\
& + \left[\beta_Z L_{xz} \frac{-4M_Z^8 + 29M_W^2 M_Z^6 - 61M_W^4 M_Z^4 + 60M_W^6 M_Z^2}{12M_W^8 - 3M_W^6 M_Z^2} \right. \\
& + L_Z \left(\frac{4M_Z^6}{3M_W^6} - \frac{7M_Z^4}{M_W^4} + \frac{9M_Z^2}{M_W^2} - \frac{16 \log(x_-)}{3} + \frac{16 \log(x_+)}{3} + \frac{20}{3} \right) \\
& \left. - 2L_{xz}^2 + \frac{8L_Z^2}{9} - \frac{8M_Z^4}{3M_W^4} + \frac{10M_Z^2}{M_W^2} - 2\pi^2 \right]. \tag{5.6}
\end{aligned}$$

The corresponding coefficients for down-type initial state read

$$\gamma_{d\bar{d},T}^{(1)} = -\frac{11}{2} \frac{1}{s_W^2} - \frac{1}{18} \frac{1}{c_W^2} + \frac{20}{9}, \tag{5.7}$$

$$\gamma_{d\bar{d},T}^{(2)} = \frac{1}{s_W^4} \left(\frac{11}{3} \pi^2 - \frac{385}{9} \right) + \frac{1}{c_W^4} \frac{52}{81} - \frac{1600}{243}, \tag{5.8}$$

$$\zeta_{d\bar{d},T}^{(1)} = \frac{9}{4} \frac{1}{s_W^2} + \frac{1}{12} \frac{1}{c_W^2} - \frac{1}{3}, \tag{5.9}$$

$$\xi_{d\bar{d},T}^{(1)} = \left(\frac{5}{2} \frac{1}{s_W^2} + \frac{1}{18} \frac{1}{c_W^2} - \frac{20}{9} \right) L_Z, \tag{5.10}$$

$$\chi_{d\bar{d},T}^{(1)} = \frac{1}{s_W^2} \left[\left(\frac{2x_-}{x_+} - 4 \right) \log(x_-) + 2 \log(x_+) \right] - \frac{4}{3} \log\left(\frac{x_+}{x_-}\right), \tag{5.11}$$

$$\begin{aligned}
(\widetilde{\chi^2})_{d\bar{d},T}^{(1)} & = \frac{4}{s_W^4} \left[\left(4 - \frac{x_-}{x_+} \right) \log^2(x_-) + \log^2(x_+) - \left(\frac{x_-}{x_+} + 3 \right) \log(x_-) \log(x_+) \right] \\
& + \frac{1}{s_W^2} \left[\left(\frac{16x_-}{3x_+} - \frac{32}{3} \right) \log^2(x_-) + \log(x_+) \left(16 - \frac{16x_-}{3x_+} \right) \log(x_-) \right. \\
& \left. - \frac{16}{3} \log^2(x_+) \right] + \frac{16}{9} \log^2\left(\frac{x_+}{x_-}\right),
\end{aligned}$$

$$\begin{aligned}
\sigma_{0d\bar{d},T}^{(1)} & = \frac{1}{s_W^2} \left[2L_{xz}^2 - \frac{L_Z^2}{2} - \frac{11M_Z^2}{M_W^2} + 2L_{top} + L_{Wtop} \left(2 - \frac{2m_t^6}{M_W^6} \right) \right. \\
& \left. + L_H \left(-\frac{M_H^6}{6M_W^6} + \frac{3M_H^4}{4M_W^4} - \frac{3M_H^2}{2M_W^2} + 1 \right) \right]
\end{aligned}$$

$$\begin{aligned}
& + \frac{\beta_H L_{x_H}}{12M_W^6 (4M_W^2 - M_H^2)} \left(2M_H^8 - 9M_W^2 M_H^6 + 24M_W^4 M_H^4 \right. \\
& \left. - 36M_W^6 M_H^2 - 4M_W^2 (M_H^6 - 2M_H^4 M_W^2) \right) \\
& + \frac{\beta_Z L_{x_Z}}{4(M_Z^2 - 4M_W^2)} M_Z^2 \left(-\frac{6M_Z^6}{M_W^6} + \frac{43M_Z^4}{M_W^4} - \frac{84M_Z^2}{M_W^2} + 68 \right) \\
& + L_Z \left(-\frac{3M_Z^6}{2M_W^6} + \frac{31M_Z^4}{4M_W^4} - \frac{17M_Z^2}{2M_W^2} + 4 \log(x_-) - 4 \log(x_+) - \frac{13}{2} \right) \\
& + \log^2(x_+) \left(\frac{3}{x_-} - \frac{3(x_-^2 + 2x_+ - 1)}{x_-(x_-^2 + x_+^2)} \right) + \frac{4 \log(x_-) \log(x_+)}{x_+} \\
& + \log^2(x_-) \left(\frac{-23x_+x_-^2 + 28x_-^2 + 10x_+}{2x_-^2(x_-^2 + x_+^2)} - \frac{5}{x_-^2 x_+} \right) \\
& + \frac{575x_-^2 + 485x_+^2}{36(x_-^2 + x_+^2)} - \frac{5x_-x_+}{2(x_-^2 + x_+^2)} + \frac{\log(x_-)(19x_+ - 10)}{2(x_-^2 + x_+^2)} \\
& + \left. \frac{M_H^4}{3M_W^4} - \frac{M_H^2}{M_W^2} + \frac{3M_Z^4}{M_W^4} - \frac{m_t^2}{M_W^2} - \frac{2m_t^4}{M_W^4} + \frac{\pi^2}{2} \right] \\
& + \frac{1}{c_W^2} \left[-\frac{L_Z^2}{18} + \left(\frac{5}{6} - \frac{M_Z^2}{M_W^2} \right) L_Z - \beta_Z L_{x_Z} \frac{M_Z^4 - 3M_W^2 M_Z^2}{4M_W^4 - M_W^2 M_Z^2} \right. \\
& \left. + \frac{(390 + 4\pi^2)x_+^2 - 4(96 + \pi^2)x_+ + 2\pi^2 + 195}{108(x_-^2 + x_+^2)} \right. \\
& \left. + \log^2(x_-) \left(\frac{x_+x_-^2 - 2x_-^2 - 2x_+}{18x_-^2(x_-^2 + x_+^2)} + \frac{1}{9x_-^2 x_+} \right) + \frac{\log(x_-)(x_+ + 2)}{18(x_-^2 + x_+^2)} \right] \\
& + \left[\beta_Z L_{x_Z} \frac{-4M_Z^8 + 29M_W^2 M_Z^6 - 61M_W^4 M_Z^4 + 60M_W^6 M_Z^2}{12M_W^8 - 3M_W^6 M_Z^2} \right. \\
& + L_Z \left(\frac{4M_Z^6}{3M_W^6} - \frac{7M_Z^4}{M_W^4} + \frac{9M_Z^2}{M_W^2} - \frac{8 \log(x_-)}{3} + \frac{8 \log(x_+)}{3} + \frac{14}{3} \right) \\
& \left. - 2L_{x_Z}^2 + \frac{8L_Z^2}{9} - \frac{8M_Z^4}{3M_W^4} + \frac{10M_Z^2}{M_W^2} - 2\pi^2 \right]. \tag{5.12}
\end{aligned}$$

Note that, as expected, the coefficients with respect to up-type and down-type initial state quarks differ only in the QED part, since they carry the same $SU(2)$ isospin and hypercharge.

In the case of production of a pair of longitudinally polarized W -bosons with up-type initial state quarks we obtain

$$\gamma_{u\bar{u},L}^{(1)} = -3 \frac{1}{s_W^2} - \frac{5}{9} \frac{1}{c_W^2} + \frac{26}{9}, \tag{5.13}$$

$$\gamma_{u\bar{u},T}^{(2)} = \frac{1}{s_W^4} \left(2\pi^2 - \frac{70}{3} \right) + \frac{1}{c_W^4} \frac{520}{81} - \frac{6400}{243}, \quad (5.14)$$

$$\zeta_{u\bar{u},L}^{(1)} = \frac{21}{4} \frac{1}{s_W^2} + \frac{13}{12} \frac{1}{c_W^2} - \frac{4}{3}, \quad (5.15)$$

$$\xi_{u\bar{u},L}^{(1)} = \left(\frac{1}{s_W^2} + \frac{5}{9} \frac{1}{c_W^2} - \frac{26}{9} \right) L_Z - \frac{1}{s_W^2} \frac{3}{2} \frac{m_t^2}{M_W^2}, \quad (5.16)$$

$$\begin{aligned} \chi_{u\bar{u},L}^{(1)} &= \frac{1}{s_W^2} \left[5 \log(x_+) - \log(x_-) \right] + \frac{3}{c_W^2} \log\left(\frac{x_+}{x_-}\right) - \frac{8}{3} \log\left(\frac{x_+}{x_-}\right) \\ &\quad + \frac{4}{3 - 2s_W^2} \log(x_+), \end{aligned} \quad (5.17)$$

$$\begin{aligned} (\widetilde{\chi^2})_{u\bar{u},L}^{(1)} &= \frac{1}{9c_W^4 s_W^4 (2s_W^2 - 3)} \left[(128s_W^{10} - 1088s_W^8 + 2720s_W^6 - 3048s_W^4 \right. \\ &\quad \left. + 1638s_W^2 - 351) \log^2(x_-) + (-256s_W^{10} + 1600s_W^8 \right. \\ &\quad \left. - 3064s_W^6 + 2316s_W^4 - 540s_W^2 - 54) \log(x_-) \log(x_+) \right. \\ &\quad \left. + \log^2(x_+) (128s_W^{10} - 512s_W^8 + 776s_W^6 - 564s_W^4 + 198s_W^2 - 27) \right], \end{aligned} \quad (5.18)$$

$$\begin{aligned} \sigma_{0u\bar{u},L}^{(1)} &= \frac{1}{s_W^2} \left[L_{x_H}^2 - \beta_H L_{x_H} \frac{M_H^2}{4(M_H^2 - 4M_W^2)} \left(\frac{M_H^6}{M_W^6} - \frac{7M_H^4}{M_W^4} + \frac{20M_H^2}{M_W^2} - 28 \right) \right. \\ &\quad \left. + L_H \left(-\frac{M_H^6}{4M_W^6} + \frac{5M_H^4}{4M_W^4} - \frac{3M_H^2}{M_W^2} + 1 \right) + L_{W \text{ top}} \left(\frac{3m_t^2}{M_W^2} - \frac{3m_t^6}{M_W^6} \right) \right. \\ &\quad \left. + \frac{L_{x_Z}^2}{2} - \frac{L_Z^2}{2} + \frac{L_{x_Z} M_Z^2 \left(-\frac{27M_Z^6}{M_W^6} + \frac{171M_Z^4}{M_W^4} - \frac{250M_Z^2}{M_W^2} + 28 \right) \beta_Z}{4M_W^2 \left(\frac{M_Z^2}{M_W^2} - 4 \right)} \right. \\ &\quad \left. + L_Z \left(-\frac{27M_Z^6}{4M_W^6} + \frac{117M_Z^4}{4M_W^4} - \frac{39M_Z^2}{2M_W^2} + 2 \log\left(\frac{x_-}{x_+}\right) - \frac{13}{2} \right) \right. \\ &\quad \left. + \frac{3L_{\text{top}} m_t^2}{M_W^2} + \frac{\log^2(x_+)}{2x_-} - \frac{5 \log^2(x_-)}{2x_+} + \frac{3m_t^2}{M_W^2} - \frac{3m_t^4}{M_W^4} \right. \\ &\quad \left. + \frac{M_H^4}{2M_W^4} - \frac{2M_H^2}{M_W^2} + \frac{27M_Z^4}{2M_W^4} - \frac{34M_Z^2}{M_W^2} - \frac{5\pi^2}{3} + \frac{575}{36} \right] \\ &\quad + \frac{1}{c_W^2} \left[-\frac{L_{x_Z}^2}{2} + \beta_Z L_{x_Z} \frac{M_Z^2}{2(M_Z^2 - 4M_W^2)} \left(\frac{M_Z^4}{M_W^4} - \frac{9M_Z^2}{M_W^2} + 18 \right) \right. \\ &\quad \left. - \frac{L_Z^2}{18} + L_Z \left(\frac{M_Z^4}{2M_W^4} - \frac{7M_Z^2}{2M_W^2} + \frac{2 \log(x_-)}{3} - \frac{2 \log(x_+)}{3} + \frac{5}{6} \right) \right. \\ &\quad \left. + \frac{\log^2(x_+)}{6x_-} - \frac{\log^2(x_-)}{6x_+} - \frac{M_Z^2}{M_W^2} + \frac{5\pi^2}{27} - \frac{731}{36} \right] \end{aligned}$$

$$\begin{aligned}
& + \left[2L_{xz}^2 + \beta_Z L_{xz} \frac{M_Z^2}{4M_W^2 - M_Z^2} \left(-\frac{6M_Z^6}{M_W^6} + \frac{34M_Z^4}{M_W^4} - \frac{39M_Z^2}{M_W^2} + 4 \right) \right. \\
& + L_Z \left(\frac{6M_Z^6}{M_W^6} - \frac{22M_Z^4}{M_W^4} + \frac{9M_Z^2}{M_W^2} - \frac{16 \log(x_-)}{3} + \frac{16 \log(x_+)}{3} + \frac{20}{3} \right) \\
& \left. + \frac{8L_Z^2}{9} - \frac{12M_Z^4}{M_W^4} + \frac{22M_Z^2}{M_W^2} + 2\pi^2 \right] - \frac{2 \log^2(x_-)}{x_+ (2s_W^2 - 3)} + \frac{448 + 36\pi^2}{27 - 18s_W^2},
\end{aligned} \tag{5.19}$$

and for down-type initial state quarks the coefficients read

$$\gamma_{\overline{d\bar{d},L}^{(1)}} = -3 \frac{1}{s_W^2} - \frac{5}{9} \frac{1}{c_W^2} + \frac{20}{9}, \tag{5.20}$$

$$\gamma_{\overline{d\bar{d},L}^{(2)}} = \frac{1}{s_W^4} \left(2\pi^2 - \frac{70}{3} \right) + \frac{1}{c_W^4} \frac{520}{81} - \frac{1600}{243}, \tag{5.21}$$

$$\zeta_{\overline{d\bar{d},L}^{(1)}} = \frac{21}{4} \frac{1}{s_W^2} + \frac{13}{12} \frac{1}{c_W^2} - \frac{1}{3}, \tag{5.22}$$

$$\xi_{\overline{d\bar{d},L}^{(1)}} = \left(\frac{1}{s_W^2} + \frac{5}{9} \frac{1}{c_W^2} - \frac{20}{9} \right) L_Z - \frac{1}{s_W^2} \frac{3}{2} \frac{m_t^2}{M_W^2}, \tag{5.23}$$

$$\begin{aligned}
\chi_{\overline{d\bar{d},L}^{(1)}} & = \frac{1}{s_W^2} \left[\log(x_-) - 5 \log(x_+) \right] + \frac{3}{c_W^2} \log\left(\frac{x_-}{x_+}\right) - \frac{4}{3} \log\left(\frac{x_+}{x_-}\right) \\
& + \frac{4}{4 - 3s_W^2} \log(x_-),
\end{aligned} \tag{5.24}$$

$$\begin{aligned}
(\widetilde{\chi^2})_{\overline{d\bar{d},L}^{(1)}} & = \frac{1}{27c_W^6 s_W^4 - 9c_W^4 s_W^6} \left[\left(-64s_W^{10} + 592s_W^8 - 1840s_W^6 + 2508s_W^4 \right. \right. \\
& - 1548s_W^2 + 351 \left. \right) \log^2(x_-) + \left(128s_W^{10} - 896s_W^8 + 1952s_W^6 \right. \\
& - 1668s_W^4 + 432s_W^2 + 54 \left. \right) \log(x_-) \log(x_+) + \log^2(x_+) \\
& \left. \times \left(-64s_W^{10} + 304s_W^8 - 544s_W^6 + 456s_W^4 - 180s_W^2 + 27 \right) \right],
\end{aligned} \tag{5.25}$$

$$\begin{aligned}
\sigma_{0\overline{d\bar{d},L}^{(1)}} & = \frac{1}{s_W^2} \left[L_{x_H}^2 - \beta_H L_{x_H} \frac{M_H^2}{4(M_H^2 - 4M_W^2)} \left(\frac{M_H^6}{M_W^6} - \frac{7M_H^4}{M_W^4} + \frac{20M_H^2}{M_W^2} - 28 \right) \right. \\
& + L_H \left(-\frac{M_H^6}{4M_W^6} + \frac{5M_H^4}{4M_W^4} - \frac{3M_H^2}{M_W^2} + 1 \right) + L_{W \text{ top}} \left(\frac{3m_t^2}{M_W^2} - \frac{3m_t^6}{M_W^6} \right) \\
& \left. + \frac{L_{xz}^2}{2} - \frac{L_Z^2}{2} + \frac{L_{xz} M_Z^2 \left(-\frac{27M_Z^6}{M_W^6} + \frac{171M_Z^4}{M_W^4} - \frac{250M_Z^2}{M_W^2} + 28 \right) \beta_Z}{4M_W^2 \left(\frac{M_Z^2}{M_W^2} - 4 \right)} \right]
\end{aligned}$$

$$\begin{aligned}
& +L_Z \left(-\frac{27M_Z^6}{4M_W^6} + \frac{117M_Z^4}{4M_W^4} - \frac{39M_Z^2}{2M_W^2} + 2 \log \left(\frac{x_-}{x_+} \right) - \frac{13}{2} \right) \\
& + \frac{3L_{top}m_t^2}{M_W^2} + \frac{\log^2(x_+)}{2x_-} - \frac{5 \log^2(x_-)}{2x_+} + \frac{3m_t^2}{M_W^2} - \frac{3m_t^4}{M_W^4} \\
& + \left[\frac{M_H^4}{2M_W^4} - \frac{2M_H^2}{M_W^2} + \frac{27M_Z^4}{2M_W^4} - \frac{34M_Z^2}{M_W^2} - \frac{5\pi^2}{3} + \frac{575}{36} \right] \\
& + \frac{1}{c_W^2} \left[-\frac{L_{xz}^2}{2} + \beta_Z L_{xz} \frac{M_Z^2}{2(M_Z^2 - 4M_W^2)} \left(\frac{M_Z^4}{M_W^4} - \frac{9M_Z^2}{M_W^2} + 18 \right) \right. \\
& - \frac{L_Z^2}{18} + L_Z \left(\frac{M_Z^4}{2M_W^4} - \frac{7M_Z^2}{2M_W^2} - \frac{2 \log(x_-)}{3} + \frac{2 \log(x_+)}{3} + \frac{5}{6} \right) \\
& \left. - \frac{\log^2(x_+)}{6x_-} + \frac{\log^2(x_-)}{6x_+} - \frac{M_Z^2}{M_W^2} + \frac{5\pi^2}{27} - \frac{731}{36} \right] \\
& + \left[2L_{xz}^2 + \beta_Z L_{xz} \frac{M_Z^2}{4M_W^2 - M_Z^2} \left(-\frac{6M_Z^6}{M_W^6} + \frac{34M_Z^4}{M_W^4} - \frac{39M_Z^2}{M_W^2} + 4 \right) \right. \\
& + L_Z \left(\frac{6M_Z^6}{M_W^6} - \frac{22M_Z^4}{M_W^4} + \frac{9M_Z^2}{M_W^2} - \frac{8 \log(x_-)}{3} + \frac{8 \log(x_+)}{3} + \frac{14}{3} \right) \\
& \left. + \frac{8L_Z^2}{9} - \frac{12M_Z^4}{M_W^4} + \frac{22M_Z^2}{M_W^2} + 2\pi^2 \right] - \frac{2 \log^2(x_-)}{x_+(4s_W^2 - 3)} + \frac{800 - 36\pi^2}{27 - 36s_W^2}.
\end{aligned} \tag{5.26}$$

The one-loop logarithmic corrections are checked according to appendix A.7. In the longitudinal case the matrix of soft anomalous dimensions and the constant contain contributions - the last two terms of eqs. (5.19,5.26)- which cannot be separated completely into particular gauge group contributions. This is due to interactions of a scalar current coupling to a vector boson. In particular, the diagrams generating this contribution are box diagrams where the charged final state Goldstone bosons couple to a neutral scalar boson and a W -boson. Here, the amplitude is of pure $SU(2)$ origin while it factorizes with respect to an s -channel Born cross section with the photon and Z -boson as intermediate gauge bosons. Such non-separable contributions arise, however, only for quark initial states and is not observed for lepton initial states. This is related to the structure of the Born cross section 2.14, where the s_W -dependence of the numerator vanishes only for lepton-charges.

5.2 Partonic Results

In this section the numerical values of radiative corrections are presented with respect to differential Born cross section, regarding W -pair production in $q\bar{q}$

annihilation, i.e. in partonic level. In the following we give the numerical results on partonic level using the input parameters given in eq. 4.57. For convenience we introduce $L^n = \log^n(\hat{s}/W^2)$. Here, \hat{s} denotes the partonic center of mass energy squared, which is different from the collider center of mass energy squared s , as will be discussed in the next section. The correction factors are labeled indicating initial states $u\bar{u}$ and $d\bar{d}$, as well as transverse and longitudinal polarization of the final states. For the particular corrections to the Born approximation with regard to specific initial and final states we obtain

$$\begin{aligned}
\delta_{u\bar{u},T}^{(1)} &= -4.85L^2 + \left[\left(-6.77 + 4\frac{x_-}{x_+} \right) \log(x_-) + 2.77 \log(x_+) + 4.86 \right] L \\
&+ \frac{1}{x_-^2 + x_+^2} \left(-0.93x_-^2 + 1.55x_-x_+ - 2.48x_+^2 - 4.97\frac{x_-^3}{x_+} \right) \log^2(x_-) \\
&+ 3\frac{x_-^2 + x_-x_+}{x_-^2 + x_+^2} \log^2(x_+) + \frac{4}{x_+} \log(x_-) \log(x_+) + 0.70 \log(x_-) \\
&+ \left(\frac{-4.97x_-^2 - 0.42x_-x_+ + 4.55x_+^2}{x_-^2 + x_+^2} - 0.70 \log(x_+) \right) \\
&+ \frac{16.51x_-^2 - 2.48x_-x_+ + 14.03x_+^2}{x_-^2 + x_+^2} - 17.23, \tag{5.27}
\end{aligned}$$

$$\begin{aligned}
\delta_{u\bar{u},T}^{(2)} &= 11.76L^4 + \left[\left(32.82 - 19.40\frac{x_-}{x_+} \right) \log(x_-) - 13.42 \log(x_+) - 17.34 \right] L^3 \\
&+ \left[\left(\frac{4.53x_-^2 - 7.52x_-x_+ + 12.04x_+^2}{x_-^2 + x_+^2} + \frac{24.08x_-^3}{(x_-^2 + x_+^2)x_+} + 4\frac{x_-^2}{x_+^2} \right. \right. \\
&- 15.07\frac{x_-}{x_+} + 22.90 \left. \right) \log^2(x_-) \\
&+ \left(-14.55\frac{x_-^2 + x_-x_+}{x_-^2 + x_+^2} + 3.83 \right) \log^2(x_+) \\
&+ \left(\frac{-0.93x_- - 19.40}{x_+} - 14.73 \right) \log(x_-) \log(x_+) + 10.52 \log(x_+) \\
&+ \left(\frac{24.08x_-^2 + 2.02x_-x_+ - 22.06x_+^2}{x_-^2 + x_+^2} + 13.13\frac{x_-}{x_+} - 23.64 \right) \log(x_-) \\
&+ \left. \frac{-80.08x_-^2 + 12.04x_-x_+ - 68.04x_+^2}{x_-^2 + x_+^2} + 78.66 \right] L^2, \tag{5.28}
\end{aligned}$$

$$\delta_{d\bar{d},T}^{(1)} = -5.00L^2 + \left[\left(-7.38 + 4\frac{x_-}{x_+} \right) \log(x_-) + 3.38 \log(x_+) + 5.41 \right] L$$

$$\begin{aligned}
& + \frac{1}{x_-^2 + x_+^2} \left(-0.93x_-^2 + 1.55x_-x_+ - 2.48x_+^2 - 4.97\frac{x_-^3}{x_+} \right) \log^2(x_-) \\
& + 3\frac{x_-^2 + x_-x_+}{x_-^2 + x_+^2} \log^2(x_+) + \frac{4}{x_+} \log(x_-) \log(x_+) - 0.85 \log(x_+) \\
& + \left(\frac{-4.97x_-^2 - 0.42x_-x_+ + 4.55x_+^2}{x_-^2 + x_+^2} + 0.85 \right) \log(x_-) \\
& + \frac{16.51x_-^2 - 2.48x_-x_+ + 14.03x_+^2}{x_-^2 + x_+^2} - 17.40, \tag{5.29}
\end{aligned}$$

$$\begin{aligned}
\delta_{d\bar{d},T}^{(2)} & = 12.52L^4 + \left[\left(36.94 - 20.01\frac{x_-}{x_+} \right) \log(x_-) - 16.93 \log(x_+) - 20.90 \right] L^3 \\
& + \left[\left(\frac{4.67x_-^2 - 7.76x_-x_+ + 12.42x_+^2}{x_-^2 + x_+^2} + 4\frac{x_-^2}{x_+^2} - 17.54\frac{x_-}{x_+} \right. \right. \\
& + \left. \left. \frac{24.85x_-^3}{(x_-^2 + x_+^2)x_+} + 27.26 \right) \log^2(x_-) \right. \\
& + \left. \left(-15.01\frac{x_-^2 + x_-x_+}{x_-^2 + x_+^2} + 5.73 \right) \log^2(x_+) \right. \\
& + \left. \left(\frac{1.54x_- - 20.01}{x_+} - 20.99 \right) \log(x_-) \log(x_+) + 16.22 \log(x_+) \right. \\
& + \left. \left(\frac{24.85x_-^2 + 2.08x_-x_+ - 22.76x_+^2}{x_-^2 + x_+^2} + 15.29\frac{x_-}{x_+} - 31.51 \right) \log(x_-) \right. \\
& + \left. \frac{-82.63x_-^2 + 12.42x_-x_+ - 70.20x_+^2}{x_-^2 + x_+^2} + 85.19 \right] L^2, \tag{5.30}
\end{aligned}$$

$$\begin{aligned}
\delta_{u\bar{u},L}^{(1)} & = -2.50L^2 + \left[-8.24 \log(x_-) + 0.97 \log(x_+) - 3.05 \right] L \\
& - \frac{2.37}{x_+} \log^2(x_-) + \frac{0.55}{x_-} \log^2(x_+) + 0.24 \log(x_-) - 0.24 \log(x_+), \\
& + 34.93,
\end{aligned}$$

$$\begin{aligned}
\delta_{u\bar{u},L}^{(2)} & = 3.12L^4 + \left[20.60 \log(x_-) - 2.42 \log(x_+) + 11.14 \right] L^3 \\
& + \left[\left(\frac{5.92}{x_+} + 24.73 \right) \log^2(x_-) + \left(-\frac{1.37}{x_-} + 0.47 \right) \log^2(x_+) \right. \\
& + 2.57 \log(x_-) \log(x_+) + 32.67 \log(x_-) - 14.46 \log(x_+) \\
& \left. - 104.31 \right] L^2, \tag{5.31}
\end{aligned}$$

$$\begin{aligned}
\delta_{d\bar{d},L}^{(1)} &= -2.65L^2 + \left[-10.07 \log(x_-) + 1.18 \log(x_+) - 2.51 \right] L \\
&\quad - \frac{2.67}{x_+} \log^2(x_-) + \frac{0.45}{x_-} \log^2(x_+) + 0.30 \log(x_-) - 0.30 \log(x_+), \\
&\quad + 31.23, \\
\delta_{d\bar{d},L}^{(2)} &= 3.52L^4 + \left[26.73 \log(x_-) - 3.14 \log(x_+) + 9.44 \right] L^3 \\
&\quad + \left[\left(\frac{7.09}{x_+} + 34.98 \right) \log^2(x_-) + \left(-\frac{1.19}{x_-} + 0.70 \right) \log^2(x_+) \right. \\
&\quad \left. + 1.86 \log(x_-) \log(x_+) + 7.80 \log(x_-) - 10.73 \log(x_+) - 92.32 \right] L^2.
\end{aligned} \tag{5.32}$$

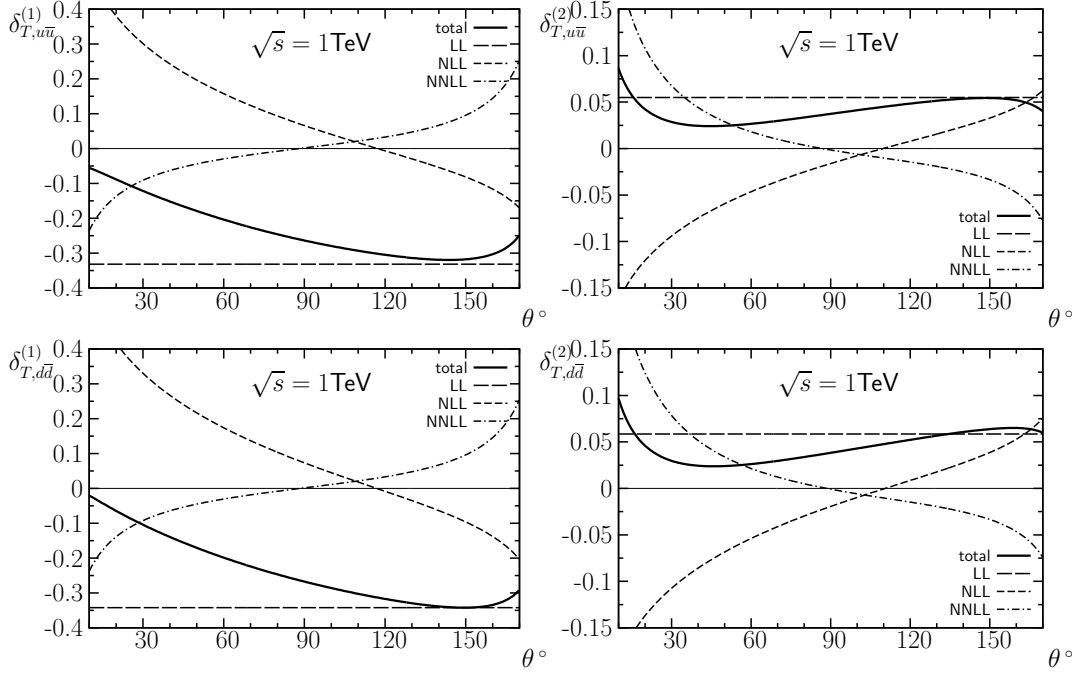


Figure 5.1: One-loop (left-hand side) and two-loop (right-hand side) corrections to the partonic differential distribution for the pair-production of transversely polarized W -boson with up-type (upper half) and down-type (lower half) quark initial states.

The corresponding corrections to the leading order differential distribution are depicted in fig. 5.1 and fig. 5.2 for transverse and longitudinally polarized W -bosons respectively. Indeed, one can barely observe a difference between

up-type and down-type quark initial states, which carry the same $SU(2)$ and $U(1)_Y$ quantum numbers as far as left-handed initial states are concerned.

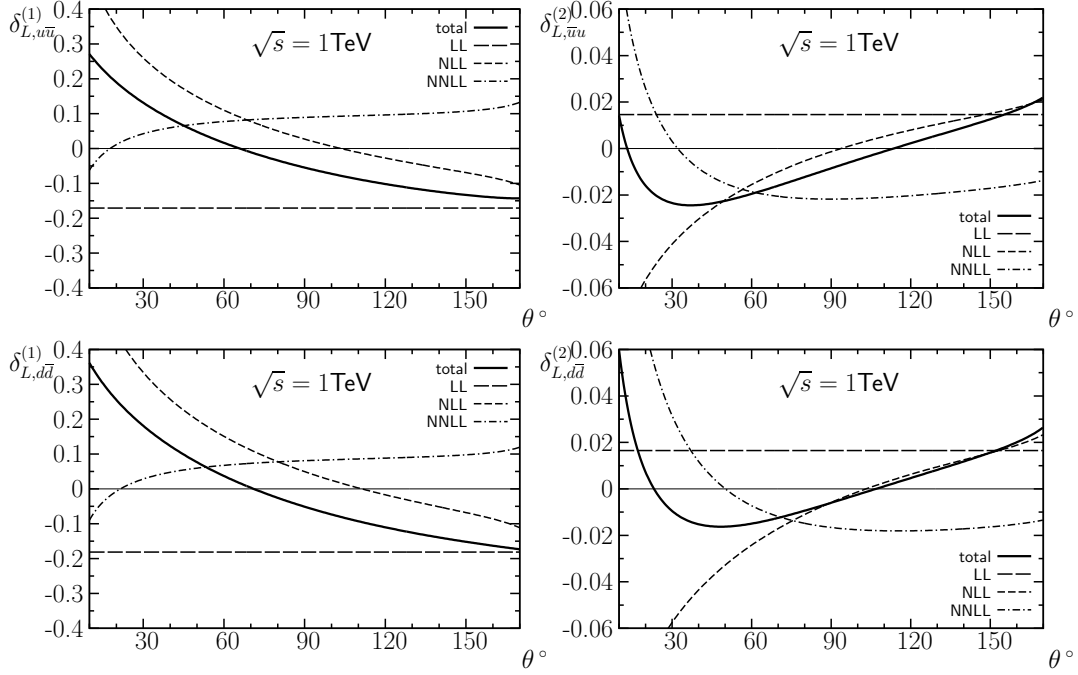


Figure 5.2: The same as fig. 5.1 but for the production of a pair of longitudinally polarized W -bosons.

5.3 Hadronic Results

In this section we study the impact of electroweak corrections to W -pair production at the LHC, i.e. W -pair production in proton-proton collisions at $\sqrt{s} = 14$ TeV. Up to now, we have only considered W -pair production in quark-antiquark annihilation, where the actual center of mass energy of the participating quarks $\sqrt{\hat{s}}$ is only a fraction of the collider energy \sqrt{s} , and obeys the relation $\hat{s} = x_1 x_2 s$. Here, x_1 and x_2 are the momentum fractions carried by the partons. To accommodate the protons substructure, the cross section on partonic level has to be convoluted with parton distribution functions $f_{h,i}(x, \mu^2)$, where $f_{h,i}(x, \mu^2)dx$ is the probability of finding a parton i in hadron h carrying a momentum fraction between x and $x + dx$. The factorization scale μ , which gives the scale where short distance effects become relevant, is chosen to be the transverse momentum p_T . After convolution with the parton distribution functions, electroweak corrections at hadronic level are obtained. The convolution with parton distribution functions is performed using the MRST package [41], providing the leading order parton distributions, which is implemented in *fortran77*. The hadronic cross section is related to the partonic cross section by

$$\frac{d\sigma}{dp_T} = \frac{1}{N_c^2} \sum_{ij} \int_0^1 dx_1 \int_0^1 dx_2 f_{h_1,i}(x_1, \mu^2) f_{h_2,j}(x_2, \mu^2) \theta(x_1 x_2 - \tau_{\min}) \frac{d\hat{\sigma}_{ij}}{p_T}, \quad (5.33)$$

where $p_T = \frac{1}{2}\sqrt{\hat{s} - 4M_W^2} \sin \theta$ is the transverse momentum of the W bosons and N_c is the number of colours. The indices i and j denote the particular initial state partons of the hadrons h_1 and h_2 . $\hat{\sigma}_{ij}$ is the partonic cross section for the subprocess with partons i and j and the sum runs over all possible i, j combinations. The quantity τ_{\min} is related to the minimum partonic energy that is needed to produce two W -bosons with a given transverse momentum p_T

$$\tau_{\min} = \frac{4(p_T^2 + M_W^2)}{s}. \quad (5.34)$$

We point out that we include only left-handed initial state quarks. On partonic level the right-handed initial states do not contribute at leading order to the production of transversely polarized W -bosons and are suppressed by s_W^4 regarding the production of a pair of longitudinally polarized W -bosons.

The p_T distribution of the partonic cross section can be obtained from the angular distribution according to

$$\frac{d\hat{\sigma}_{ij}}{p_T} = \left| \frac{d \cos \theta}{dp_T} \right| \left(\frac{d\hat{\sigma}_{ij}(x_+, x_-)}{d \cos \theta} + \frac{d\hat{\sigma}_{ij}(x_-, x_+)}{d \cos \theta} \right), \quad 0 \leq \cos \theta \leq 1, \quad (5.35)$$

with the Jacobian given by

$$\left| \frac{d \cos \theta}{dp_T} \right| = \frac{4p_T}{\sqrt{s(x_1 x_2 s - 4M_W^2)} \sqrt{x_1 x_2 - \tau_{\min}}}. \quad (5.36)$$

To implement the numerical results in an integration algorithm we perform a variable transformation

$$\begin{aligned} x_1 &= (1 - \tau)z_1^2 + \tau_{\min}, \\ x_2 &= \frac{(1 - \tau)z_1^2 z_2^2 + \tau_{\min}}{(1 - \tau)z_1^2 + \tau}, \end{aligned} \quad (5.37)$$

to get rid of a singularity of the integrand at $x_1 x_2 = \tau_{\min}$ in eq. 5.35 and stabilize the numerical integration. The p_T distribution which enters the integration algorithm then takes the form

$$\begin{aligned} \frac{d\sigma}{dp_T} &= \frac{16p_T}{N_c^2 s} \sum_{ij} \int_0^1 dz_1 \int_0^1 dz_2 C(z_1, z_2, \tau) f_{h_1, i}(x_1, \mu^2) f_{h_2, j}(x_2, \mu^2) \\ &\times \left(\frac{d\hat{\sigma}_{ij}(x_+, x_-)}{d \cos \theta} + \frac{d\hat{\sigma}_{ij}(x_-, x_+)}{d \cos \theta} \right) \end{aligned} \quad (5.38)$$

where

$$C(z_1, z_2, \tau) = \frac{1}{\sqrt{z_1^2 z_2^2 + 4p_T^2 / (s(1 - \tau_{\min}))}} \frac{(1 - \tau_{\min})z_1^2}{(1 - \tau_{\min})z_1^2 + \tau_{\min}}. \quad (5.39)$$

The numerical results are obtained using the integration routine *CUHRE*, which is provided in the *CUBA* library [42].

The p_T distributions of the differential cross section at leading order, and including higher order corrections, are depicted in figs. (5.3,5.4) for the transverse and longitudinal case. The relative higher order corrections with respect to the Born approximation are illustrated in fig. 5.5. We find a strong enhancement of the p_T distribution due to next-to-leading order corrections. For the production of transversely polarized W -pairs the one-loop corrections amount to 40% at $p_T = 1$ TeV and 60% at $p_T = 2$ TeV. The two-loop contributions amount to 10% corrections at $p_T = 1$ TeV and 20% at $p_T = 2$ TeV. In the longitudinal case the radiative corrections are not as large as the ones regarding the transverse case. This is because the Casimir operators, which govern the leading logarithmic contributions, are smaller for the Goldstone bosons, describing the longitudinal degrees of freedom, than the ones for the transversely polarized W -bosons. Here, the one-loop corrections amount to 15% (30%) at $p_T = 1$ (2) TeV. The two-loop contribution does not exceed a few percent up to $p_T = 2$ TeV.

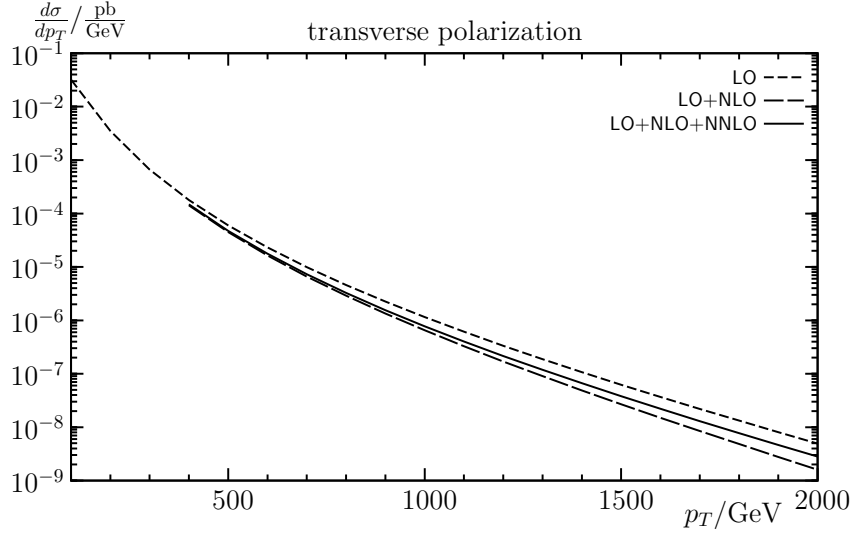


Figure 5.3: The p_T distribution for the production of transversely polarized W pairs. LO denotes the leading order contribution and NLO(NNLO) denotes the one-loop and two-loop corrections relative to the leading order.

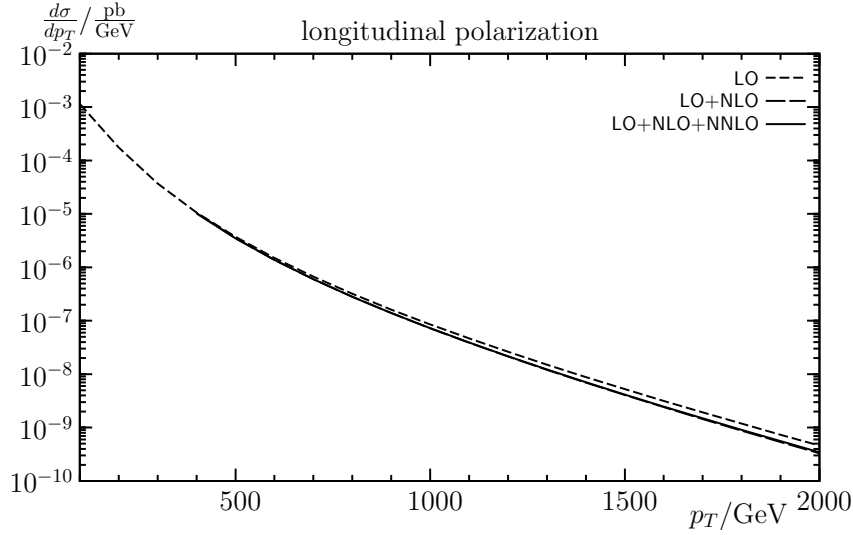


Figure 5.4: p_T distribution for the production of longitudinally polarized W pairs with same notation as fig. 5.3.

Finally, let us consider the invariant mass distribution for W -pair production, where the invariant mass is given by $M_{WW} = \sqrt{(k_1 + k_2)^2}$, with $k_{1,2}$ being

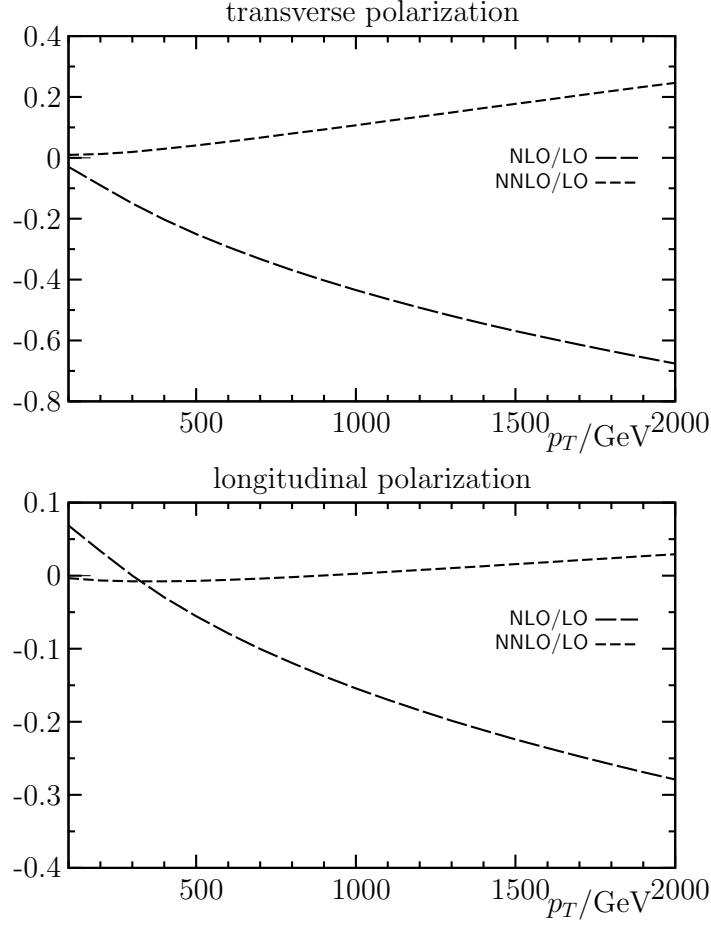


Figure 5.5: p_T distribution of one-loop and two-loop corrections relative to the leading order for the production of transverse and longitudinally polarized W pairs.

the momenta of the produced W -bosons. The invariant mass distribution reads

$$\frac{d\sigma}{dM_{WW}} = \frac{1}{N_c^2} \sum_{ij} \int_0^1 dx_1 \int_0^1 dx_2 f_{h_1,i}(x_1, \mu^2) f_{h_2,j}(x_2, \mu^2) \frac{d\hat{\sigma}_{ij}(M_{WW}^2)}{dM_{WW}}, \quad (5.40)$$

where

$$\frac{d\hat{\sigma}_{ij}(M_{WW}^2)}{dM_{WW}} = \int_{-\alpha}^{\alpha} d\cos\theta \frac{d\hat{\sigma}_{ij}(M_{WW}^2)}{d\cos\theta} \delta(\sqrt{x_1 x_2 s} - M_{WW}). \quad (5.41)$$

The leading order invariant mass distribution for W -pair production is depicted in fig. 5.6 with an angular cutoff $\alpha = 0.866$, corresponding to 30 de-

grees. In fig. 5.7 the radiative corrections to this distributions are illustrated. We observe the corrections to be of similar form and size with respect to the ones obtained for lepton colliders, figs. (4.4, 4.5). This is due to the fact that the dominant contribution to radiative corrections is of $SU(2)$ nature, with quarks and leptons having the same $SU(2)$ quantum numbers.

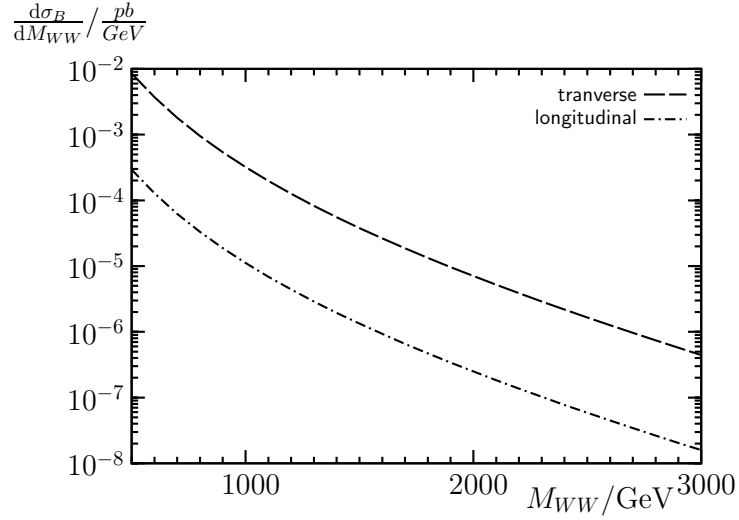


Figure 5.6: The invariant mass distribution relative to the Born approximation for the production of transversely and longitudinally polarized W pairs.

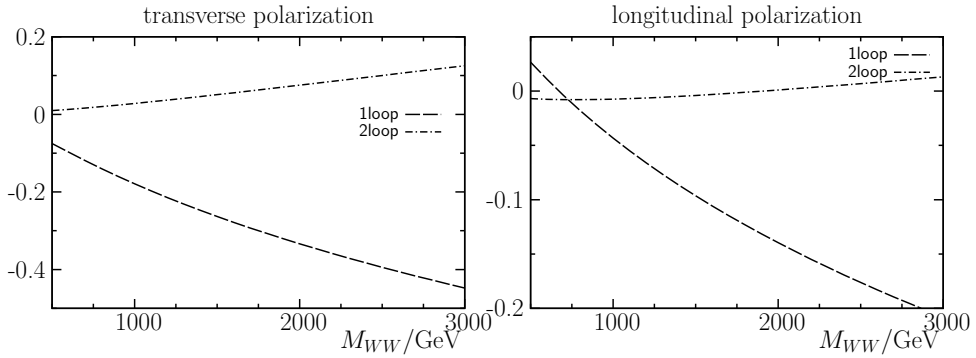


Figure 5.7: The electroweak one-loop and two-loop corrections to the invariant mass distribution relative to the Born approximation.

Note that also the leading order cross section is obtained in the high energy limit, therefore the p_T and M_{WW} distribution for small p_T are not reproduced correctly. The uncertainty of the theoretical predictions for on-shell

W -pair production at large scattering angles is driven by the unknown two-loop linear logarithmic terms and $\mathcal{O}(\alpha^3)$ corrections. We restrict ourselves to logarithmic enhanced two-loop corrections. In principle, with the coefficients presented in this work, the NNLL three-loop terms can be obtained with the evolution equation approach. The only difficulties are related to the Yukawa sector in the longitudinal part. However, for the pair-production of longitudinally polarized W -bosons, the three-loop corrections turn out to be in the size of a few per mille for center of mass energies of few TeV and, therefore, are negligible. The three-loop corrections regarding the production of transversely polarized W -pairs are in the one percent range for center of mass energies of 1-2 GeV, due to large cancellations of the leading and next-to-leading logarithms. Thus, for LHC distributions, the inclusion of three-loop terms is not necessary. Yet, to include these corrections is straightforward as long as only the transverse part is concerned.

The inclusion of the N^3LL term would be desirable to improve the theoretical accuracy. Concerning the longitudinal case, a rough estimate of the N^3LL term can be obtained by looking into the four fermion process. Since the Goldstone bosons (i.e. the longitudinal degrees of freedom of the W -bosons) exhibit the same quantum charges as fermions, a glance at the four fermion process provides us with an estimate of the N^3LL contribution. For the fermion pair production such terms are known to contribute about 1–2% of the cross section [14]. Therefore, we assume that this contribution is fairly negligible with respect to the production of longitudinally polarized W -pairs. For the case of transverse W -bosons, however, these contributions are not possible to estimate and might lead to significant contributions to radiative corrections, since the two-loop corrections already rise up to 20% for the p_T distribution and 10% for invariant mass distribution.

To derive two-loop N^3LL corrections the two-loop values of the soft anomalous dimensions ζ and ξ have to be known, such that an explicit two-loop calculation is necessary. For the production of longitudinally polarized W -pairs, where only s-channel diagrams contribute at leading order, these coefficients can be found in the two-loop corrections to the vertex form factors. The case of production of transversely polarized W -pair is more involved because here two-loop corrections to the full process have to be taken into account.

Chapter 6

Conclusions

The production of W -pairs is an important process both for LHC and ILC. First of all, the W -pair provides a probe of the triple gauge coupling, which couples a pair of W -bosons and a neutral gauge boson. This coupling uniquely appears in that form in the Electroweak Standard Model. On the other hand, W -pairs have to be considered as a background to many processes, in particular for the Higgs search in the channel $H \rightarrow W^+W^-$. Hence precise theoretical predictions to the both Higgs decay and the background are desired in order to disentangle the background from a possible Higgs signature.

In this work we evaluated electroweak corrections to the on-shell W -pair production at both lepton and hadron colliders. To derive the higher order corrections we adopted the evolution equation approach which provides a powerful tool to derive leading logarithmic corrections without performing a full loop calculation in the desired order of perturbation theory. It is shown that in the high energy regime the radiative can be split in two parts, one related to exchange of massive gauge bosons and another one related to exchange of the massless photon. This decomposition leads to two differential equations, the hard evolution equation and the infrared evolution equation. These two sets of evolution equations completely determine the dependence of the amplitudes on the two dimensionless variables Q/M_W and Q/λ up to the initial conditions which are fixed by the matching procedure. We applied this approach to derive next-to-next-to leading logarithmic corrections at two-loop level.

We observed large cancellations in particular between the next-to-leading and next-to-next-to leading logarithms for almost the whole angular distribution for both the production of transverse vector bosons and scalar (Goldstone) bosons. Hence, to include only NLL in a logarithmic approximation seems

to rather worsen the accuracy and one is better off when only the leading logarithmic corrections are included.

In this work only left-handed initial states have been considered. For the transverse part right-handed initial states do not contribute at leading order and are therefore fairly negligible. For the longitudinal part the right-handed initial states do couple only by hypercharge, and are suppressed by s_W^4 with respect to the right-handed initial states. Yet it is desirable to include processes involving right-handed initial quarks to account for the non-polarized initial states in hadron colliders.

For lepton colliders, the polarization of the initial state particles is technically possible, such that the exclusion of right-handed electrons does not cause any trouble, whereas this is not the case for LHC. Here, the exclusion of partons lead to errors which could easily be removed by taking into account right-handed initial states. Therefore, this is a desirable task for forthcoming calculations.

Furthermore, we restricted ourselves to quark initial states. At LHC, also processes with initial state gluons contribute. However, compared to the process $qq \rightarrow WW$, the cross section of $gg \rightarrow W^+W^-$ is about an order of magnitude smaller [40].

We should emphasize that we made use of the high energy approximation, which is strictly only valid for large scattering angles and breaks down at small production angles where the angular dependent logarithms become large. Yet it provides a fairly good approximation for nearly the whole angular regime. The quality of this approximation is discussed in detail in [21].

Appendix A

Appendix

A.1 Reduction of Gamma Matrices

Any product consisting of Dirac matrices $\Gamma^{\alpha\dots\beta} = \gamma^\alpha \dots \gamma^\beta$ can be decomposed in a basic set of Dirac matrices

$$\begin{aligned} 1 & \text{ scalar ,} \\ \gamma_\mu & \text{ vector ,} \\ \sigma_{\mu\nu} & \text{ tensor ,} \\ \gamma_\mu \gamma_5 & \text{ pseudo-vector ,} \\ \gamma_5 & \text{ pseudo-scalar ,} \end{aligned}$$

according to

$$\Gamma_{\text{red}}^\mu = \frac{1}{4}(c_1 + c_2 \gamma_5 + c_3^\mu \gamma_\mu + c_4^\mu \gamma_\mu \gamma_5 + c_5^{\mu\nu} \sigma_{\mu\nu}), \quad (\text{A.1})$$

with $\sigma_{\mu\nu} = \frac{i}{2}[\gamma_\mu, \gamma_\nu]$. The coefficients are given by

$$\begin{aligned} c_1 &= \text{Tr}[\Gamma], \\ c_2 &= \text{Tr}[\gamma_5 \Gamma], \\ c_3^\mu &= \text{Tr}[\gamma^\mu \Gamma], \\ c_4^\mu &= -\text{Tr}[\gamma^\mu \gamma_5 \Gamma], \\ c_5^{\mu\nu} &= \frac{1}{2} \text{Tr}[\sigma^{\mu\nu} \Gamma]. \end{aligned} \quad (\text{A.2})$$

A.2 Group Theory

A $SU(N)$ transformation on N -component spinor fields ψ is given by

$$\psi' = \exp(i\theta_a T^a) \psi. \quad (\text{A.3})$$

The generators of the transformation T_a are specified by their commutation relations

$$[T^a, T^b] = i f^{abc} T^c, \quad (\text{A.4})$$

where f^{abc} is the totally antisymmetric structure constant of $SU(N)$ and satisfy the anticommutation relation

$$\{T^a, T^b\} = \frac{1}{N} \delta^{ab} + d^{abc} T^c, \quad (\text{A.5})$$

where d^{abc} is the totally symmetric. Therewith

$$T^a T^b = \frac{1}{2N} \delta^{ab} + \frac{1}{2} d^{abc} T^c + \frac{1}{2} i f^{abc} T^c. \quad (\text{A.6})$$

For an irreducible representation

$$\text{Tr}[T^a T^b] = T_R \delta^{ab}, \quad (\text{A.7})$$

where the Dynkin index $T_R = 1/2$ for $SU(N)$. In the fundamental representation, the Casimir operator is given by

$$\sum_a (T^a)_{ij} (T^a)_{jk} = C_F \delta_{ik}, \quad (\text{A.8})$$

with

$$C_F = \frac{N^2 - 1}{2N}. \quad (\text{A.9})$$

For the adjoint representation, the $N^2 - 1$ dimensional representation matrices are given by the structure constants

$$(T^b)_{ac} = i f^{abc}. \quad (\text{A.10})$$

The Casimir operator in the adjoint representation reads

$$\sum_{ab} f^{abc} f^{abd} = C_A \delta^{ab}, \quad (\text{A.11})$$

with

$$C_A = N. \quad (\text{A.12})$$

A.3 Explicit Values of Charges

Explicit values of the gauge charges are

	Y/2	Q	T^3	$C_{SU(2)}$
$\nu_L, \bar{\nu}_l$	$\mp\frac{1}{2}$	0	$\pm\frac{1}{2}$	$\frac{3}{4}$
l_L, \bar{l}_L	$\mp\frac{1}{2}$	∓ 1	$\mp\frac{1}{2}$	$\frac{3}{4}$
l_R, \bar{l}_R	∓ 1	∓ 1	0	0
u_L, \bar{u}_L	$\pm\frac{1}{6}$	$\pm\frac{2}{3}$	$\pm\frac{1}{2}$	$\frac{3}{4}$
d_L, \bar{d}_L	$\pm\frac{1}{6}$	$\mp\frac{1}{3}$	$\mp\frac{1}{2}$	$\frac{3}{4}$
u_R, \bar{u}_R	$\pm\frac{2}{3}$	$\pm\frac{2}{3}$	0	0
d_R, \bar{d}_R	$\mp\frac{1}{3}$	$\mp\frac{1}{3}$	0	0
W^\pm	0	± 1	± 1	2
W^3	0	0	0	2
B	0	0	0	0

The scalar doublet $\Phi = (\phi^+, \phi_0)$, $\Phi^* = (\phi^-, \phi_0^*)$ transform according to the fundamental representation and its quantum numbers correspond to those of the left-handed leptons with

$$\begin{aligned} \phi^+ &\leftrightarrow \bar{l}_L, & \phi_0 &\leftrightarrow \bar{\nu}_L, \\ \phi^- &\leftrightarrow l_L, & \phi_0^* &\leftrightarrow \nu_L. \end{aligned} \quad (\text{A.13})$$

The electric charge, hypercharge and the weak isospin component T_3 obey the Gell-Mann-Nishijima relation

$$Q = \frac{Y}{2} + T_3. \quad (\text{A.14})$$

A.4 Summation of Light Fermion

In section 3.1 we introduced

$$\begin{aligned} \gamma_{ff}^{(2)} &= -2C_F \left[\left(\frac{67}{9} - \frac{\pi^2}{3} \right) C_A - \frac{4}{9}(5n_f + 2n_s)T_F \right], \\ \beta_0 &= \frac{11}{3}C_A - \frac{4}{3}T_F n_f - \frac{1}{3}T_F n_s, \end{aligned}$$

where $n_f = 6$ is the number of light fermions and $n_s = 1$ the number of scalar doublets. In the Electroweak Standard Model, however, the particular fermions carry different electromagnetic charge and hypercharge. Therefore one must not simply plug in the number of light fermions but take into account the correct charges of the underlying theory.

The sum of the charge squared of all standard model fermions per generation \sum_f in $U(1)_Y$ and $U(1)_{em}$ is given in the following table.

	ν_L	l_L	l_R	u_L	d_L	u_R	d_R	\sum_f
$Y^2/4$	$\frac{1}{4}$	$\frac{1}{4}$	1	$3 \times \frac{1}{36}$	$3 \times \frac{1}{36}$	$3 \times \frac{4}{9}$	$3 \times \frac{1}{9}$	$\frac{10}{3}$
Q^2	0	1	1	$3 \times \frac{4}{9}$	$3 \times \frac{1}{9}$	$3 \times \frac{4}{9}$	$3 \times \frac{1}{9}$	$\frac{16}{3}$

Thus one has to replace

$$T_F n_f \rightarrow \frac{5}{3} N_g \quad \text{for } U(1)_Y, \quad (\text{A.15})$$

$$T_F n_f \rightarrow \frac{8}{3} N_g \quad \text{for } U(1)_{em}. \quad (\text{A.16})$$

in the hard evolution equation, where $s \gg m_t^2$. Here, $N_g = 3$, denotes the number of generations. For the infrared evolution equation the top mass is non-negligible and has to exclude the top contribution in n_f such that

$$T_F n_f \rightarrow \frac{20}{3} \quad \text{for } U(1)_{em} \text{ with heavy top.} \quad (\text{A.17})$$

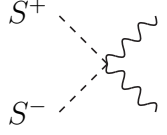
A.5 Feynman Rules of $U(1)_Y$

The Feynman rules to the spontaneously broken $U(1)_Y$ theory are given with respect to the quantum charge $Y/2$ which are presented in A.3.

$$\begin{array}{c} \text{---} \\ \diagup \\ \psi \\ \diagdown \\ \text{---} \\ \bar{\psi} \end{array} = -ig' \frac{Y_f}{2} \gamma^\mu, \quad (\text{A.18})$$

$$\begin{array}{c} \text{---} \\ \diagup \\ k_1 \text{---} S^+ \\ \diagdown \\ k_2 \text{---} S^- \\ \text{---} \end{array} = -ig' \frac{Y_S}{2} (k_1 - k_2)^\mu \quad \text{for } S = (\phi^-, \phi^0, H), \quad (\text{A.19})$$

$$\begin{array}{c} \text{---} \\ \diagup \\ H \\ \diagdown \\ \text{---} \end{array} = -ig' \frac{s_W}{c_W} M_W Y_H^2 g^{\mu\nu}, \quad (\text{A.20})$$



$$= -ig'^2 \frac{Y_S^2}{2} g^{\mu\nu}. \quad (\text{A.21})$$

The momenta k_1 and k_2 of the second diagram are assumed as incoming. We restrict ourselves to $U(1)_Y$ radiative corrections such that scalar self-couplings are not taken into account since they involve only $SU(2)$ couplings.

A.6 Counter Terms

The counterterms in the on-shell scheme are presented with the divergent part

$$\Delta = \frac{2}{\epsilon} - \gamma_E + \log(4\pi) \quad \text{for } D = 4 - \epsilon. \quad (\text{A.22})$$

The wave function renormalization constant of fermions f is given in terms of electromagnetic charge Q_f and its weak isospin component I_3 .

$$\begin{aligned} \delta Z_f &= -\Delta \frac{\left((2Q_f^2 s_W^2 + 1) c_W^2 + 2(I_3 - Q_f s_W^2)^2 \right)}{2c_W^2 s_W^2} + Q_f^2 \log\left(\frac{\lambda^2}{\mu^2}\right) \\ &+ \frac{\log\left(\frac{M^2}{\mu^2}\right) \left(c_W^2 + 2(I_3 - Q_f s_W^2)^2 \right)}{2c_W^2 s_W^2} + \frac{I_3^2}{2c_W^2 s_W^2} - \frac{Q_f I_3}{c_W^2} \\ &+ \frac{L_Z (I_3 - Q_f s_W^2)^2}{c_W^2 s_W^2} + Q_f^2 \left(\frac{s_W^2}{2c_W^2} + \frac{1}{2} \right) + \frac{1}{4s_W^2}, \\ \delta Z_W &= -\frac{5\Delta}{6s_W^2} + \frac{5}{6s_W^2} \log\left(\frac{M_W^2}{\mu^2}\right) + 2 \log\left(\frac{M_W^2}{\lambda^2}\right) + \frac{L_{top}}{s_W^2} \\ &+ \frac{M_W^6 - m_t^6}{M_W^6 s_W^2} L_{Wtop} + \beta_H L_{x_H} \left(\frac{M_H^4}{12M_W^4 s_W^2} - \frac{M_H^6}{24M_W^6 s_W^2} \right) \\ &+ L_H \left(-\frac{M_H^6}{12M_W^6 s_W^2} + \frac{3M_H^4}{8M_W^4 s_W^2} - \frac{3M_H^2}{4M_W^2 s_W^2} + \frac{1}{2s_W^2} \right) \\ &+ \frac{\beta_H L_{x_H}}{M_H^2 - 4M_W^2} \left(-\frac{M_H^8}{24M_W^6 s_W^2} + \frac{7M_H^6}{24M_W^4 s_W^2} - \frac{M_H^4}{M_W^2 s_W^2} + \frac{3M_H^2}{2s_W^2} \right) \\ &+ \beta_Z L_{x_Z} \left(\frac{(8s_W^2 - 9) M_Z^6}{24s_W^2 M_W^6} + \frac{(8c_W^2 + 1) M_Z^4}{12M_W^4 s_W^2} - \frac{2c_W^2 M_Z^2}{M_W^2 s_W^2} \right) \end{aligned}$$

$$\begin{aligned}
& + \frac{\beta_Z L_{xz}}{M_Z^2 - 4M_W^2} \left(\frac{(8s_W^2 - 9) M_Z^8}{24M_W^6 s_W^2} + \frac{(68c_W^2 + 7) M_Z^6}{24M_W^4 s_W^2} \right. \\
& \left. - \frac{(7s_W^4 - 13s_W^2 + 7) M_Z^4}{2c_W^2 M_W^2 s_W^2} + \frac{3(s_W^4 - 5c_W^4) M_Z^2}{2c_W^2 s_W^2} \right) \\
& + L_Z \left(\frac{(8s_W^2 - 9) M_Z^6}{12s_W^2 M_W^6} + \frac{(28c_W^2 + 3) M_Z^4}{8M_W^4 s_W^2} - \frac{(10s_W^4 - 17s_W^2 + 9) M_Z^2}{4c_W^2 M_W^2 s_W^2} \right. \\
& \left. + \frac{s_W^2}{2c_W^2} - \frac{5c_W^2}{2s_W^2} \right) - \frac{m_t^4}{M_W^4 s_W^2} - \frac{m_t^2}{2M_W^2 s_W^2} - \frac{M_H^2}{2M_W^2 s_W^2} + \frac{M_H^4}{6M_W^4 s_W^2} \\
& + \frac{(96M_W^2 c_W^4 + 12M_W^2 c_W^2) M_Z^4}{72c_W^2 M_W^6 s_W^2} - \frac{(360c_W^4 M_W^4 + 36c_W^2 M_W^4) M_Z^2}{72c_W^2 M_W^6 s_W^2} \\
& - \frac{35}{18s_W^2} + \frac{32}{9} + \frac{s_W^2}{c_W^2} + \frac{23c_W^2}{9s_W^2}. \tag{A.23}
\end{aligned}$$

The self energy contribution and mass counterterms needed for the Goldstone boson equivalence theorem at one-loop read

$$\begin{aligned}
\Sigma_L^W(M_W^2) &= \left(-\frac{M_W^2}{c_W^2} + \frac{m_t^2(3 - 3s_W^2)}{2c_W^2 s_W^2} + \frac{M_Z^2(2s_W^4 - 4s_W^2 + 2)}{2c_W^2 s_W^2} \right) \\
&\times \left(\log\left(\frac{M_W^2}{\mu^2}\right) - \Delta \right) + L_H \left(\frac{M_H^6}{8M_W^4 s_W^2} - \frac{M_H^4}{2M_W^2 s_W^2} - \frac{M_H^2}{8s_W^2} \right) \\
&\frac{3L_{Wtop} m_t^6}{2M_W^4 s_W^2} + \frac{(12c_W^2 M_W^2 - 24c_W^2 L_{Wtop} M_W^2) m_t^4}{8c_W^2 M_W^4 s_W^2} \\
&+ \frac{m_t^2}{8c_W^2 M_W^4 s_W^2} (12c_W^2 L_{top} M_W^4 + 12c_W^2 L_{Wtop} M_W^4 \\
&- 24c_W^2 M_W^4) + \beta_H L_{xH} \left(\frac{M_H^6}{8M_W^4 s_W^2} - \frac{M_H^4}{4M_W^2 s_W^2} - \frac{3M_H^2}{8s_W^2} \right) \\
&+ \beta_Z L_{xz} \left(\frac{(9 - 8s_W^2) M_Z^6}{8s_W^2 M_W^4} + \frac{(6s_W^2 - 7) M_Z^4}{4M_W^2 s_W^2} \right. \\
&+ \left. \frac{(8s_W^4 - 25s_W^2 + 13) M_Z^2}{8c_W^2 s_W^2} \right) + L_Z \left(\frac{(9 - 8s_W^2) M_Z^6}{8s_W^2 M_W^4} \right. \\
&+ \left. \frac{(7s_W^2 - 8) M_Z^4}{2s_W^2 M_W^2} + \frac{(24s_W^4 - 59s_W^2 + 31) M_Z^2}{8c_W^2 s_W^2} \right) \\
&+ \frac{M_Z^2 (16c_W^4 M_W^4 + 4c_W^2 M_W^4)}{8c_W^2 M_W^4 s_W^2} + \frac{2M_W^2}{c_W^2}, \\
\Sigma^{W\phi}(M_W^2) &= \left(\frac{3m_t^2}{2M s_W^2} - \frac{M(2s_W + 1)}{4c_W s_W} \right) \left(\Delta - \log\left(\frac{M^2}{\mu^2}\right) \right) - \frac{3L_{Wtop} m_t^6}{2M^5 s_W^2}
\end{aligned}$$

$$\begin{aligned}
& + \frac{3L_{Wtop}m_t^4}{M^3s_W^2} - \frac{3m_t^4}{2M^3s_W^2} - \frac{3L_{top}m_t^2}{2Ms_W^2} - \frac{3L_{Wtop}m_t^2}{2Ms_W^2} + \frac{3m_t^2}{Ms_W^2} \\
& + L_{x_H}\beta_H \left(-\frac{M_H^6}{8M^5s_W^2} + \frac{M_H^4}{4M^3s_W^2} + \frac{M_H^2}{4Ms_W^2} \right) \\
& + L_H \left[-\frac{M_H^6}{8M^5s_W^2} - \frac{M_H^4}{4M(M^2 - M_H^2)s_W^2} + \frac{M_H^4}{2M^3s_W^2} \right. \\
& \left. - \frac{M_H^2}{4Ms_W^2} + \frac{MM_H^2}{2(M^2 - M_H^2)s_W^2} + \frac{M}{4s_W^2} - \frac{M^3}{4(M^2 - M_H^2)s_W^2} \right] \\
& + L_Z \left(\left(-\frac{c_W^2}{8M^3s_W^2} + \frac{1}{8M^3s_W^2} - \frac{5}{4M^3} - \frac{s_W^2}{8M^3c_W^2} \right) M_Z^4 \right. \\
& \left. + \left(\frac{c_W^2}{4Ms_W^2} + \frac{7}{2M} - \frac{1}{2Ms_W^2} + \frac{3s_W^2}{4Mc_W^2} \right) M_Z^2 \right) \\
& + L_{x_Z}\beta_Z \left(\left(-\frac{c_W^2}{8M^3s_W^2} + \frac{1}{8M^3s_W^2} - \frac{5}{4M^3} - \frac{s_W^2}{8M^3c_W^2} \right) M_Z^4 \right. \\
& \left. + \left(\frac{s_W^2}{2Mc_W^2} + \frac{1}{M} - \frac{1}{4Ms_W^2} \right) M_Z^2 \right) + \frac{M_H^4}{4M^3s_W^2} - \frac{M_H^2}{2Ms_W^2} \\
& - \frac{7Ms_W^2}{4c_W^2} - \frac{3M}{2} + \frac{M_Z^2(9 - 8s_W^2)}{4Mc_W^2} + \frac{Mc_W^2}{4s_W^2} - \frac{M}{2s_W^2}, \\
\partial M_W^2 = & \left(\frac{M^2(s_W^2 + 5)}{6c_W^2s_W^2} - \frac{M_Z^2(s_W^2 - 1)^2}{c_W^2s_W^2} - \frac{3m_t^2}{2s_W^2} \right) \left(\Delta - \log \left(\frac{M^2}{\mu^2} \right) \right) \\
& + L_{x_H}\beta_H \left(-\frac{M_H^6}{24M^4s_W^2} + \frac{M_H^4}{6M^2s_W^2} - \frac{M_H^2}{2s_W^2} \right) \\
& + L_H \left(-\frac{M_H^6}{24M^4s_W^2} + \frac{M_H^4}{4M^2s_W^2} - \frac{3M_H^2}{4s_W^2} \right) + L_{top} \left(\frac{3m_t^2}{2s_W^2} - \frac{M^2}{s_W^2} \right) \\
& + L_{Wtop} \left(-\frac{m_t^6}{2M^4s_W^2} + \frac{3m_t^2}{2s_W^2} - \frac{M^2}{s_W^2} \right) \\
& + L_Z \left(\frac{(8s_W^2 - 9)M_Z^6}{24s_W^2M^4} + \frac{(10c_W^2 + 1)M_Z^4}{4M^2s_W^2} + \frac{(1 - 3s_W^2)M_Z^2}{4c_W^2s_W^2} \right) \\
& + L_{x_Z}\beta_Z \left(\frac{(8s_W^2 - 9)M_Z^6}{24s_W^2M^4} + \frac{(12 - 11s_W^2)M_Z^4}{6s_W^2M^2} \right. \\
& \left. + \frac{(5c_W^4 - s_W^4)M_Z^2}{2c_W^2s_W^2} \right) - \frac{m_t^4}{2M^2s_W^2} - \frac{m_t^2}{s_W^2} \\
& - \frac{(856c_W^4M^6 - 144s_W^4M^6 - 692c_W^2M^6 + 712c_W^2s_W^2M^6)}{72M^4c_W^2s_W^2}
\end{aligned}$$

$$\begin{aligned}
& -\frac{M_Z^4(-48M^2c_W^4 - 6M^2c_W^2)}{72M^4c_W^2s_W^2} - \frac{M_Z^2(432c_W^4M^4 + 36c_W^2M^4)}{72M^4c_W^2s_W^2} \\
& + \frac{M_H^4}{12M^2s_W^2} - \frac{M_H^2}{2s_W^2},
\end{aligned} \tag{A.24}$$

The counterterms to the electromagnetic coupling constant, the sinus of the weak mixing angle and the neutral vector boson propagators are

$$\delta Z_e = \frac{1}{2}\Delta\alpha - \frac{8}{9}L_{top} + \frac{11}{6}\log\left(\frac{\mu^2}{M_W^2}\right) - \frac{1}{3} + \frac{11}{6}\Delta,$$

where $\Delta\alpha$ is given in eq. 4.11,

$$\begin{aligned}
\delta Z_{sw} = & \left(\log\left(\frac{M^2}{\mu^2}\right) + \Delta\right) \left(\frac{M_Z^2(s_W^2 - 1)^2}{2M^2s_W^4} + \frac{25}{12s_W^2} - \frac{1}{2s_W^4} + \frac{11}{6}\right) \\
& + L_{x_H}\beta_H \left(\frac{c_W^2M_H^6}{48M^6s_W^4} - \frac{c_W^2M_H^4}{12M^4s_W^4} + \frac{c_W^2M_H^2}{4M^2s_W^4}\right) \\
& + L_{Wtop} \left(\frac{c_W^2m_t^6}{4M^6s_W^4} - \frac{3c_W^2m_t^2}{4M^2s_W^4} + \frac{c_W^2}{2s_W^4}\right) \\
& + L_{top} \frac{-32s_W^4 + 24s_W^2 + 18c_W^2 - 9}{36s_W^4} \\
& + L_{x_{HZ}}\beta_{HZ} \left(-\frac{M_H^6c_W^6}{48M^6s_W^4} + \frac{M_H^4c_W^4}{12M^4s_W^4} - \frac{M_H^2c_W^2}{4M^2s_W^4}\right) \\
& + L_H \left(\frac{M_H^6(c_W^2 - c_W^6)}{48M^6s_W^4} - \frac{M_H^4(1 - s_W^2)}{8s_W^2M^4}\right) \\
& + i\pi\beta_{Zt} \left(\left(\frac{4c_W^2}{3M^2s_W^2} + \frac{c_W^2}{4M^2s_W^4} - \frac{16c_W^2}{9M^2}\right)m_t^2 + \frac{2}{3s_W^2} - \frac{1}{4s_W^4} - \frac{8}{9}\right) \\
& + L_{x_{zt}}\beta_{Zt} \left(\frac{16m_t^2c_W^2}{9M^2} - \frac{4m_t^2c_W^2}{3M^2s_W^2} - \frac{m_t^2c_W^2}{4M^2s_W^4} - \frac{2}{3s_W^2} + \frac{1}{4s_W^4} + \frac{8}{9}\right) \\
& + i\pi\beta_Z \left(\frac{5c_W^6}{2s_W^4} - \frac{c_W^4}{3s_W^2} + \frac{13c_W^4}{8s_W^4} + \frac{c_W^2}{12s_W^2} - \frac{5}{6}c_W^2 - \frac{1}{24}\right) \\
& + L_Z \left(\frac{(8c_W^4 + c_W^2)M_Z^6}{48M^6s_W^4} - \frac{(10c_W^4 + c_W^2)M_Z^4}{8M^4s_W^4} + \frac{(3s_W^2 - 1)M_Z^2}{8M^2s_W^4}\right. \\
& \left. + \frac{10}{3s_W^2} + \frac{M_H^6c_W^6}{48M^6s_W^4} - \frac{M_H^4c_W^4}{8M^4s_W^4} + \frac{3M_H^2c_W^2}{8M^2s_W^4} - \frac{55}{24s_W^4} - \frac{40}{9}\right) \\
& + L_{x_Z}\beta_Z \left(\frac{(8c_W^4 + c_W^2)M_Z^6}{48M^6s_W^4} - \frac{(11c_W^4 + c_W^2)M_Z^4}{12M^4s_W^4} + \frac{(s_W^4 - 5c_W^4)M_Z^2}{4M^2s_W^4}\right)
\end{aligned}$$

$$\begin{aligned}
& + \frac{5c_W^2}{6} + \frac{c_W^4}{3s_W^2} - \frac{c_W^2}{12s_W^2} - \frac{5c_W^6}{2s_W^4} - \frac{13c_W^4}{8s_W^4} + \frac{1}{24} \Big) - \frac{20}{3s_W^2} + \frac{311}{72s_W^4} \\
& + M_Z^4 \left(-\frac{c_W^4}{3M^4 s_W^4} - \frac{c_W^2}{24M^4 s_W^4} \right) + M_H^4 \left(\frac{c_W^4}{24M^4 s_W^4} - \frac{c_W^2}{24M^4 s_W^4} \right) \\
& + M_Z^2 \left(\frac{3c_W^4}{M^2 s_W^4} + \frac{c_W^2}{4M^2 s_W^4} \right) + m_t^2 \left(\frac{32c_W^2}{9M^2} - \frac{8c_W^2}{3M^2 s_W^2} \right) + \frac{m_t^4 c_W^2}{4M^4 s_W^4} \\
& - \frac{5c_W^6}{s_W^4} + \frac{2c_W^4}{3s_W^2} + \frac{47c_W^4}{18s_W^4} + \frac{85c_W^2}{18s_W^2} - \frac{173c_W^2}{36s_W^4} + \frac{5c_W^2}{3} + 8, \\
\delta Z_{AA} &= -\Delta\alpha + \frac{16}{9}L_{top} - \frac{23}{3}\log\left(\frac{\mu^2}{M_W^2}\right) + \frac{2}{3} - \frac{23}{3}\Delta, \\
\delta Z_{AZ} &= \left(\Delta + \log\left(\frac{M^2}{\mu^2}\right)\right) \left(-\frac{34s_W}{3c_W} - \frac{7}{3c_W s_W}\right) \\
& + L_{top} \left(\frac{32s_W}{9c_W} - \frac{4}{3c_W s_W}\right) + L_Z \left(\frac{160s_W}{9c_W} - \frac{20}{3c_W s_W}\right) \\
& + i\pi\beta_{Zt} \left(\frac{64c_W s_W m_t^2}{9M^2} - \frac{8c_W m_t^2}{3M^2 s_W} + \frac{32s_W}{9c_W} - \frac{4}{3c_W s_W}\right) \\
& + i\pi\beta_Z \left(\frac{32c_W^3}{3s_W} + \frac{8}{3}s_W c_W + \frac{19c_W}{3s_W} + \frac{s_W}{3c_W}\right. \\
& \left. - \frac{L_{xz}(32c_W^4 + (8s_W^2 + 19)c_W^2 + s_W^2)}{3s_W c_W}\right) - \frac{328s_W}{9c_W} + \frac{40}{3s_W c_W} \\
& - \frac{64c_W^3}{3s_W} - \frac{128m_t^2 s_W c_W}{9M^2} - \frac{16s_W c_W}{3} + \frac{16m_t^2 c_W}{3M^2 s_W} - \frac{116c_W}{9s_W}, \\
\delta Z_{ZA} &= \frac{4c_W}{s_W} \left(\log\left(\frac{\mu}{M_W}\right) - \Delta\right), \\
\delta Z_{ZZ} &= \left(\Delta + \log\left(\frac{M^2}{\mu^2}\right)\right) \left(-\frac{23s_W^2}{3c_W^2} + \frac{5}{3c_W^2} - \frac{5}{6c_W^2 s_W^2}\right) \\
& + \frac{L_{xHz}\beta_{HZ} \left(-\frac{c_W^2 M_H^8}{24M^6 s_W^2} + \frac{7M_H^6}{24M^4 s_W^2} - \frac{M_H^4}{M^2 c_W^2 s_W^2} + \frac{3M_H^2}{2c_W^4 s_W^2}\right)}{M_H^2 - 4M_Z^2} \\
& + L_{xHz}\beta_{HZ} \left(\frac{M_H^4(1-s_W^2)}{12s_W^2 M^4} - \frac{M_H^6 c_W^4}{24M^6 s_W^2}\right) + L_H \left(-\frac{c_W^2(c_W^2+1)M_H^6}{24M^6 s_W^2}\right. \\
& + \frac{(4c_W^2+5)M_H^4}{24M^4 s_W^2} + \frac{(s_W^2-9)M_H^2}{12M^2 c_W^2 s_W^2} + \frac{1}{2c_W^4 s_W^2} \Big) + L_Z \left(\frac{(c_W^4+c_W^2)M_H^6}{24M^6 s_W^2}\right. \\
& \left. + \frac{(4s_W^2-9)M_H^4}{24M^4 s_W^2} + \frac{(c_W^2+8)M_H^2}{12M^2 c_W^2 s_W^2} + \frac{c_W^2(43-80s_W^2)-6}{12c_W^4 s_W^2}\right)
\end{aligned}$$

$$\begin{aligned}
& + \frac{i\pi\beta_Z}{12(4M^2 - M_Z^2)c_W^2 s_W^2} \left((39(M_Z^2 - 2M^2) - 16M^2 s_W^2) c_W^4 \right. \\
& + 2s_W^2 (-20s_W^2 M^2 - 2M^2 + M_Z^2) c_W^2 + (2M^2 - M_Z^2) s_W^4 \\
& \left. + 120M^2 c_W^6 \right) + \frac{i\pi\beta_{Zt}}{18M^2 c_W^2 (M^2 - 4m_t^2 c_W^2) s_W^2} \left((32s_W^4 - 24s_W^2 + 9) M^4 \right. \\
& \left. - 2m_t^2 c_W^2 (32s_W^4 - 24s_W^2 + 9) M^2 + 2m_t^4 c_W^4 (64s_W^4 - 48s_W^2 - 9) \right) \\
& - \frac{L_{xzt}\beta_{Zt}}{18M_Z^2 (M_Z^2 - 4m_t^2) c_W^2 s_W^2} \left(32(4m_t^4 - 2M_Z^2 m_t^2 + M_Z^4) s_W^4 \right. \\
& \left. - 24(4m_t^4 - 2M_Z^2 m_t^2 + M_Z^4) s_W^2 + 9(-2m_t^4 - 2M_Z^2 m_t^2 + M_Z^4) \right) \\
& + L_{xz}\beta_Z \left(\frac{2(60c_W^6 + (39 - 8s_W^2) c_W^4 + (2s_W^2 - 20s_W^4) c_W^2 - s_W^4) M^2}{12(M_Z^2 - 4M^2) c_W^2 s_W^2} \right. \\
& \left. - \frac{s_W^4 + 37c_W^2 s_W^2 - 39c_W^2}{12c_W^2 s_W^2} \right) + \frac{L_{top}(32s_W^4 - 24s_W^2 + 9)}{18c_W^2 s_W^2} \\
& + \frac{c_W^2 M_H^4}{12M^4 s_W^2} + \frac{M_H^4}{12M^4 s_W^2} - \frac{M_H^2}{6M^2 s_W^2} - \frac{M_H^2}{3M^2 c_W^2 s_W^2} \\
& - \frac{8m_t^2}{3M^2} + \frac{2c_W^2}{3} + \frac{32m_t^2 s_W^2}{9M^2} - \frac{29s_W^2}{4c_W^2} + \frac{5s_W^2}{3} \\
& + \frac{16}{3c_W^2} - \frac{5c_W^4}{s_W^2} - \frac{m_t^2}{2M^2 s_W^2} + \frac{41c_W^2}{12s_W^2} - \frac{101}{36c_W^2 s_W^2} + \frac{1}{c_W^4 s_W^2} + \frac{5}{18},
\end{aligned} \tag{A.25}$$

A.7 Checks of One-Loop Logarithms

The one-loop coefficients of Sudakov logarithms are related to Casimir operators of the external particles [43]. We consider here only virtual corrections to the W -pair production in fermion antifermion annihilation to check against our calculation. The electroweak (W^\pm and Z) and electromagnetic corrections are given separately. For convenience we introduce $a = \frac{\alpha}{4\pi}$, $a_Y = \frac{\alpha}{4\pi c_W^2}$ and $a_W = \frac{\alpha}{4\pi s_W^2}$. The corrections are presented in the form $\mathcal{A}^{(1)} = \delta_{\mathcal{A}}^{(1)} \mathcal{A}_{\text{Born}}$ with

$$\delta_{\mathcal{A}}^{(1)} = \delta_{\mathcal{A}}^{\text{LL,ew}} + \delta_{\mathcal{A}}^{\text{NLL,ew}} + \delta_{\mathcal{A}}^{\text{ang NLL,ew}} + \delta_{\mathcal{A}}^{\text{LL,em}} + \delta_{\mathcal{A}}^{\text{NLL,em}} + \delta_{\mathcal{A}}^{\text{ang NLL,em}}. \tag{A.26}$$

For $f_L \bar{f}_L \rightarrow W^+ W^-$, with $f = e, u, d$, it is

$$\delta_{\mathcal{A}}^{\text{LL,ew}} = - \left[a_Y \left(\frac{Y_f}{2} \right)^2 - a_W \frac{11}{4} \right] \log^2 \left(\frac{s}{M_W^2} \right),$$

$$\begin{aligned}
\delta_{\mathcal{A}}^{\text{NLL,ew}} &= \left[a[-2 - 2Q_f^2] + a_Y 2[Q_f^2 - 2T_f^3 Q_f + (T_f^3)^2] \right. \\
&\quad \left. + a_W [2 + 2(T_f^3)^2] \right] \log\left(\frac{M_Z^2}{M_W^2}\right) + a_Y 3\left(\frac{Y_f}{2}\right)^2 \\
&\quad \left. + a_W \frac{65}{12} \right] \log\left(\frac{s}{M_W^2}\right), \\
\delta_{\mathcal{A}}^{\text{ang NLL,ew}} &= \left[a\left(-4Q_f \log\left(\frac{x_-}{x_+}\right)\right) + a_W \left(\left(4T_f^3 - 2 + 2\frac{x_-}{x_+}\right) \log(x_-) \right. \right. \\
&\quad \left. \left. - 4T_f^3 \log(x_+)\right) \right] \log\left(\frac{s}{M_Z^2}\right), \\
\delta_{\mathcal{A}}^{\text{LL,em}} &= a \left[\left(2 + Q_f^2\right) \log^2\left(\frac{s}{M_W^2}\right) - Q_f^2 \log^2\left(\frac{s}{\lambda^2}\right) \right. \\
&\quad \left. - 2 \log\left(\frac{s}{\lambda^2}\right) \log\left(\frac{s}{M_W^2}\right) \right], \\
\delta_{\mathcal{A}}^{\text{NLL,em}} &= a \left[\left(-2 - 3Q_f^2\right) \log\left(\frac{s}{M_W^2}\right) + \left(2 + 3Q_f^2\right) \log\left(\frac{s}{\lambda^2}\right) \right], \\
\delta_{\mathcal{A}}^{\text{ang NLL,em}} &= a 4Q_f \log\left(\frac{x_-}{x_+}\right) \log\left(\frac{s}{\lambda^2}\right), \tag{A.27}
\end{aligned}$$

and for $f_L \bar{f}_L \rightarrow \phi^+ \phi^-$ it is

$$\begin{aligned}
\delta_{\mathcal{A}}^{\text{LL}} &= -\left[a_Y \left(\left(\frac{Y_f}{2}\right)^2 + \frac{1}{4} \right) + a_W \frac{3}{2} \right] \log^2\left(\frac{s}{M_W^2}\right), \\
\delta_{\mathcal{A}}^{\text{NLL,ew}} &= \left[\left(a[-2 - 2Q_f^2] + a_Y 2 \left(Q_f^2 - 2T_f^3 Q_f + (T_f^3)^2 + \frac{1}{4} \right) \right) \right. \\
&\quad \left. + a_W \left(2(T_f^3)^2 + \frac{1}{2} - \frac{3}{2} \frac{m t^2}{M_W^2} \right) \right] \log\left(\frac{M_Z^2}{M_W^2}\right) + a_Y \left(3 \left(\frac{Y_f}{2}\right)^2 + 1 \right) \\
&\quad \left. + a_W \frac{21}{4} \right] \log\left(\frac{s}{M_W^2}\right), \\
\delta_{\mathcal{A}}^{\text{ang NLL,ew}} &= a \left[\left(-4Q_f \log\left(\frac{x_-}{x_+}\right) \right) + a_Y \left(2 \left(\frac{Y_f}{2}\right) \log\left(\frac{x_-}{x_+}\right) \right) \right. \\
&\quad \left. + a_W \left(2T_f^3 \log(x_-) \right) - \frac{4a}{s_W^4 R_{f\phi}} \log(x_-) \right] \log\left(\frac{s}{M_W^2}\right), \\
&\quad \text{where } R_{f\phi} = -\frac{1}{2c_W^2} \left(\frac{Y_f}{2}\right) - \frac{1}{2c_W^2} T_f^3, \\
\delta_{\mathcal{A}}^{\text{LL,em}} &= a \left[\left(2 + Q_f^2 \right) \log^2\left(\frac{s}{M_W^2}\right) - Q_f^2 \log^2\left(\frac{s}{\lambda^2}\right) \right. \\
&\quad \left. - 2 \log\left(\frac{s}{\lambda^2}\right) \log\left(\frac{s}{M_W^2}\right) \right],
\end{aligned}$$

$$\begin{aligned}
\delta_{\mathcal{A}}^{\text{NLL,em}} &= a \left[(-2 - 3Q_f^2) \log \left(\frac{s}{M_W^2} \right) + (2 + 3Q_f^2) \log \left(\frac{s}{\lambda^2} \right) \right], \\
\delta_{\mathcal{A}}^{\text{ang NLL,em}} &= a 4Q_f \log \left(\frac{x_-}{x_+} \right) \log \left(\frac{s}{\lambda^2} \right).
\end{aligned} \tag{A.28}$$

For the W boson the charges of the W^- are used. Thus for up-quarks in the initial states the quantum numbers of the antiquark \bar{u} has to be used since this is the one coupling to the W^- . Note that in the above formulae all virtual electromagnetic are included, while we subtracted QED logarithms which cancel for inclusive corrections.

Bibliography

- [1] J.M. Cornwall and G. Tiktopoulos, *Phys. Rev. Lett.* **35** (1975) 338; *Phys. Rev.* D13 (1976) 3370.
- [2] J. Frenkel and J.C. Taylor, *Nucl. Phys.* B116 (1976) 185.
- [3] D. Amati, R. Petronzio and G. Veneziano, *Nucl. Phys.* B146 (1978) 29.
- [4] A.H. Mueller *Phys. Rev.* D20 (1979) 2037;
J.C. Collins, *Phys. Rev.* D22 (1980) 1478; in *Perturbative QCD*, ed.
A.H. Mueller, 1989, p. 573.
- [5] A. Sen, *Phys. Rev.* D24 (1981) 3281.
- [6] A. Sen, *Phys. Rev.* D28 (1983) 860.
- [7] T. Kinoshita, *J. Math. Phys.* **3** (1962) 650.
- [8] T. D. Lee and M. Nauenberg, *Phys. Rev.* **133** (1964) B1549.
- [9] M. Ciafaloni, P. Ciafaloni and D. Comelli, *Phys. Rev. Lett.* **84** (2000) 4810 [arXiv:hep-ph/0001142].
- [10] A. Denner and S. Pozzorini, *Eur. Phys. J. C* **18** (2001) 461 [arXiv:hep-ph/0010201].
- [11] V.S. Fadin, L.N. Lipatov, A.D. Martin and M. Melles, *Phys. Rev.* D61 (2000) 094002.
- [12] J.H. Kühn, A.A. Penin and V.A. Smirnov, *Eur. Phys. J. C*17 (2000) 97;
Nucl. Phys. Proc. Suppl. 89 (2000) 94.
- [13] J. H. Kuhn, S. Moch, A. A. Penin and V. A. Smirnov, *Nucl. Phys. B* **616** (2001) 286 [Erratum-ibid. B **648** (2003) 455] [arXiv:hep-ph/0106298].

-
- [14] B. Jantzen, J. H. Kuhn, A. A. Penin and V. A. Smirnov, Nucl. Phys. B **731** (2005) 188 [Erratum-ibid. B **752** (2006) 327] [arXiv:hep-ph/0509157].
- [15] J. H. Kuhn, F. Metzler and A. A. Penin, Nucl. Phys. B **795** (2008) 277 [Erratum-ibid. **818** (2009) 135] [arXiv:0709.4055 [hep-ph]].
- [16] J. M. Cornwall, D. N. Levin and G. Tiktopoulos, Phys. Rev. D **10**, 1145 (1974) [Erratum-ibid. D **11**, 972 (1975)]. M. S. Chanowitz and M. K. Gaillard, Nucl. Phys. B **261** (1985) 379.
- [17] H. G. J. Veltman, Phys. Rev. D **41** (1990) 2294.
- [18] Y. P. Yao and C. P. Yuan, Phys. Rev. D **38** (1988) 2237.
- [19] M. Böhm, A. Denner, H. Joos Gauge “Theories of the Strong and Electroweak Interaction”
- [20] A. Denner, arXiv:0709.1075v1 [hep-ph]
- [21] W. Beenakker, A. Denner, S. Dittmaier, R. Mertig and T. Sack, Nucl. Phys. B **410**, 245 (1993).
- [22] Z. Bern, A. De Freitas and L. J. Dixon, JHEP **0306** (2003) 028 [arXiv:hep-ph/0304168].
- [23] E. W. N. Glover and M. E. Tejeda-Yeomans, JHEP **0306** (2003) 033 [arXiv:hep-ph/0304169].
- [24] T. Kodaira and L. Trentedue, *Phys. Lett.* B112 (1982) 66;
T.H. Davies and W.J. Stirling, *Nucl. Phys.* B244 (1984) 337;
G.P. Korchemsky and A.V. Radyushkin, *Nucl. Phys.* B283 (1989) 342.
- [25] K. Hagiwara, R. D. Peccei, D. Zeppenfeld and K. Hikasa, Nucl. Phys. B **282** (1987) 253. J. Fleischer, F. Jegerlehner and M. Zralek, Z. Phys. C **42** (1989) 409.
- [26] M. Bohm, A. Denner, T. Sack, W. Beenakker, F. A. Berends and H. Kuijff, Nucl. Phys. B **304** (1988) 463.
- [27] W. Beenakker, K. Kolodziej and T. Sack, Phys. Lett. B **258** (1991) 469. W. Beenakker, F. A. Berends and T. Sack, Nucl. Phys. B **367** (1991) 287. J. Fleischer, K. Kolodziej and F. Jegerlehner, Phys. Rev. D **47** (1993) 830. S. Dittmaier, M. Bohm and A. Denner, Nucl. Phys. B **376** (1992) 29 [Erratum-ibid. B **391** (1993) 483].

-
- [28] A. Denner, S. Dittmaier, M. Roth and L. H. Wieders, Nucl. Phys. B **724** (2005) 247 [arXiv:hep-ph/0505042].
- [29] G. Degrossi, S. Fanchiotti and A. Sirlin, Nucl. Phys. B **351** (1991) 49.
- [30] S. Fanchiotti, B. A. Kniehl and A. Sirlin, Phys. Rev. D **48** (1993) 307 [arXiv:hep-ph/9212285].
- [31] W. J. Marciano and A. Sirlin, Phys. Rev. D **22** (1980) 2695 [Erratum-
ibid. D **31** (1985) 213].
- [32] P. Nogueira, J. Comput. Phys. **105** (1993) 279.
- [33] R. Mertig, M. Bohm and A. Denner, Comput. Phys. Commun. **64** (1991) 345.
- [34] G. Passarino and M. Veltman, *Nucl. Phys.* B160 (1979) 151.
- [35] M. Roth and A. Denner, Nucl. Phys. B **479** (1996) 495 [arXiv:hep-ph/9605420].
- [36] T. Hahn and M. Perez-Victoria, Comput. Phys. Commun. **118** (1999) 153 [arXiv:hep-ph/9807565].
- [37] J.C. Collins, Phys. Rev. D **22** (1980) 1478; Adv. Ser. Direct. High Energy Phys. **5** (1989) 573
- [38] M. Melles, *Phys.Rev.* D64 (2001) 014011.
- [39] M. Beccaria *et al.*, *Phys. Rev.* D61 (2000) 011301; D61 (2000) 073005; M. Beccaria, F.M. Renard and C. Verzegnassi, *Phys. Rev.* D63 (2001) 053013.
- [40] S. Frixione, Nucl. Phys. B **410** (1993) 280.
- [41] A. D. Martin, R. G. Roberts, W. J. Stirling and R. S. Thorne, Phys. Lett. B **531** (2002) 216 [arXiv:hep-ph/0201127].
- [42] T. Hahn, Comput. Phys. Commun. **168** (2005) 78 [arXiv:hep-ph/0404043].
- [43] A. Denner and S. Pozzorini, Preprint PSI-PR-00-15, hep-ph/0010201.

Acknowledgment

First of all, I would like to thank Prof. Johann H. Kühn for giving me the opportunity to work on this interesting topic, his support, and his patience. I thank Prof. Matthias Steinhauser for agreeing to be the second referee for my thesis. I am grateful to Peter Marquard and Christoph Reiser for carefully reading parts of the manuscript. Also many thanks go to my collaborators Prof. Alexander A. Penin and Sandro Uccirati. I am grateful Throughout my time at the Institute for Theoretical Particle Physics i have enjoyed a pleasant and inspiring atmosphere, and I have profited a lot from discussions with several colleagues. In particular, I am thankful to my fellow PhD students Joachim Brod, Matthias Kauth, Philipp Maierhöfer, Philip Kant and Nicolai Zerf and everybody who joined our weekly soccer match.

Last, but not least, I would like to thank my parents, my brother, and my friends, for their patience and support during my studies.

Curriculum Vitae

Personal Information:

Name: Falk Metzler
Date of Birth: 18.08.1978
Place of Birth: Karlsruhe, Germany
Nationality: german
Marital Status: single

Education:

school attendance: 1985 - 1989 Elementary School Karlsruhe
1989 - 1999 Max-Planck-Gymnasium Karlsruhe
Studies: 1999 - 2005 Physics at the University of Karlsruhe
Diploma Thesis: Elektroschwache Strahlungskorrekturen zur
 W -Paar Produktion bei hohen Energien
Referee: Prof. Dr. J.H. Kühn
Diploma: 23.05.2005, grade 1.2
Promotion: Juli 2005- Juli 2009
Physics at the University of Karlsruhe
Day of Exam : 03.07.2009
Title : Electroweak Corrections to W -pair Production
at LHC and ILC
Referees: Prof. Dr. J.H. Kühn
Prof. Dr. M. Steinhauser

